Development of an Efficient Calculation Method Based on Evolutionary Programming for Optimal Power Flow Considering Transient and Voltage Stabilities

過度安定度と電圧安定度を考慮した進化的プログラミングに基づいた効果的な最適潮流計算手法の開発

by

Tangpatiphan　Kritsana
タンパティパーン　クリサナ

A dissertation submitted in partial fulfillment of the requirements
of the degree of Doctor of Philosophy in the
Graduate School of Engineering, The University of Tokyo

December 2009

Contents

ACKNOWLEDGEMENTS

I would like to express my heartfelt gratitude to my advisor, Professor Akihiko Yokoyama, for his kind guidance, constant encouragement, and constructive suggestions throughout my study in his laboratory. It was my very great pleasure to conduct this research with him.

Indispensably, I also wish to express sincere appreciations to the committee members of my Ph.D. dissertation, Professor Kenji Yamaji, Professor Kunihiko Hidaka, Professor Haruhito Taniguchi, Professor Takafumi Koseki, Professor Junpei Baba, who kindly provide me a great deal of valuable suggestions and comments during my thesis work. Moreover, I would like to express my frank appreciation to Dr. Kithsiri Madapatha Liyanage for his kind and useful comments during the laboratory meeting.

I also wish to extend my sincere thanks to Mr. Norihito Shimada for his kind assistance and various technical supports for my research. Special thanks are conveyed to Dr. Surachai Chaitusaney and Dr. Jun Zhang, my closed and respectful seniors, for their kindness, encouragement, and help in both research matters and life in Japan. In addition, I would like to thank all members in Yokoyama Laboratory, Mr. Shinji Ooya, Mr. Ko Sekita, Mr. Nattawut Paensuwan, Mr. Ken-ichi Kawabe, Mr. Hiroshi Irie, Mr. Taisuke Masuta, Mr. Nguyen Hoang Viet and others, which are not mentioned here, for their goodwill, friendship, and guidance on both my research and Japanese study.

Sincere gratitude is conveyed to Ministry of Education, Culture, Sports, Science and Technology (MEXT) for providing me the scholarship and giving me the great chance to study at the University of Tokyo.

Grateful acknowledgements are expressed to the COE (Centers of Excellence) Program for providing me financial supports when I have to present my research papers overseas and organizing several helpful seminars. At the same time, sincere appreciations are expressed to all staffs of Japanese class in both international student center and faculty of engineering. Their Japanese classes really help me to understand Japanese language and culture.

Finally, this is a good opportunity to express the utmost gratitude to my parents, lovely sister, and Miss Supreeya Sirisaengsawarng for their timeless love, support, and encouragement throughout my doctoral study in Japan.

Tangpatiphan Kritsana
Tokyo
December 2009

List of Figures

Chapter 1

Chapter 2

Chapter 3

Chapter 4

Chapter 5

Appendix

List of Tables

Appendix

CHAPTER 1

INTRODUCTION

1.1 General Introduction

In electric power system, the optimization problems play a crucial role in many aspects such as cost minimization, profit maximization etc. The process of seeking optimum for these problems usually consists of modeling and solving [1]. In the past, the problems were modeled in such a way that the classical optimization techniques, such as gradient-based optimization algorithm and linear programming etc. [2], could handle and then the optimal solutions were gained. Unfortunately, a large number of optimization problems in present electric power system become more complex and larger in size. The process of problem modeling, approximation, and assumptions in order to apply the classical optimization techniques seems to be more difficult and unacceptable. In addition, the classical optimization techniques are powerless to obtain the desired solution, when they are applied to solve optimization problems which are highly non-linear, non-smooth, and non-convex in nature. Therefore, the development of state-of-the-art methods becomes very important.

To respond to the above-mentioned need, novel and modern heuristic methods such as Evolutionary Programming (EP) [1, 3], Genetic Algorithm (GA), Simulated Annealing (SA), Tabu Search (TS), Artificial Neutral Network (ANN), etc., have been developed continuously to surpass limitations of the classical techniques. Among them, EP was proved to be a promising algorithm for solving constrained optimization problems. Due to its characteristics, which are independent on gradient search, less complex in algorithm, and unrestricted to types of objective functions and constraints in optimization problems, the application of EP now becomes popular in many fields and particularly necessary for solving highly non-linear optimization problems.

In this dissertation, the application of EP-based methods to optimal power flow (OPF) problem, one of the most important optimization problems in power system operation, is explored and presented. The transient and voltage stability issues, which play an important role on major blackouts in many countries, are also considered in the OPF problem. This dissertation is organized as follows. Chapter 1 gives the overviews and objective of this research. Chapter 2 presents the formulations of different types of OPF problems. Chapter 3 explains the mechanisms and main components of the proposed EP-based methods. Chapter 4 is of the topic on the proposed artificial neural network for transient stability assessment. Chapter 5 reports the results of different types of OPF problems solved by the proposed EP-based methods. Finally the conclusion is drawn in Chapter 6.

1.2 Overview of Evolutionary Programming (EP)

In 1960's, the EP technique was originally developed by Lawrence Fogel [1] and firstly used finite state machines as the based structure to be evolved. In 1990's, EP was later developed to solve optimization problem in the real space. After that, EP becomes an important tool widely used to solve various practical optimization problems.

The EP technique is a stochastic and iterative optimization method in the area of evolutionary computation emphasizing on evolution process. It works by evolving a population of candidate or potential solutions toward the global solution through the use of mutation operator and selection scheme. The population comprises a set of individuals representing the trial solutions in an optimization problem. During each evolution, a new population (offspring) is formed from an existing population (parent) through the use of a mutation operator. This mutation operator produces a new population by perturbing each individual in the parent population with a random number such as Gaussian random number etc. It is possible to use more than one mutation operator to a single parent to provide the diversification to the candidate solutions. The degree of optimality of each candidate solution (individual) is measured by its fitness, which can be defined as a value of the objective function in the optimization problem [4]. The selection scheme based on the fitness value of both parent and offspring will be performed to create the new parent for the next evolution. In the process of mutation, the fitness of the parent population and the number of evolutions or iterations are two key factors that define how far offspring can be mutated. Firstly, a parent with good fitness will generate an offspring in its vicinity, and on the contrary a parent with bad fitness will let an offspring move far away from it. This will give a chance to an offspring to improve the quality in terms of fitness from its parent. Secondly, at the beginning evolution, a large mutated distance of an offspring from its parent is allowed, then when the number of evolutions increases, the distance gets smaller and smaller, and lastly EP converges to the optimal solution.

An example of the general optimization problem [2] can be formulated as follows:

$$\begin{aligned} &\text{Min} && F(X) \\ &\text{when} && X = (x_1, \cdots, x_n)^T \subseteq \Re^n \\ &\text{Subject to} && g(X) = 0 \\ & && h(X) \le 0 \end{aligned} \tag{1.1}$$

where $g(X)$ and $h(X)$ express the equality and inequality constraints respectively.

Generally, EP [4] has the main steps for obtaining the optimal solution as follows:

- *Initialization*

The P candidate solutions or individuals of the problem are randomly selected to form the initial population by using some distribution random numbers, e.g. uniform random number Gaussian random number etc.

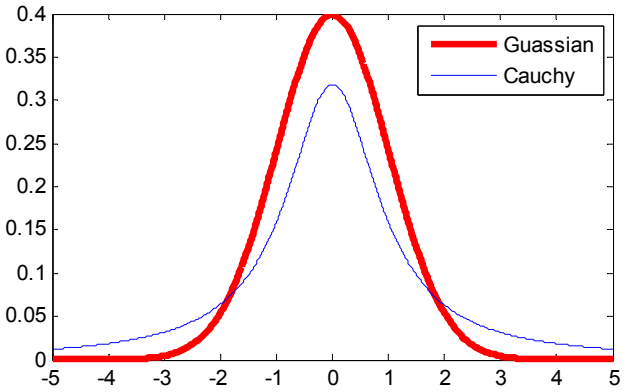

Fig. 1.1 The comparison between Gaussian and Cauchy distribution functions

- *Mutation*

From the present set of candidate solutions, the offspring will be created on a one-by-one basis using mutation scale (σ) and probability distribution functions, e.g. Gaussian distribution, Cauchy distribution, Levy distribution etc. The offspring will be obtained according to the following equation.

$$x_i' = x_i + \sigma_i \times D(0,1) \tag{1.2}$$

where $D(0,1)$ is the probability distribution function; σ is mutation scale which can be the function of the fitness value; number of iteration and other parameters; x_i' and x' are the offspring and parent respectively.

The mutation scale should provide the opportunity to the offspring to avoid local optimums and help the algorithm to converge to the optimal solution. The types of distribution function $D(0,1)$ also have influence on quality of the solution. In Fig. 1.1, Gaussian and Cauchy distribution functions are plotted. From this figure, it can be seen that the Cauchy mutation has a longer tail than Gaussian mutation. Obviously, the Cauchy mutation can produce the offspring, which is quite different (far) from their parent. Therefore, Cauchy mutation is suitable for searching in large neighborhood whereas Gaussian mutation is good at searching in the local neighborhood. In addition, mutation operators both Gaussian and Cauchy can be applied to a population at the same time to enhance search template.

- *Selection*

In this process, the current parent and offspring populations are combined together making the combined population and the new parent population will be selected from the combined population based on their fitness. For optimization to occur or the movement to the global optimum, the fitter or better solutions should have a greater chance of selection. Note that fitness should reflect the quality of a solution. In the minimization problem, an individual with a high objective function value should have lower fitness than that with a low objective function value. For example if the value of objective function is F, the fitness (f) can be defined as $1/F$. A selection technique intensively used is a tournament scheme described in the following.

$$w_t = \begin{cases} 1 & f_i > f_r \\ 0 & otherwise \end{cases}$$

$$s_i = \sum_{t=1}^{N_t} w_t \tag{1.3}$$

In the tournament scheme, each individual has to compete with N_t individuals randomly selected from the combined population on a one-by-one basis. According to Eq. (1.3) if the fitness value of the individual (f_i) is greater than that of the selected opponent (f_r), the individual scores 1 or wins. Otherwise, it scores 0 or loses.

When all individuals in the combined population get their competition scores (s_i), they will be ranked in descending order according to their competition score. The first P individuals with higher competition score are transcribed along with their fitness to form a new parent population of the next generation.

To select the potential individuals for the next generation, other selection schemes used in Simulated Annealing (SA) or Genetic Algorithm (GA) can be applied. In addition, since almost all selection schemes try to give a chance to weak individuals to survive, there will be a case that an individual with the best fitness will not be selected. To solve the problem, elitism can be also used to keep the best individual of each evolution.

- *Stopping Criteria*

The above-mentioned mutation and the selection processes will be repeated until the convergence condition or stopping criterion is satisfied. The maximum generation number can be used as a stopping criterion. Another possible criterion is based on an improvement of solution, i.e. the EP processes will be terminated if there is no improvement of the solutions over the specific generation number.

Various versions of EP algorithms can be found in [2]. Based on the characteristic of EP algorithm described above, the parallel algorithm can be easily put into the search template. By doing so, the computational time of EP will be definitely decreased.

The procedure of EP for solving optimization problem can be simply shown as follows:

Step 1: Load all data, set $g = 1$
Step 2: Initialization & Fitness evaluation
Step 3: Mutation & Fitness evaluation
Step 4: Selection
Step 5: If g < G_{max}, set $g = g + 1$ and go back to Step 3. Otherwise, terminate the process.

1.3 Application of EP to Power System Optimization Problems

In this section, the examples of EP application toward various kinds of optimization problems in electric power system, i.e. economic load dispatch, optimal power flow, unit commitment, transmission expansion planning, power flow control by facts, optimal placement of distributed generators in distribution networks, and transient & subtransient parameter estimation, are briefly illustrated. The results presented in this chapter show that EP works well on both the real-valued functions and mixed integer functions. This emphasizes that EP can be a promising tool to solve the optimization problems in the future.

1.3.1 Economic Load Dispatch (ELD)

Economic load dispatch is an optimization problem in power system operation. The main task is to allocate the available power generation in system to supply the load. The primary objective function is to minimize total fuel cost of all generating units while satisfying all operational constraints of available generators.

The representation of solution (individual) in EP algorithm is a set of power generation of all generators $X_i = [P_i, ..., P_{NG}]$. In [5], various kinds of mutation operators are applied to generate an offspring from its parent as below:

Gaussian Mutation (CEP)

$$P_i' = P_i + N(0, \sigma_i^2) \tag{1.4}$$

where $N(0, \sigma_i)$ is Gaussian random variable with mean 0 and standard deviation σ_i.

Cauchy Mutation (FEP)

$$P_i' = P_i + \sigma_i \times C(0,1) \tag{1.5}$$

where $C(0,1)$ is Cauchy random variable with scale parameter $t = 1$ centered at zero.

Mean of Gaussian and Cauchy mutations (MFEP)

$$P_i' = P_i + \sigma_i / 2\{N(0,1) + C(0,1)\} \tag{1.6}$$

Selection of the Better One from Gaussian and Cauchy mutations (IFEP)

$$\begin{aligned} P_{1i}' &= P_i + \sigma_i \times N(0,1) \\ P_{2i}' &= P_i + \sigma_i \times C(0,1) \end{aligned} \tag{1.7}$$

From IFEP, the objective function values of both offspring are evaluated and compared. The better one will be chosen.

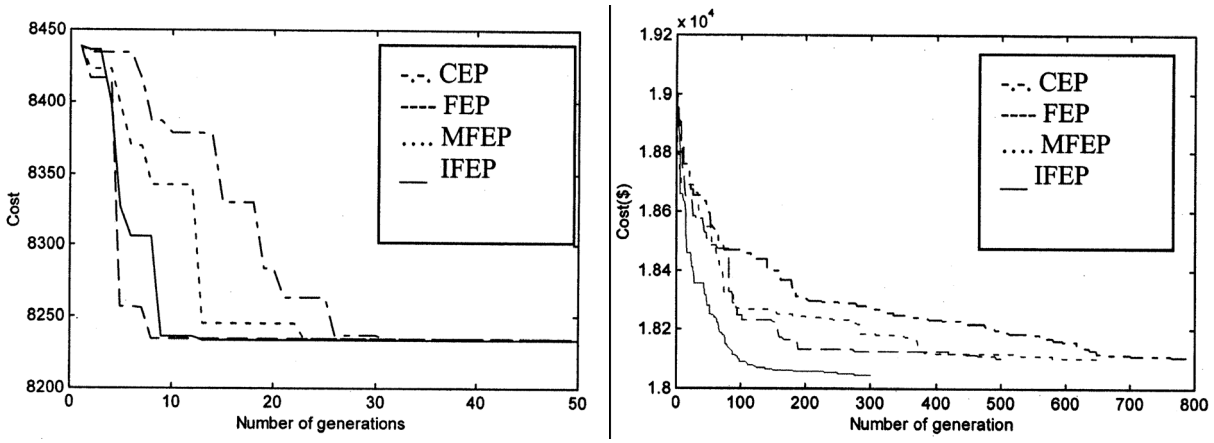

(a) 13-unit case (b) 40-unit case

Fig. 1.2 Convergence comparisons between different types of EP algorithms for ELD problem

Above EP algorithm with the competition in selection process is tested with fuel cost with valve-point loading. The valve-point loading effect normally occurs in a thermal generating unit causing the fuel cost function non-smooth and non-convex. The results show that mutation operator in FEP type performs better than other types in a small system (13-unit case) as shown in Fig. 1.2a, but IFEP type gives the best solution and the fastest convergence rate in bigger system (40-unit case) as shown in Fig. 1.2b. However, IFEP type requires computatioanl time slightly higher than others because it has to produce two solutions per one mutation. In addition, the results of all types of EP-based methods in [5] outperform those obtained by Genetic Algorithm (GA).

1.3.2 Optimal Power Flow (OPF)

It can be said that OPF problem is an extension problem of ELD. In OPF, the solution is not only power generation but also other controllable parameters in a power system such as voltages at generator bus, transformer tap settings, etc. The constraints in ELD are also extended. The real loss in the system is calculated and added into power balance equation whereas in ELD the system loss is obtained by approximation. All additional variable limits in the system are considered as inequality constraints, for instance voltage limit at load bus, line flow limit on the transmission line, stability limit etc. Various objection functions can be considered in OPF, for example fuel cost minimization, system loss minimization, optimal voltage profile, power transfer maximization, and load shedding minimization under an emergency condition and in some cases the multi-objective is taken into account. The minimization of both fuel cost and system loss at the same time is one of the multi-objective functions. Therefore, the OPF problem is a large scale of non-linear optimization problem requiring a powerful tool to solve it.

In [6], EP algorithm is a selected tool to solve OPF with cost minimization. The control variables or solutions are the power generation, voltage at generator bus, and transformer tap position. To handle the inequality constraints, the original objective function is added by the penalty terms. The EP algorithm is tested on IEEE 30-bus system with three different types of

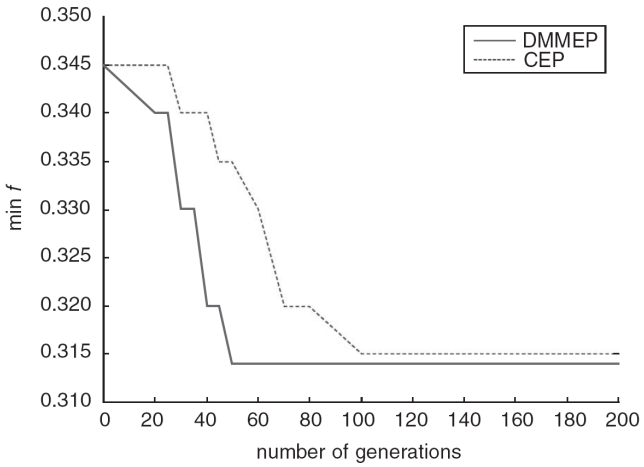

Fig. 1.3 Convergence natures of DMMEP and CEP for multi-objective OPF problem

cost function; namely quadratic, piecewise quadratic and quadratic with sine component curves. The results show that EP works well with both smooth and non-smooth cost functions.

In [7], the optimal reactive power dispatch which is the active loss minimization is considered as an objective function. The results in this paper show that the EP method is able to undertake global search with a fast convergence rate and a feature of robust computation, and possesses an inherent capability for parallel processing. From the simulation study, it has been found that the results of EP are always better than that obtained using the quasi Newton method, one of the classical optimization techniques, under all circumstances.

In [8, 9], multi-objective optimization problems, which consider loss minimization, cost minimization of reactive power source installment, and voltage deviation minimization simultaneously, are solved by EP. In [9], a dynamic mutation and metropolis selection EP method (DMMEP) is proposed and compared with the conventional EP (CEP). The results on the multi-objective OPF problem show that DMMEP converges to the solution much faster than CEP as shown in Fig. 1.3.

1.3.3 Unit Commitment (UC)

UC is an operation scheduling function [10], which hourly schedules the *on* and *off* times of all generating units in the whole system with the minimum cost while satisfying the forecasted power demand plus the system reliability, and considering start-up and shut-down costs and minimum-up and minimum-down times of each generating unit. For hourly schedule of generating unit, ELD will be calculated to obtain the operating cost of each hour. In terms of time scales, UC is hourly operation decision with one-day or one-week horizon. The UC problem formulation [11] can be expressed as follows:

$$\text{Min} \quad TC = TFC + TSUC + TSDC \tag{1.8}$$

where TC is total cost for scheduling period; TFC is the total fuel cost of committed units (calculated from ELD) for scheduling period; $TSUC$ is the total start-up cost; and $TSDC$ is the total shut-down cost.

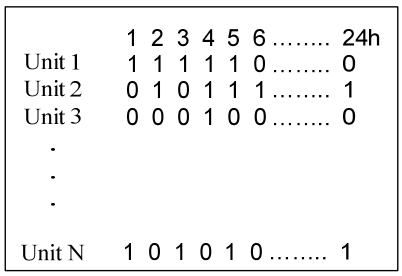

Fig. 1.4 Solution representation of UC problem

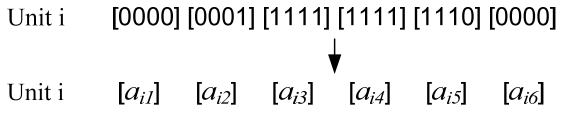

Fig. 1.5 Solution representation of EP for UC problem

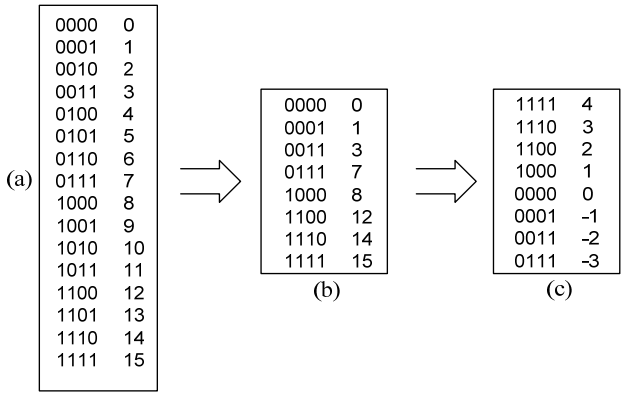

Fig. 1.6 Defining the unit's operating code for UC problem

The main constraints are as follows: all committed unit capacity should meet the hourly power demand and spinning reserve (normally 10% of hourly demand). Minimum-up and minimum-down times of each generating unit must be ensuring. In other words, once the unit is committed or decommitted, there is a minimum time before it can be decommitted or recommitted. In each hour, the committed units should also supply power demand within their maximum and minimum limits etc.

The solution of UC problem is principally the status of all generating units in each hour and it is demonstrated in Fig. 1.4. In this figure, '1' indicates that the unit is 'on-line' and '0' indicates that the unit is 'shut-down' or 'off-line'. Because EP fundamentally treats the candidate solution as real number, the modification is needed. The original '0' and '1' schedules are transformed to real number as shown in Fig. 1.5. The a_{ij} refers to as "state variable" of unit i at the j-th reduced period. Therefore, the representation of an individual becomes $S_k = [a_{i1}, a_{i2}\ a_{i3}, a_{i4}, a_{i5}, a_{i6}]$. These elements take on the integer values shown in Fig. 1.6a.

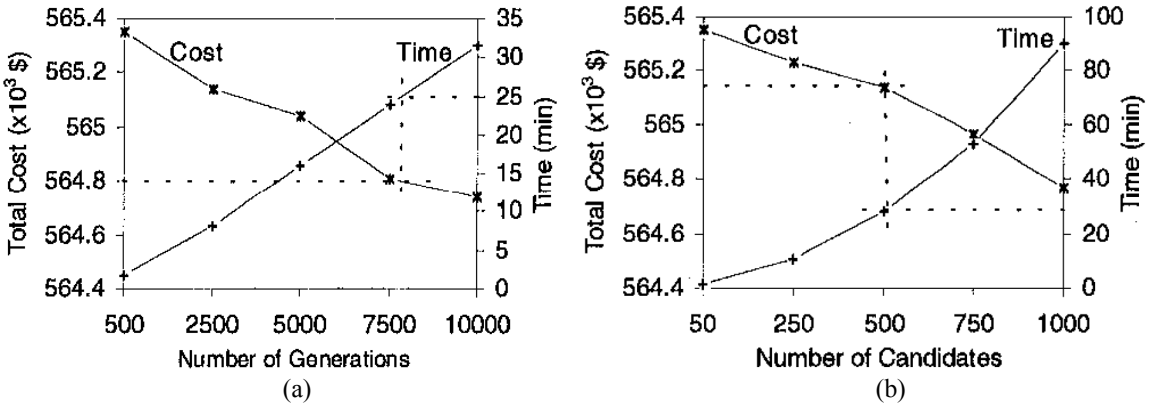

Fig. 1.7 EP performances for UC problem

To add minimum-up and minimum-down time constraints (Let say both are 4 hrs), firstly the coding begins with a simple binary system (Fig. 1.6a) and then eliminates the combinations that violate the constraints (Fig. 1.6b) and lastly it is rearranged with respect to the number of on-line hours (Fig. 1.6c). For example, "-2" and "2" indicate a unit run for 2 hours; in the first case the unit is brought on-line and in the second case the unit is brought off-line.

The EP is used to solve UC problem with 10-unit case. The EP performances, when the number of generations is increased and when the number of *P* candidates is increased, are plotted in Fig.1.7. At the same computational time (25 minutes), EP algorithm performs much better with "more generations" ($564800) than it does with "more candidates" ($565150). Fig. 1.7 also indicates that the execution time increases in a quadratic manner with the increase of the population size whereas the execution time increases almost in a linear manner with the increase of the generation number.

In addition, the EP gives the better performance for UC problem compared to solution obtained from GA, e.g. less computational time and lower total cost.

1.3.4 Transmission Expansion Planning

In case that the existing transmission network is fully committed, the new transmission is needed to equip to the system in order to supply power in a secure manner. Briefly, in this problem, the objective is to identify where and what type of equipment (transmission line) should be installed to minimize the investment and operating costs while subject to investment constraints; limitation of the number of circuits in one path (arc) etc. The representation of EP algorithm in [12] is $S_k = [n_{k,ij}$; for all $\text{arc}_{ij}]$,when $n_{k,ij}$ denotes the number of circuits in arc_{ij} of individual k and arc_{ij} denotes the transmission path connecting between node i and node j. The mutation process creates a single offspring from its parent as below:

$$n'_{k,ij} = \text{integer}\left[n_{k,ij} + N(0, \sigma^2_{k,ij}) \right]$$
$$\sigma_{k,ij} = \beta \cdot n_{ij,\max} \cdot F(S_k) / F_{\min} \qquad (1.9)$$

where $n_{ij,\max}$ denotes the maximum number of circuits in an arc_{ij}; β is a scaling factor.

Table 1.1 Performance of various algorithms for transmission planning problem

Algorithm	Number of fitness evaluations before the best solution is created	Number of fitness evaluations requires to achieve convergence
GA	598	881
SA	594	754
Hybrid	470	528
EP	224	320

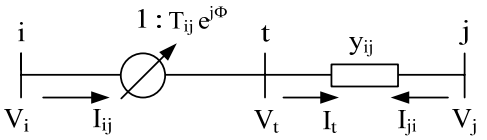

Fig. 1.8 Phase shifter with tap change equivalent circuit

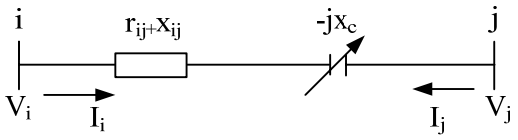

Fig. 1.9 Series compensator equivalent circuit

Table 1.1 summarizes the performance of the EP algorithm proposed in [12] and the results which were obtained using a genetic algorithm (GA), a simulated annealing (SA) technique, and a hybrid method that integrates features of GA, SA and Tabu Search (TS). It can be seen that the EP approach is shown to have a better performance than others in terms of the smallest number of fitness evolutions.

1.3.5 Power Flow Control by FACTS

The development of FACTS (flexible AC transmission systems) based on power electronic devices such as thyristor etc. has many benefits on both steady state power flow control and dynamics stability control. Under some emergency conditions in power system, the power flow in critical lines has to be limited or to be controlled. This power flow is sometimes beyond the control ability of generator. However, this can be achieved by controlling FACTS parameters.

In [13] phase shifter and series compensator based on an unified power flow controller (UPFC) device, one type of the FACTS devices, are equipped to the system at a specific location. They can be used to regulate both angles and magnitudes of branch voltages. Their equivalent circuits are modeled in Figs. 1.8 and 1.9.

By controlling parameters of T_{ij}, Φ and x_c, power flow in the line equipped with the devices can be controlled. The objective function is to minimize active power loss and to control power flow in critical lines to a specific value under emergency conditions, such as circuit outages etc., while subject to power balance and parameter limits of phase shifters and series compensators. The objective function (F) can be formulated as below:

$$\text{Min } F = P_{loss} + \sum_{k \in CL} \lambda_k \left(|P_k| - P_k^{MAX} \right)^2 \tag{1.10}$$

where λ_k is a penalty factor for the critical line k; P_k is power flow in the critical line k; P_k^{MAX} is the limited power flow on branch k; CL is a set of the critical lines under emergency condition.

Table 1.2 Results of power flows of branches with and without power flow control

	Initial conditions		Optimal Results	
Branches	(10,22)	(8,28)	(10,22)	(8,28)
Case 1	0.080	0.021	0.0766	0.0254
Case 2	0.086	0.147	0.100	0.100
Case 3	0.231	0.158	0.100	0.100

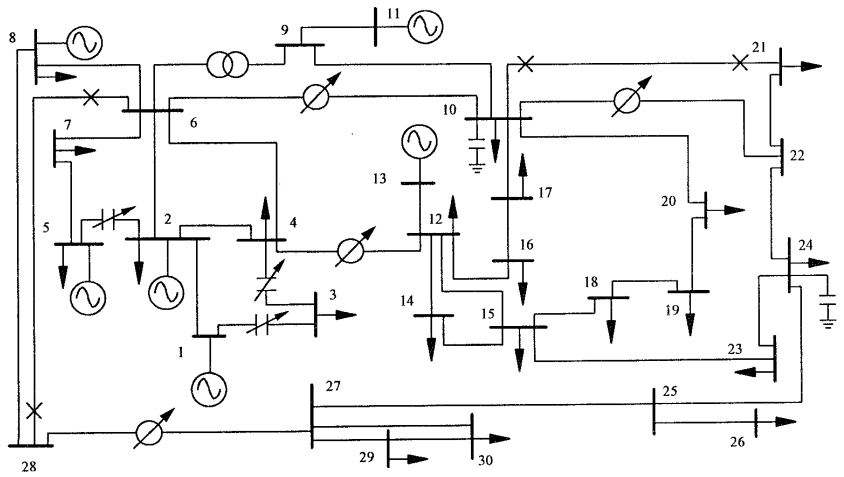

Fig. 1.10 Modified IEEE 30-bus system with FATCS devices

The locations of four phase shifters and three series compensators in modified IEEE 30-bus system are shown in Fig. 1.10.

Three cases have been studied. Case 1 is the normal operation state. Case 2 and 3 are contingency states. Case 2 has one circuit outage of branch (6, 28). Case 3 has two circuit outages of branches (6, 28) and (10, 21). Two branches (10, 22) and (8, 28) are selected as the limited power flow branches whose limits are set to 0.1 p.u. The results of all cases are tabulated in Table 1.2. After optimization, the power flows in branches (10, 22) and (8, 28) are regulated back into their limit in both case 2 and case 3 as shown in the table.

1.3.6 Optimal Placement of Distributed Generators in Distribution Networks

Due to a high cost of electrical network expansion in order to meet load growth, distributed generation (DG), defined as an electric power source connected directly to the distribution network on customer side, can be a promising choice to delay expensive infrastructure investment. The rising interest in DG is not only due to the economical reasons but also government incentives to create a combination of a generation group that is less dependent on only one type of power source. The optimal location can also lead to significant reduction in feeder losses. However, DG's installation can cause some disturbances to the system such as power quality etc. Normally, the energy provided by DG, is more expensive than that provided by large central generators. Therefore, the placement location and sizing of DG on the distribution system are important issues on the power system planning.

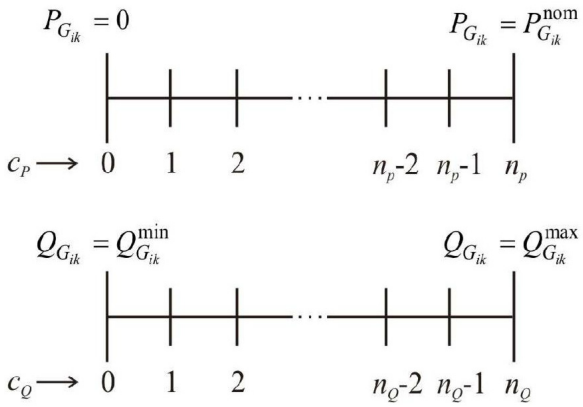

Fig. 1.11 Active and reactive generated power intervals of DG

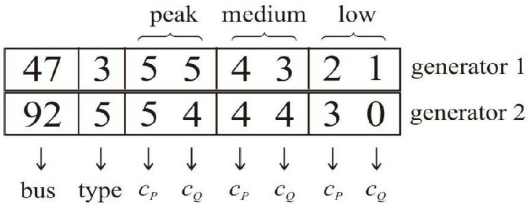

Fig. 1.12 Representation of an EP candidate solution for optimal placement of DGs

The objective of DG's installation is to minimize the supply cost i.e. the total cost paid by the utility in order to supply the feeder loads while considering the investment and operation cost of DGs and bus voltage variation. The objective in [14] is formulated as follows:

$$\text{Max} \quad F = C_T^B - C_T^A - \lambda_v P_v \tag{1.11}$$

where $C^B{}_T$ is the total load supply cost for a period before DG's installation; $C^A{}_T$ is the total load supply cost for a period after DG's installation, which includes the supply cost from substation and DGs as well as cost of DG's installation. The third term is a penalty function in which the DG's operation makes the generation bus voltages exceed a specified variation tolerance.

The load daily variation is considered by three demand levels i.e. peak, intermediate, and low (it assumes to be equal for whole year). DG is considered as a negative constant load with maximum and minimum limits of active and reactive capacity. The possible generation interval of a DG is divided into discrete levels as shown in Fig.1.11.

The numbers c_P and c_Q are an integer located between 0 and n_P and between 0 to n_Q respectively. This number expresses the amount of active and reactive power supply from a DG based on its nominal capacity (P_G^{nom}) in each load demand level. The solution of the problem consists of position, nominal capacity (type), and operation schedule (c_P and c_Q) of DGs. Therefore, the representation of an EP candidate solution is depicted in Fig. 1.12.

Table 1.3 Comparison of system loss and supply cost before and after the installation of two DGs

Parameters	Before	After
Substation (MWh/day)	149,82	120,90
Generator 1 (MWh/day)	-	12,44
Generator 2 (MWh/day)	-	9,50
Load (MWh/day)	134,93	134,93
Losses (MWh/day)	14,89	7,91
Active losses (peak) (%)	13,35	8,73
Supply costs ($)	$16{,}41.10^6$	$16{,}16.10^6$

The algorithm is tested with a part of distribution system in Brazil and the horizon time for evaluation of the DG's installation is 5 years. The maximum number of the installed DGs is 2. Solved by the EP algorithm, the optimal installations of two DGs are obtained at bus 128 (Generator 1) and 116 (Generator 2). Table 1.3 shows the comparison of system loss and supply cost before and after the installation of two DGs. The results show that by adding two DGs into the distribution system, the total loss in feeder lines and the total supply cost including the investment of DG's installation are remarkably reduced.

1.3.7 Transient and Subtransient Parameter Estimation

The issue of dynamic parameter estimation of a generator is important for power system analysis, control system design, and fault analysis. The accuracy of dynamic parameter estimation indicates the accuracy of dynamic analysis of a power system. As known, the dynamic parameters of a generator clearly play a very significant role on the power system stability analysis. Generally, the generator parameters are estimated by observing stimulus and response data. The objective of this problem is to minimize a value of the squared predictive error, which is a function of dynamic generator parameters. The dynamic model of a generator [15] can be simply written as follows:

$$\begin{aligned} \dot{x}(t) &= A(p)x(t) + B(p)u(t) + B_e(p)y_e(t) + w(t) \\ y(t_k) &= C(p)x(t_k) + C_e(p)y_e(t_k) + v(t_k) \end{aligned} \tag{1.12}$$

and

$$\begin{aligned} p &= [X_d, X'_d, X''_d, X_q, X''_q, T'_{do}, T''_{do}, T''_{qo}, M, D, S_d] \\ x(t) &= [\Delta\delta, \Delta\omega, \Delta E'_q, \Delta E''_q, \Delta E''_d, \Delta E_{fd}] \end{aligned} \tag{1.13}$$

where p is the parameter vector to be estimated, $x(t)$ is state variable; $y(t_k)$ and $y_e(t_k)$ are the output signal at time step t_k; $w(t)$ and $v(t_k)$ are the system and measurement noises respectively.

The objective function is to minimize an error function of the real response and estimated response from the set of parameters (p).

$$\text{Min} \quad F(p) = E(e(p,t_k))^T$$

Table 1.4 Numerical results of transient and subtransient parameter estimation

		X_d	X_d'	X_d''	X_q	X_q''	T_{do}'	T_{do}''	T_{qo}''	M	D	S_d	Max Errors
True Values		2.0	0.244	0.185	1.91	0.212	4.18	0.75	0.743	6.5	5.012	1.0	
Case 1	EP	2.009	0.243	0.184	1.922	0.214	4.240	0.737	0.732	6.398	4.919	1.010	1.86% (D)
	CEKF	1.997	0.245	0.185	1.904	0.213	4.187	0.750	0.745	6.482	5.017	1.005	0.47% (S_d)
Case 2	EP	2.035	0.238	0.180	1.854	0.207	4.259	0.757	0.769	6.319	4.891	0.988	3.50% (T_{qo}'')
	CEKF	2.049	0.240	0.188	1.879	0.209	4.280	0.759	0.754	6.673	4.883	0.976	2.66% (M)
Case 3	EP	2.127	0.234	0.191	1.811	0.213	3.858	0.684	0.777	6.324	4.675	0.941	8.73% (T_{do}'')
	CEKF	1.894	0.257	0.223	1.450	0.251	3.329	0.928	0.737	6.100	4.468	0.889	24.08% (X_q)
Case 4	EP	1.782	0.210	0.154	2.147	0.242	3.521	0.857	0.660	6.306	5.688	0.940	16.51% (X_d'')
	CEKF	4.100	0.082	0.033	3.743	0.182	6.389	1.401	0.201	14.569	6.969	0.405	124.15% (M)

where

$$e(p,t_k) = y(t_k) - C(p)x(t_k) + C_e(p)y_e(t_k)$$

$$E(e(t)) = \frac{1}{T}\sum_{t=1}^{T} e(t) \tag{1.14}$$

where $e(p,t_k)$ is the error function. $x(t_k)$ is value of state variable at time t_k, which is obtained from integral process by a numerical method; T is the number of components in vector $e(p,t_k)$.

Ref. [15] introduces an adaptive mutation scale (σ) in EP algorithm, which is different from a fixed adaptive mutation scale in some previous applications. The adaptive scaling factor guarantees that if the objective function increases, the scaling factor will be kept large for the extended search area to make sure that any better solution will not be ignored. On the other hand, if the objective function decreases, the scaling factor will reduce to make a smooth convergence.

The corrected extended Kalman Filter (CEKF) is used as the comparison method. Four case studies are conducted with different noise levels (Noises in Case 1 are zero and in Case 4 are the highest). The results solved by EP and CEKF are tabulated in Table 1.4. The results indicate that in no noise (Case 1) or in low noise (Case 2), the results of CEKF are the same or even better than those of EP. However, in high-noise (Cases 3 and 4), the performance of CEKF deteriorates while EP still gives the satisfactory results. This shows that EP is a robust search to obtain good parameter estimation from the data, which is full of noises.

1.4 Overview of Optimal Power Flow (OPF) problem

The OPF has had a long history in its development. It was first discussed by Carpenter in 1962 [16–18]. It was introduced as an extension of conventional economic dispatch to determine the optimal settings for control variables while respecting various constraints and took a long time to become a successful algorithm that could be applied in everyday use.

The OPF is a power system optimization problem designed to optimize a prescribed objective function F(**x**,**u**) while at the same time satisfying equality constraints g(**x**,**u**,**p**)=0 and inequality constraints h(**x**,**u**,**y**)≤0. g(**x**,**u**,**p**) represents bus power balance equations which are the functions of vector **x**, **u** and **p**. h(**x**,**u**,**y**) is the inequality constraints. **x** is the vector of state variables including all load bus voltage magnitudes, all bus voltage angles excluding slack bus. **u** is the vector of control variables corresponding to real power generations of all PV buses excluding slack bus, voltage magnitudes of PV buses and slack bus, tap settings of variable-tap transformer, phase shifter angles, switched capacitor settings. **p** is the vector of demand variables including real and reactive power loads. **y** is the vector of output variables including slack bus's real power generation, reactive power generation of all generators, and line and transformer loadings. Some objectives and related constraints commonly found in OPF problems are listed in Table 1.5.

Table 1.5 Objectives and related constraints commonly found in OPF problem [10, 17]

Objectives	Constraints
1. Active power objectives • Minimize generation cost • Minimize transmission loss • Maximize power transfer 2. Reactive power objectives • Minimize transmission loss 3. General objectives • Minimize deviation from a target schedule • Minimize control shifts to alleviate violations • Minimize load shedding • Optimize voltage profile 4. Environmental dispatch objectives • Minimize emissions	1. Limits on control variables • Generator output in MW • Transformer tap limits • Generator bus voltage limits • Shunt capacitor range 2. Operating limits on • Line and transformer flows (MVA, Amps, MW, MVAR) • MW and MVAR interchange • MW and MVAR reserve margins • Load bus voltage limits • Voltage angle difference limits 3. Security constraints limit • Limit on operations with simulated line outage

The objective function used in OPF normally is selected based on the operational condition of the power system. For example, during the normal operation, fuel cost minimization or gas emission minimization may be selected, whereas during the emergency condition such as line fault etc., load shedding minimization or voltage profile optimization may be considered. In addition, in some cases multiple objective functions (fuel cost minimization and gas emission minimization) can also be taken into consideration at the same time. In such a case, the scaling factor is needed to define in order to weight the importance of each objective function.

For OPF studies, the power system network is typically modeled at the main transmission level, including transmission units. The model may also include other auxiliary generating units and representation of internal or external parts of the system are used in deciding the optimum state of the system [10].

1.5 Literature Review of Optimization Techniques for OPF

Since the OPF is an optimization problem, the purpose of optimization is to determine the optimal setting of all control variables with respect to a predefined objective.

A wide variety of optimization techniques have been applied to solving OPF problems. Basically, it can be classified into the classical optimization approach and artificial-intelligence based approach. The former lacks in the ability of finding the global optimum whereas the latter consumes extensive computation time. Most of the optimization techniques, applied to OPF problem in the past, were in classical optimization approaches. However, due to advances of current computer technology, many artificial intelligence (AI) techniques have been proposed to solve the OPF problem. A review of literatures focused on these two kinds of optimization approaches is stated in the following:

1.5.1 OPF Problem with Classical Optimization Techniques

The OPF literature up to 1993 has been surveyed by J.A Momoh et al. [19, 20]. They classified classical optimization techniques applied to solve OPF problems into six categories as shown below:

1. Nonlinear programming (NLP),
2. Quadratic programming (QP),
3. Newton-based solution of optimality conditions,
4. Linear programming (LP),
5. Hybrid versions of linear programming and integer programming, and
6. Interior point methods.

For each category, they mentioned a theory in brief and displayed the statistics of its application to OPF problems as follows:

Non-Linear Programming (NLP)

Nonlinear programming (NLP) deals with problems involving nonlinear objective function and constraints. The constraints may consist of equality and/or inequality formulations. The inequality can be specified by being bounded both above and below.

Several methods such as sequential unconstrained minimization technique (SUMT), Lagrange multiplier based, and the modular in-core nonlinear optimization system (MINOS) augmented concept have been used to solve OPF problems. This class assumes nonlinear objectives and constraints. A survey of most commonly found applications revealed that about 8% of OPF formulations employed general purpose packages applied for both real-time on-line and off-line operational problems.

Quadratic Programming (QP)

Quadratic programming is a special form of nonlinear programming whose objective function is quadratic with linear or linearized constraints. Several QP methods in this category

(about 15%) have been used to solve OPF (loss, voltage economic dispatch) type of problems. Quasi-Newton and sensitivity-based methods have been employed for solving real on-line OPF problems.

Newton-Based Solutions

In this approach, the necessary conditions of optimality commonly referred to as the Kuhn-Tucker conditions are obtained. In general, these are nonlinear equations requiring iterative methods of solution. The Newton method is favored for its quadratic convergence properties.

Linear Programming (LP)

Linear programming treats problems with constraints and objective function formulated in linear forms with non-negative variables. The simplex method is known to be quite effective for solving LP problems.

Roughly 25% of the papers reviewed in [19, 20] solve the OPF problems using LP based techniques. The most commonly used technique is the revised simplex method. The objective functions (voltage, loss, economic dispatch and VAR) are linearized to enable an LP solution.

Mixed Integer Programming (MIP)

Mixed integer programming (MIP) is a particular type of linear programming whose constraint equations involve variables restricted to being integers. Integer programming and mixed integer programming, like nonlinear programming are extremely demanding of computer resources and the number of discrete variables is an important indicator of how difficult and MIP problem will be to solve.

Literature in this category employs a mixture of linear and mixed integer programming techniques to solve typical OPF problems such as VAR planning (power loss minimization). The mathematical optimization technique assumes linear objectives, and the constraints are a combination of linear and nonlinear with discrete or integer variables.

Interior Point Methods

The interior point method, recently re-discovered by Karmarkar, has stunned the operational research community since the scheme solves LP problem faster and is perhaps better than the conventional simplex algorithm. The extension of the interior point method to apply to NLP and QP problems has shown superior qualities and promising results. The interior point methods convert the inequality constraints to equalities by the introduction of nonnegative slack variables. A logarithmic barrier function of the slack variables is then added to the objective function, multiplied by the barrier parameter, which is gradually reduced to zero during the solution process.

1.5.2 OPF Problem with Artificial Intelligence Based Optimization Techniques

The OPF programs based on classical optimization approaches reviewed in the previous section are used daily to solve very large OPF problems. However, they are not guaranteed to converge to global optimum of the general non-convex OPF problem, although there are some empirical evidences on the uniqueness of the OPF solution within the domain of interest.

Moreover, the classical optimization techniques need some mathematical assumptions, such as convex and smooth objective functions, linear constraints, to solve the problem. Several disadvantages of the classical optimization techniques have been concluded by M. A. Abido [21] in the following paragraph.

Nonlinear programming based procedures have many drawbacks such as insecure convergence properties and algorithmic complexity. Quadratic programming based techniques have some disadvantages associated with the piecewise quadratic cost approximation. Newton-based techniques have a drawback of the convergence characteristics that are sensitive to the initial conditions and they may even fail to converge due to the inappropriate initial conditions. Sequential unconstrained minimization techniques are known to exhibit numerical difficulties when the penalty factors become extremely large. Although linear programming methods are fast and reliable, they have some disadvantages associated with the piecewise linear cost approximation. Interior point methods have been reported as computationally efficient; however, if the step size is not chosen properly, the sub-linear problem may have a solution that is infeasible in the original nonlinear domain [22]. In addition, interior point methods, in general, suffer from bad initial, termination, and optimality criteria and, in most cases, are unable to solve nonlinear and quadratic objective functions [18].

Since there are recent attempts to overcome the limitations of the classical optimization approaches, the application of artificial intelligence (AI) techniques to solve optimization problem has emerged. Some of AI techniques, such as Simulated Annealing (SA), Tabu Search (TS), Genetic Algorithm (GA), hybrid Tabu Search/Simulated Annealing (TS/SA), Evolutionary Programming (EP), Improved Evolutionary Programming (IEP), and Particle Swarm Optimization (PSO), have been introduced to solve the OPF problems. A brief review of each algorithm has been concluded as follows:

Simulated Annealing (SA)

A new technique to obtain near to optimum solutions of optimization problems entitled Simulated Annealing (SA) was proposed by Scott Kirkpatrick, C. Daniel Gelatt and Mario P. Vecchi in 1983. SA has been tested in several optimization problems showing a great ability for not been trapped in local minima. Due to its implementation simplicity and good results shown, its use has been growing since mid 80's. SA techniques were originally inspired by the formation of crystals in the solids during cooling. The method itself has a direct analogy with thermodynamics, specifically with the way that liquids freeze and crystallize.

SA is a method based on local search in which each movement is accepted if it improves the objective function. Other possible solutions are also accepted according to a probabilistic criterion. Such probabilistic nature is based on annealing process and they are obtained as a function of the system temperature.

The SA strategy starts with a "high" temperature giving a high probability to accept non-improving movement. The temperature and probabilistic levels diminish as long as the algorithm advances to the optimal solution. Therefore, SA has the ability to escape from local minima by accepting non-improving solutions during the first and medium stages of the algorithm [23]. The main drawback of SA procedure is that the annealing procedure is very CPU consuming although its convergence has been theoretically improved.

Tabu Search (TS)

TS is an AI-based method firstly proposed by Glover that guides the search for the optimal solution making use of flexible memory system, which exploits the history of the search. It consists of the systematic prohibition of some solutions to prevent cycling and to avoid the risk of trapping in local minima. New solutions are searched in the neighborhood of the current one. The neighborhood is defined as a set of the points reachable with a suitable sequence of local perturbations, starting from the current solution.

To prevent cycling movement, Tabu list of T length is introduced to prevent moving back to the previous solution just visited. In addition, some aspiration criteria, which allow overriding of Tabu status, can be introduced if that move is still found to lead to a better cost with respect to the cost of the current optimum.

One of the most important features of TS is that a new configuration may be accepted even if the value of the objective function is worse than that of the current solution prompted by using short-term and long-term process. In this way it is possible to avoid being trapped in local minima [24].

TS approach is proposed to solve OPF problem, which is examined on standard IEEE 30-bus test system with different objectives and generator cost curves. The results are promising and show the effectiveness and robustness of the proposed approach [25].

Genetic Algorithm (GA)

GA is computational procedures, which use ideas borrowed from evolution genetics in that they solve problems by maintaining populations that survive and evolve through chance and rule "survival of fittest".

In a simple genetic algorithm, individuals are simplified to a chromosome that codes for the variable of the problem. The strength of an individual is the objective function that must be optimized. A population of candidates evolves by genetic operators: mutation, crossover and selection. The characteristics of good candidates have more chance to be inherited, because good candidates live longer. Therefore, the average strength of the population rises through the generations. Finally, the population stabilizes, because no better individual can be found. At this stage, the algorithm has converged, and most of the individuals in the population are mostly identical, and represent sub-optimal to the problem [26, 27].

GA is applied to solve the OPF problem with a versatile FACTS device, i.e. Unified Power Flow Controller (UPFC), with the modified IEEE 14-bus test system. The results show that UPFC does not contribute much on cost reduction but it can help to reduce reactive power loss and increase the voltage stability margin [26].

Hybrid Tabu Search/Simulated Annealing (TS/SA)

A hybrid TS/SA approach is an integrated approach between TS and SA by using TS as a main algorithm. The trial generated neighborhood solution of SA is used for generating neighborhood solution for TS. In addition, the probabilistic acceptance criterion of SA is used instead of aspiration criteria of TS. Cooling schedule and Tabu list restriction are also used in this approach [28].

The hybrid TS/SA is proposed to minimize the generator fuel cost in OPF problem with FACTS devices when power flow controls are not needed. The IEEE 30-bus system is used to test the performance of the hybrid TS/SA algorithm. The results show that the cost saving is increased when more FACTS devices are added in the system. In addition, the hybrid TS/SA method contributes to better solutions and requires less CPU times than using TS or SA alone [29].

Evolutionary Programming (EP)

Similar to GA, the EP technique is a stochastic and iterative optimization method in the area of evolutionary computation, which uses the mechanics of evolution to produce optimal solutions to a given problem. However, EP works on real value coded strings rather than binary strings used by GA. It works by evolving a population of candidate solutions toward the global minimum through the use of mutation operator and selection scheme. During each iteration, a new population (offspring) is formed from an existing population (parent) through the use of a mutation operator. The mutation operator produces offspring by perturbing the parent with some probability distribution functions. The degree of optimality of each candidate solution (individual) is measured by its fitness, which can be defined as a value of the objective function of the problem being optimized [4]. By applying a competition scheme, the individuals in the population compete with each other. The winning individuals form a resultant population, which is transcribed to the next generation.

The EP is employed to minimize the generator fuel cost in OPF problem with FACTS devices. The IEEE 30-bus system is a test case to investigate the performance of EP algorithm with three different generation cost curves. The results show that EP approach can obtain the satisfactory results for all types of cost curves [6].

Also, EP is applied to handle power flow control in the OPF problem with FACTS devices on the modified IEEE 30-bus test system. The security constraints are considered in the OPF problem by setting the line flow limit of some critical transmission lines under the emergency case. The results show that the application of EP can effectively find out the global solution [13].

Improved Evolutionary programming (IEP)

To prevent premature convergence and to balance the exploration and exploitation abilities, an improved EP (IEP) was proposed by using multiple sub-populations to perform parallel search with random initialization in the divided solution space, and applying multiple mutation operators to enhance search template. Moreover, probabilistic update strategy based on annealing schedule like SA is utilized to avoid the dependence on fitness function and to avoid being trapped in local optimum. Moreover, re-assignment of individuals of every sub-population is designed to fuse information and enhance population diversity [30].

IEP is applied to solve the OPF problem with three different types of generator fuel cost curves. It is shown that total generator fuel cost solved by IEP is less expensive than those solved by EP, TS, and hybrid TS/SA [31].

Moreover, due to its characteristic, IEP can easily facilitate parallel implementation to reduce the computational time without sacrificing the quality of solution.

Particle Swarm Optimization (PSO)

PSO is an efficient and reliable evolutionary-based approach which combines social psychology principles in socio-cognition human agents and evolutionary computations. PSO has been motivated by the behavior of organisms such as fish schooling and bird flocking. Unlike the other heuristic techniques, PSO has a flexible and well-balanced mechanism to enhance and adapt to the global and local exploration abilities. It works by moving particles (changing positions) over a multi-dimensional search space using local and global information of P_{best} (the best position reached by a particular particle) and G_{best} (the best position reached by all particles) until the computational limitation is exceeded.

In [21], PSO is applied to solve the OPF problem with different objectives that include fuel cost minimization, voltage profile improvement, and voltage stability enhancement. The results confirm the potential of PSO and show its effectiveness and superiority over the classical gradient and GA techniques.

1.6 Objectives of This Research

The objectives of this research can be summarized as follows.

1. Study and formulate the OPF problems with transient and voltage stability considerations.
2. Propose and develop new versions of the EP-based methods to solve the problems.
3. Examine the sensitivity of parameters used in the proposed method on the obtained solutions and simulation time.
4. Compare the effectiveness of new EP-based methods with the conventional EP and in some cases if possible with other heuristic methods.
5. Compare the results between the different OPF problems.

1.7 Structure of Dissertation

This research proposes the EP-based methods to solve the OPF problem with the considerations of transient and voltage stability issues. Fig. 1.13 shows the structure of this research. This dissertation is organized in as follows. Four types of the OPF problems are formulated in Chapter 2. In Chapter 3, the procedure and main components of the EP-based methods are elaborated. Chapter 4 is of the topic on the proposed artificial neural network for transient stability assessment used in Transient Stability Constrained Optimal Power Flow (TSCOPF) problem. Chapter 5 reports all results of different types of OPF problems solved by the proposed EP-based methods. Finally the conclusion is drawn in Chapter 6.

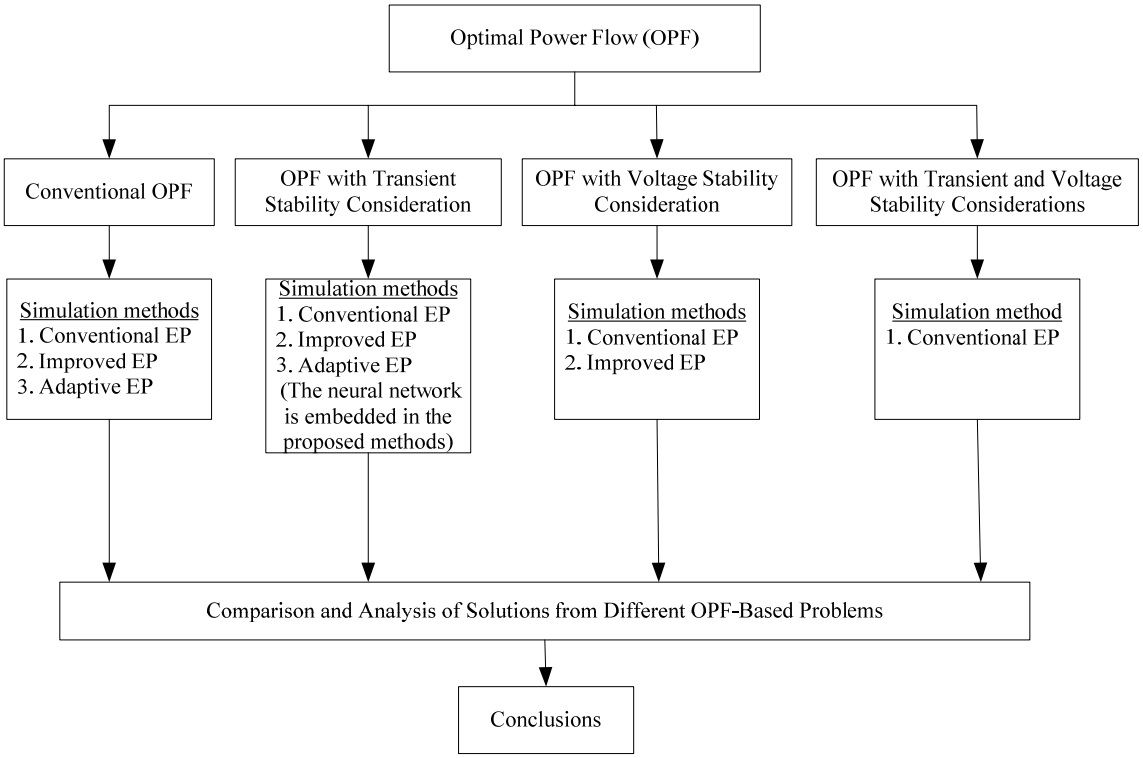

1. INTRODUCTION

---

2. OPTIMAL POWER FLOW (OPF) WITH TRANSIENT AND VOLTAGE STABILITY CONSIDERATIONS
3. EVOLUTIONARY PROGRAMMING (EP)-BASED METHODS

---

4. ARTIFICIAL NEURAL NETWORK (ANN) FOR TRANSIENT STABILITY ASSESSMENT
5. NUMERICAL RESULTS AND DISCUSSION

---

6. CONCLUSIONS

REFERENCES
LIST OF PUBLICATIONS

Fig. 1.13 Structure of this dissertation

References

[1] Z. Michalewicz and M. Michalewicz: "Evolutionary Computation Techniques and Their Applications", in *Proc. 1997 IEEE Int. Conf. on Intelligence Processing Systems*, Oct. 1997.

[2] J. Xu, J. Zhang, and X. Song: "Evolutionary Programming: The-state-of-the-art", in *Proc. the 6th World Congress on Intelligence Control and Automation*, Jun. 2006.

[3] W. Gao: "Comparison Study of Genetic Algorithm and Evolutionary Programming", in *Proc. 3rd Conf. on Machine Learning and Cybernetics*, August 2004.

[4] L. L. Lai: "Intelligent System Applications in Power Engineering: Evolutionary Programming and Neural Networks", New York, John Wiley & Sons, 1998.

[5] N. Sinha, R. Chakrabarti, and P. K. Chattapadhyay: "Evolutionary Programming Techniques for Economic Load Dispatch", *IEEE Trans. on Evolutionary Computation*, Vol. 7, No. 1, pp. 83–94, Feb. 2003.

[6] J. Yuryerich and K. P. Wong: "Evolutionary Programming Based on Optimal Flow Flow", *IEEE Trans. on Power Systems*, Vol. 14, No. 4, Nov. 1999.

[7] Q. H. Wu and J. T. Ma: "Power System Optimal Reactive Power Dispatch Using Evolutionary Programming", *IEEE Trans. on Power Systems*, Vol. 10, No. 3, pp. 1243–1249, Aug. 1995.

[8] V. Gopalakrishmnan, P. Thirunavukkarasu, and R. Prasanna: "Reactive Power Planning Using Hybrid Evolutionary Programming Method", in *Proc. IEEE PES Power Systems Conf. and Expo.*, Oct. 2004.

[9] C. Jiang and C. Wang: "Improved Evolutionary Programming with Dynamic Mutation and Metropolis Criteria for Multi-Objective Reactive Power Optimization", in Proc. *IEE Gener. Transm. Distrib.*, Vol. 152, No. 2, Mar. 2005.

[10] J. A. Momoh: Electric Power System Applications of Optimization, Marcel Dekker, New York, 2001.

[11] K. A. Juste, H. kita, E. Tanaka, and J. Hasegawa: "An Evolutionary Programming Solution to the unit Commitment Problem", *IEEE Trans. on Power Systems*, Vol. 14, No. 4, Nov. 1999.

[12] J. L. Ceciliano and R. Nieva: "Transmission Network Planning Using Evolutionary Programming", in *Proc. the 1999 Congress on Evolutionary Programming*, Jul, 1999.

[13] L. L. Lai and J. T. Ma: "Power Flow Control in FACTS using Evolutionary Programming", in *Proc. IEEE Porto Power Tech Conference*, 1995.

[14] B. A. de Souza, J. M. C. de Albuquerque: "Optimal Placement of Distributed Generators Networks Using Evolutionary Programming", in *Proc. Transm. & Distr. Conf. and Expo.*, Aug, 2006.

[15] L. L. Lai and J. T. Ma: "Application of Evolutionary Programming to Transient and Subtransient Parameter Estimation", *IEEE Trans. on Power Systems*, Vol. 11, No. 3, pp. 523–530, Sep. 1996.

[16] A. J. Wood, B. F. Woollenberg: Power Generation, Operation, and Control, John Wiley & Sons, New York, 1996.

[17] J. C. Das: Power System Analysis: Short-Circuit Load Flow and Harmonics, Marcel Decker, New York, 2002.

[18] J. A. Momoh and J. Z. Zhu: "Improved Interior Point Method for OPF Problems", *IEEE Transactions on Power Systems*, Vol. 14, No. 3, pp. 1114–1120, 1999.

[19] J. A. Momoh, M. E. El-Hawary, and R. Adapa: "A Review of Selected Optimal Power Flow Literature to 1993 Part I: Nonlinear and Quadratic Programming Approaches", *IEEE Trans. Power Syst.*, Vol.14, No.1, pp.96–104, 1999.

[20] J. A. Momoh, M. E. El-Hawary, and R. Adapa: "A Review of Selected Optimal Power Flow Literature to 1993 Part II: Newton, Linear Programming and Interior Point Methods", *IEEE Trans. Power Syst.*, Vol. 14, No.1, pp. 105–111, 1999.

[21] M. A. Abido: "Optimal Power Flow Using Particle Swarm Optimization", *International Journal of Electrical Power and Energy Systems*, Vol. 24, pp. 563–571, 2002.

[22] X. Yan, and V. H. Quintana: "Improving an Interior Point Based OPF by Dynamic Adjustments of Step Sizes and Tolerances", *IEEE Transactions on Power Systems*, Vol. 14, No. 2, pp. 709–717, 1999.

[23] C. A. Roa-Sepulveda and B. J. Pavez-Lazo: "A Solution to the Optimal Power Flow Using Simulated Annealing", *International Journal of Electrical Power and Energy Systems*, Vol. 25, pp. 47–57, 2002.

[24] Fanni, A. Manunza, M. Marchesi, and F. Pilo: "Tabu Search Metaheuristics for Global Optimization of Electromagnetic Problems", *IEEE Transactions on Magnetics*, Vol. 34, No. 5, pp. 2960–2963, 1998.

[25] M. A. Abido: "Optimal Power Flow Using Tabu Search Algorithm", *Electric Power System Components and Systems*, Vo. 30, pp. 469–483, 2002.

[26] H. C. Leung and T. S. Chung: "Optimal Power Flow with a Versatile FACTS Controller by Genetic Algorithm Approach", *IEEE Power Engineering Society Meeting*, Vol. 4, pp. 2806–2811, 2000.

[27] G. Bakirtzis, P. N. Biskas, C. E. Zoumas, and V. Petridis: "Optimal Power Flow by Enhanced Genetic Algorithm", *IEEE Transactions on Power Systems*, Vol. 17, No. 2, pp. 229–236, 2002.

[28] W. Ongsakul and P. Bhasaputra: "Optimal Power Flow with FACTS Devices by Hybrid TS/SA Approach", *International Journal of Electrical Power and Energy Systems*, Vol. 24, pp. 851-857, 2002.

[29] W. Ongsakul and P. Bhasaputra: "Optimal Power Flow with Multi-type of FACTS Devices by Hybrid TS/SA Approach", in *Proc*. *IEEE ICIT*, 2002.

[30] L. Wang, D. Z. Zheng, and F. Tang: "An Improved Evolutionary Programming for Optimization", in *Proc. the 4th World Congress on Intelligent Control and Automation*, pp. 1769–1773, 2002.

[31] W. Ongsakul and T. Tantimaporn: "Optimal Power Flow by Improved Evolutionary Programming", *Electric Power Components and Systems*, Vol. 34, No. 1, pp. 79–95, 2006.

CHAPTER 2

OPTIMAL POWER FLOW (OPF) PROBLEM WITH TRANSIENT AND VOLTAGE STABILITY CONSIDERATIONS

2.1 Introduction

This chapter will mainly describes the statements and formulations of four different OPF problems, namely conventional OPF, transient stability constrained OPF (TSCOPF), OPF with steady-state voltage stability consideration, and OPF with both transient and voltage stability considerations. The corresponding objectives and constraints in each problem are clearly illustrated. Furthermore, the strategies to cope with the related constraints both equality and inequality ones are explained here.

To analyze the OPF problem with fuel cost minimization, the input-output characteristic of a thermal generating unit is an important issue to be first mentioned. The higher the accuracy of the characteristic representation is the more realistic the solution of OPF problem will be. In this dissertation, three different input-output characteristics are considered in the simulation.

Characteristic Representation of Thermal Generating Unit

In analyzing the problems associated with the controlled operation of power systems, there are many possible parameters of interest. Fundamental to the economic operating problem, is the set of input-output characteristics of a thermal power generating unit [1]. Typically, the data used to create the input-output characteristic are obtained from design calculations or from heat rate tests. The input of the unit can be used in terms of heat rate (MBtu/hr) or converted into total generation cost per hour ($/hr) whereas the output is normally the net electrical output of the generating unit in MW.

To simplify the characteristic representation of a generating unit, the input-output characteristic can be modeled as a smooth and convex curve shown in Fig. 2.1. The characteristic shown is idealized in that it is presented as the smooth, convex curve. The minimum output of unit is caused by fuel combustion stability and inherent steam generator design constraints.

However, for large steam turbine generators, the input-output characteristics shown in Fig. 2.1 are not always as smooth as indicated. Large steam turbine generators will have a number of steam admission valves that are opened in sequence to obtain ever-increasing output of the thermal generating unit. When a valve is first opened, the throttling losses increase rapidly and then, reduce gradually until the opening of next valve. The valve-point loading effect exhibits a greater variation in the input-output curve as shown in Fig. 2.2. Points A, B, and C are the operating points when valves are opened.

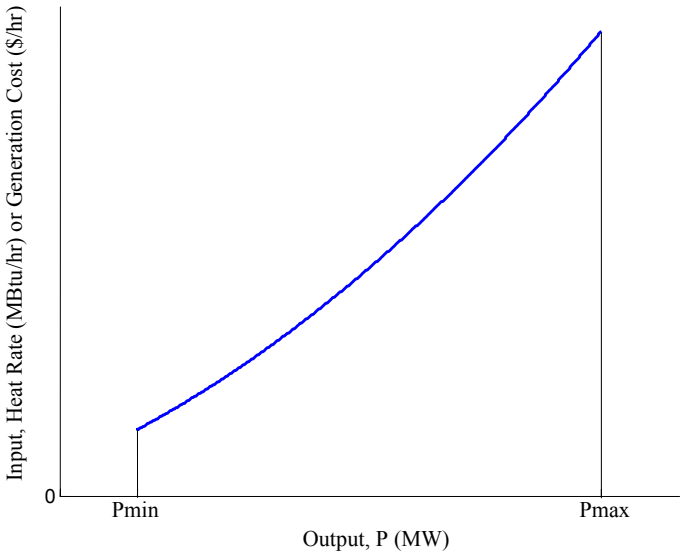

Fig. 2.1 Input-output curve of a thermal generating unit

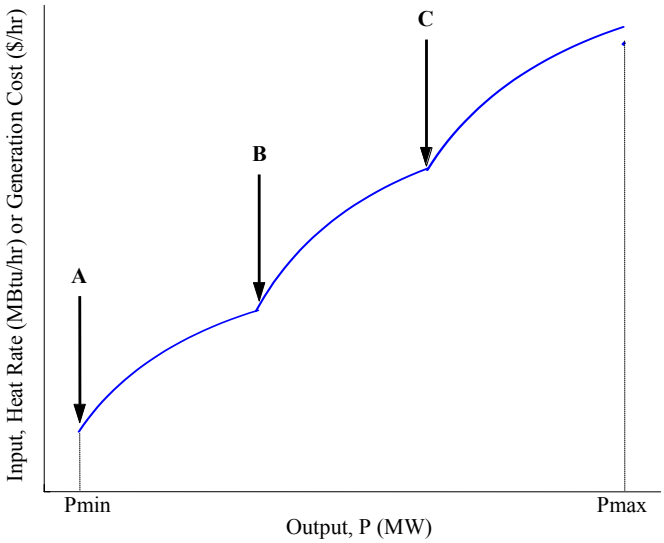

Fig. 2.2 Input-output curve of a thermal generating unit with three valve points

Besides, a power system operation usually uses a combined-cycle unit as a peak load serving unit. It consists of a series of single-cycle gas turbines in conjunction with some heat-recovery steam generators (HRSGs) [2]. Fig. 2.3 shows the input-output characteristic of a combined cycle plant with two gas turbines.

In conclusion, Fig. 2.1 represents the rough approximation of input ($/hr)-output (MW) characteristic of a thermal generating unit, Fig. 2.2 gives the more accurate representation of input-output characteristic of a generating unit when three valve-point loading effects are taken

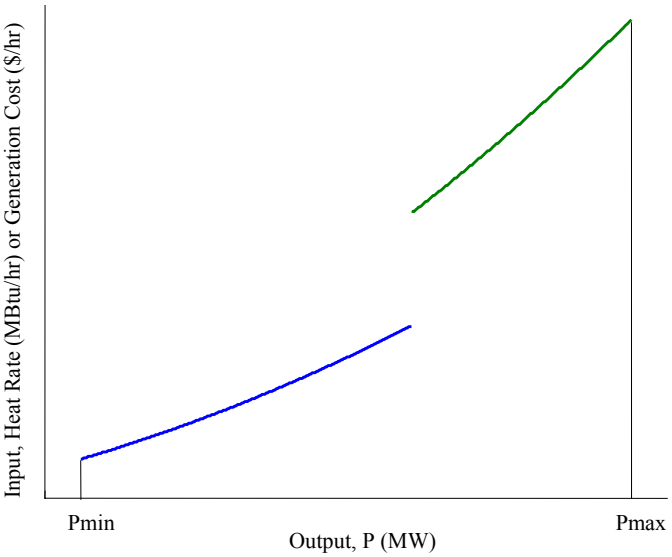

Fig. 2.3 Input-output curve of a combined-cycle unit with two gas turbines

into consideration, and Fig. 2.3 represents the approximation of input-output characteristic of a combined 2-thermal generating unit. Based on this assumption, these three types of input-output characteristic of the thermal unit can be represented by the quadratic, quadratic with sine component, and piecewise quadratic curves respectively. These three cost curves will be used in the OPF simulation in order to investigate the effectiveness of the proposed algorithms.

Please note that most of the classical optimization problems can handle the OPF problem only when the cost curve of a thermal generating unit is represented by the quadratic function (Fig. 2.1), which is simple but not so accurate. Linear Programming (LP) is even worse. It cannot deal with this simple quadratic function. The linearization process is required to convert from the quadratic function to piecewise linear function. Undoubtedly, this approximation will degrade the accuracy of the OPF solution when in the future the cost curve of the generating unit will become more and more complicated. On the other hand, the proposed EP-based methods do not have such limitation. They can solve the OPF problem with any type of generator cost curve even though the cost curve is non-smooth or non-convex.

2.2 Conventional OPF Problem

The OPF is an optimization problem that optimizes a selected objective while satisfying network equality and inequality constraints. The general OPF problem can be expressed as:

$$\text{Min or Max} \quad F(\mathbf{x},\mathbf{u}) \tag{2.1}$$

$$\text{Subject to} \quad g(\mathbf{x},\mathbf{u},\mathbf{p})=0, \tag{2.2}$$

$$h(\mathbf{x},\mathbf{u},\mathbf{y})\leq 0, \tag{2.3}$$

where

$F(\mathbf{x},\mathbf{u})$ is the objective function to be optimized.

$g(\mathbf{x},\mathbf{u},\mathbf{p})$ is the equality constraint representing bus power balance equations.

$h(\mathbf{x},\mathbf{u},\mathbf{y})$ is the system operating constraint.

$\mathbf{x}$ is the vector of state variables including load bus voltage magnitudes and all bus voltage angles excluding the angle at the slack bus.

$\mathbf{u}$ is the vector of control variables including real power generation outputs except at the slack bus, voltage magnitudes of all PV buses including the slack bus, and transformer tap settings.

$\mathbf{p}$ is the vector of the demand variables including the real power demand and reactive power demand of all buses.

$\mathbf{y}$ is the vector of the output variables including real power generation at the slack bus, reactive power generation of all generators, and power flows in transmission lines and transformer loadings.

2.2.1 Objective Function

In the OPF problem formulation, a wide variety of objectives can be selected. In this dissertation, the selected objective of the OPF problem is to minimize the total generator fuel cost. This objective is primarily used in the operation and planning of a power system. It can be expressed mathematically as:

$$F = \sum_{i=1}^{NG} F_i(P_{Gi}) \tag{2.4}$$

where

F is the total generation cost.

$F_i(P_{Gi})$ is the i-th generating unit's generation cost which is a function of real power generation output.

P_{Gi} is the real power generation output (in MW) of the i-th generator,

NG is the number of generating units.

Note that due to the flexibility of the EP-based methods, the fuel cost curve in Eq. (2.4) is not limited to be only a quadratic or linear function.

2.2.2 Equality Constraints

The equality constraints in the OPF problem are network power balance equations at each node. The real and reactive power balance equations in polar form can be expressed as follows:

$$P_i - \sum_{j=1}^{N} V_i V_j Y_{ij} \cos(\theta_{ij} - \delta_i + \delta_j) = 0 \qquad i=1, 2, \ldots, N \tag{2.5}$$

$$Q_i + \sum_{j=1}^{N} V_i V_j Y_{ij} \sin(\theta_{ij} - \delta_i + \delta_j) = 0 \qquad i=1, 2, \ldots, N \tag{2.6}$$

where

P_i is the real power injection at bus i.
Q_i is the reactive power injection at bus i.
V_i, V_j are the voltage magnitude of bus i and j.
Y_{ij} is the magnitude of the ij-th element of bus admittance matrix.
θ_{ij} is the angle of the ij-th element of bus admittance matrix.
δ_i, δ_j are the voltage angle of bus i and j.
N is the number of buses.

The power injection at each bus can be obtained by subtracting total power generation with total load. The equations for computing real and reactive power injection are expressed as:

$$P_i = P_{Gi} - P_{Di} \tag{2.7}$$

$$Q_i = Q_{Gi} - Q_{Di} \tag{2.8}$$

where

P_{Gi} is the total real power generation at bus i.
P_{Di} is the total real power load at bus i.
Q_{Gi} is the total reactive power generation at bus i.
Q_{Di} is the total reactive power load at bus i.

2.2.3 Inequality Constraints

The operation of power system network is constrained by limits of equipment loading and operating requirements. These operating limits and requirements cause inequality constraints imposed on the OPF problem, such as generation constraints, transformer constraints, security constraints, etc. The inequality constraints imposed on the OPF are listed as follows:

$$P_{Gi}^{\min} \le P_{Gi} \le P_{Gi}^{\max} \qquad i = 1, 2, \ldots, NG \tag{2.9}$$

$$V_i^{\min} \le V_i \le V_i^{\max} \qquad i = 1, 2, \ldots, N \tag{2.10}$$

$$t_i^{\min} \le t_i \le t_i^{\max} \qquad i = 1, 2, \ldots, NT \tag{2.11}$$

$$Q_{Gi}^{\min} \le Q_{Gi} \le Q_{Gi}^{\max} \qquad i = 1, 2, \ldots, NG \tag{2.12}$$

$$\left|S_{Li}\right| \le S_{Li}^{\max} \qquad i = 1, 2, \ldots, NL \tag{2.13}$$

where,

P_{Gi} is the real power generation at bus *i.*

$P_{Gi}^{\min}, P_{Gi}^{\max}$ are the lower and upper limits of real power generation at bus *i*.

V_i is the generator voltage magnitude at bus *i*.

$V_i^{\min}, V_i^{\max}$ are the lower and upper limits of voltage magnitude at bus *i*.

t_i is the transformer tap setting of the *i*-th transformer.

$t_i^{\min}, t_i^{\max}$ are the lower and upper limits of the tap setting of the *i*-th transformer.

Q_{Gi} is the reactive power generation at bus *i.*

$Q_{Gi}^{\min}, Q_{Gi}^{\max}$ are the lower and upper limits of reactive power generation at bus *i*.

$|S_{Li}|$ is the *i*-th line or transformer loading.

$S_{Li}^{\max}$ is the *i*-th line or transformer loading limit.

NT is the number of transformers.

NL is the number of branches.

2.2.4 OPF Problem Formulation

In conclusion, the conventional OPF problem has now been formulated as follows:

$$\begin{array}{ll} \text{Min} & \text{Eq. (2.4)} \\ \text{Subject to} & \text{Eqs. (2.7) – (2.13)} \end{array} \tag{2.14}$$

2.3 Transient Stability Constrained OPF (TSCOPF) Problem

The solution obtained from the conventional OPF, which considers only the static constraints, does not guarantee transient stability in the system when subject to possible contingencies such as line fault. Besides, a large amount of financial loss normally incurred by loss of synchronism in power system has been reported in many countries. As a result, a novel OPF is proposed by adding the transient stability constraints into the conventional OPF problem. It is so called transient stability constrained optimal power flow (TSCOPF) [3].

The transient stability constraints consist of additional equality constraints i.e. a set of differential-algebraic equations (DAEs) that describes the dynamic behavior of rotor angle after undergoing severe disturbances and the additional inequality constraints i.e. stability criteria for indicating whether or not the system is stable after the contingency. The criterion widely used is maximum allowable deviation of rotor angle with respect to Center of Inertia (COI). To handle the transient stability equality constraints, in [3, 4] a set of DAEs is first converted into numerically equivalent algebraic equations using some numerical methods such as modified Euler's method, and then step-by-step simulation (Time domain simulation) is performed to observe the rotor angle deviation.

Some literatures try to tackle this problem. In [3] multi-contingency transient stability constraints are considered in TSCOPF and both binding and non-binding contingencies are elaborated. In [5], the transcription technique is proposed to handle transient stability constraints by converting TSCOPF that is a semi-infinite optimization problem into a finite optimization problem in Euclidean space.

Inherently, TSCOPF problem is a non-linear, non-smooth, and multimodal optimization problem i.e. there exist more than one local optimum. Formerly, in order to obtain a solution of TSCOPF, conventional methods such as, primal-dual interior-point method [3] and linear programming (LP) [4] are applied. However, these methods have many drawbacks as mentioned earlier in Chapter 1. As a result, the TSCOPF problem is still a challenging problem and a powerful tool is needed for solving it.

2.3.1 Transient Stability Constraints

Transient stability [6] is the ability of a power system to maintain synchronism when subject to a severe transient disturbance such as a fault on the transmission network and loss of generator and load etc. After the disturbance, if the generator rotor angle separation between the machines in the system remains within the certain bounds (limits), it can be said that the system maintains synchronism.

The transient stability constraints consist of equality constraint i.e. swing equations and inequality constraint i.e. transient stability limits. In this study, the classical model of synchronous generator is used. This model basically represents a synchronous machine by a constant voltage source behind a transient reactance and the mechanical power input remains constant during the transient period.

The transient stability analysis of the i-th synchronous generator can be done by solving a set of DAEs (swing equation) that describes the motion of rotor angle as follows:

$$\begin{aligned} \dot{\delta}_i &= \omega_i - \omega_R \\ 2H_i\dot{\omega}_i &= \omega_R(P_{mi} - P_{ei} - D_i\omega_i) \end{aligned} \qquad i = 1,2,...,NG \tag{2.15}$$

where $$P_{ei} = E_i^2 G'_{ii} + \sum_{\substack{j=1 \\ j\neq i}}^{NG}\left[E_i E_j B'_{ij}\sin(\delta_i - \delta_j) + E_i E_j G'_{ij}\cos(\delta_i - \delta_j)\right]$$

ω_R, ω_i are rated rotor speed and rotor speed of the i-th generator.
P_{mi} is the mechanical input of the i-th generator.
P_{ei} is the electrical output of the i-th generator.
E_i, E_j are constant voltages behind a transient reactance of the i- and j-th generators.
D_i is the damping coefficient of the i-th generator.
G'_{ij}, B'_{ij} are the real and imaginary parts of the ij-th element of reduced Y_{bus}.
δ_i, δ_j are the rotor angles of the i- and j-th generators.
H_i is inertia constant of the i-th generator.

The reduced Y_{bus} can be obtained by eliminating all buses except for generator buses. All steps for building the reduced Y_{bus} can be found in [7]. The value of D_i in this paper is assumed to be zero (no damping).

To include DAEs into TSCOPF problem, the DAEs in Eq. (2.15) are converted into numerically equivalent algebraic equations by using implicit trapezoidal rule as follows:

$$\begin{aligned} \delta_i^{t+\Delta t} &= \delta_i^t + \frac{\Delta t}{2}\left[\omega_i^{t+\Delta t} + \omega_i^t\right] \qquad t = t_0, t_0 + \Delta t, ..., T \\ \omega_i^{t+\Delta t} &= \omega_i^t + \frac{\Delta t}{2}\left[\frac{\omega_R}{2H_i}\left(P_{mi} - P_{ei}^{t+\Delta t}\right) + \frac{\omega_R}{2H_i}\left(P_{mi} - P_{ei}^t\right)\right] \end{aligned} \tag{2.16}$$

where $$P_{ei}^t = E_i^2 G''^t_{ii} + \sum_{\substack{j=1 \\ j\neq i}}^{NG}\left[E_i E_j B''^t_{ij}\sin(\delta_i^t - \delta_j^t) + E_i E_j G''^t_{ij}\cos(\delta_i^t - \delta_j^t)\right]$$

δ_i^t, ω_i^t are rotor angle and rotor speed of the i-th generator at time t.
G''^t_{ij}, B''^t_{ij} are real and imaginary parts of the ij-th element of the reduced Y_{bus} at time t.
Δt is integration step width.
T is the maximum integration period.
$\delta_i^{t_0}$, $\omega_i^{t_0}$ are rotor angle and rotor speed immediately before the fault occurs.

The constant mechanical output P_{mi} that equals $P_{ei}^{t_0}$, and E_i can be obtained from load flow solution. In Eq. (2.16), which forms equality constraints, the generator rotor angle of time t+Δt

can be calculated by using information at time $t+\Delta t$ and time t. To solve this implicit function, numerical techniques can be applied.

To determine whether the system is stable or not, the maximum allowable deviation of rotor angle with respect to COI is adopted. The position of COI at time t can be expressed as follows:

$$\delta_{COI}^{t} = \frac{\sum_{i=1}^{NG} H_i \delta_i^t}{\sum_{i=1}^{NG} H_i} \tag{2.17}$$

The transient stability limit, which is inequality constraints, can be formulated as below:

$$\left|\delta_i^t - \delta_{COI}^t\right| \le \delta_{MAX} \qquad t = t_0, t_0 + \Delta t, ..., T \tag{2.18}$$

where δ_{MAX} is the maximum allowable deviation of rotor angle with respect to COI. This stability limit is acceptable for utility engineers and is widely used [4]. In practical, the out-of-step relay can be set to a specific value in order to trip if the any generator rotor angle goes beyond the threshold when the fault occurs.

2.3.2 TSCOPF Problem Formulation

Finally, the TSCOPF problem has now been formulated as follows:

Min	Eq. (2.4)	
Subject to	Eqs. (2.7) – (2.13)	
	Eqs. (2.16) and (2.18)	(2.19)

Similarly, multi-contingency transient stability constrained OPF (MC-TSCOPF) problem, which can guarantee the transient stability after multiple possible contingencies, can be formulated by adding transient stability limits of each considered contingency as the additional constraints into the formulation shown in Eq. (2.19).

2.4 OPF with Steady-State Voltage Stability Consideration

In addition to transient stability mentioned in the previous session, voltage stability issue also play a crucial rule on the major blackouts around the world during the last decades. The voltage stability problems are reported in several countries, i.e. France, Belgium, Sweden Germany, Japan, USA [8, 9]. Consequently, the consideration of voltage stability in power system operation is essential and should be added into the conventional OPF in order to guarantee a sufficient stability margin for both normal and emergency operations.

Voltage stability is associated with the ability of a power system to maintain acceptable voltages at all nodes in the system under normal condition and after being subject to a disturbance [6] such as load increase and transmission-line outage etc. Generally, voltage stability can be categorized into steady-state and dynamic analysis. Although the dynamic analysis is needed for deep understanding of this phenomenon, the steady-state provides a faster estimation how far the current system status is from the voltage collapse point. As a result, voltage stability indices are very important for voltage stability study. Among various voltage stability indices summarized in [10], the indicator L originally developed in [11] is selected for voltage stability estimation. The indicator L is widely used in many researches for steady-state voltage stability study. For example, in [12] the indicator L is employed for voltage stability consideration in composite power system reliability evaluation, in [13] the indicator L is used as a main criterion in OPF problem for load curtailment minimization. Moreover, in [14] the indicator L is treated as an additional constraint in the OPF problem.

2.4.1 Indicator L

The indicator L is a quantitative measure for estimating the voltage stability margin of the current operating point. It is derived from the solution of the power flow equations based on the fact that at the voltage collapse point, the Jacobian matrix of load flow becomes singular. The value of indicator L less than 1 can guarantee the voltage stability. To calculate the indicator, firstly the hybrid representation derived from the original admittance matrix (Y_{bus}) is formulated as follows:

$$\begin{bmatrix} V_L \\ I_G \end{bmatrix} = \begin{bmatrix} Z_{LL} & F_{LG} \\ K_{GL} & Y_{GG} \end{bmatrix} \begin{bmatrix} I_L \\ V_G \end{bmatrix} \tag{2.20}$$

where

V_L, I_L	are the voltage and current vectors at the load buses.
V_G, I_G	are the voltage and current vectors at generator buses including slack bus.
Z_{LL}, F_{LG}, K_{GL}, Y_{GG}	are the sub-matrices of the hybrid matrix.

The hybrid representation is obtained by a partial inversion, where the voltages at the load buses are exchanged against their currents. Through the utilization of this representation, the indicator L at load bus j can then be calculated as follows:

$$L_j = \left| 1 + \frac{\overline{V}_{0j}}{\overline{V}_j} \right| = \left| \frac{S_j + S_{jcorr}}{Y^*_{jj+} \cdot V_j^2} \right| \tag{2.21}$$

and

$$\overline{V}_{0j} = -\sum_{i=1}^{NG} F_{ji} \cdot \overline{V}_i \,,$$

$$S_{jcorr} = \left(\sum_{\substack{i=1 \\ i \neq j}}^{NLB} \frac{Z^*_{ji}}{Z^*_{jj}} \cdot \frac{S_i}{\overline{V}_i} \right) \cdot \overline{V}_j$$

$$Y_{jj+} = \frac{1}{Z_{jj}} \tag{2.22}$$

where

F_{ji}	is the ji-th element of sub-matrix F_{LG}.
Z_{jj}	is the jj-th element of sub-matrix Z_{LL}.
Z^*_{jj}, Z^*_{ji}	are the conjugate of jj-th and ji-th elements of sub-matrix Z_{LL}.
S_i	is the complex power demands at load bus i.
V_j	is the voltage magnitude at bus j.
$\overline{V}_i$, $\overline{V}_j$	are voltages at generator bus i and load bus j respectively.

From Eq. (2.21), the indicator L at load bus j is a function of the term V_{0j} or S_{jcorr} which is influenced by all generator voltages or all active and reactive load demands. The V_{0j} physically indicates the equivalent voltage of all generator buses and S_{jcorr} represents equivalent complex power of all other load buses except bus j. The value of indicator L is in between 0 (no load) and 1 (voltage collapse). The relationship between the value of indicator L and voltage level at a specific load bus when the loading factor is increased is depicted in Fig. 2.4. It can be seen that when the operating point is moving to the voltage collapse point, the value of indicator L increases rapidly approaching to the value of 1.

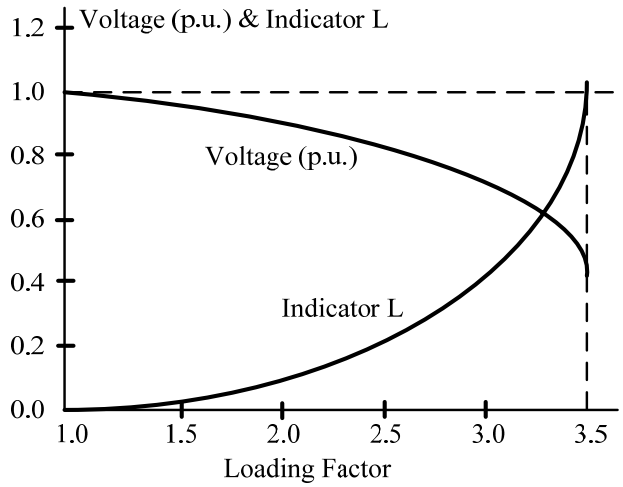

Fig. 2.4 The relationship between the value of indicator L and voltage level

The advantages of indicator L are listed below:

- It has a simple structure and can be handled easily.
- There is no need of repetitive power flow solution (Fast Calculation).
- The weakest bus (Max (L_j)) can be identified.
- The accuracy in predicting is satisfactory.

By considering the indicator L as a voltage stability degree, a new objective function of the OPF problem with voltage stability consideration is formulated. The objective function is the sum of the fuel cost of all generating units and the maximum value of indicator L among all load buses (indicator L at the weakest bus). The problem can be seen as a trade-off between the generator fuel cost minimization and the voltage stability margin maximization.

$$F = \sum_{i=1}^{NG} F_i(P_{Gi}) + \alpha\left(Max(L_j)\right) \tag{2.23}$$

where

F is the objective function of OPF with voltage stability consideration.
α is the scaling factor.
L_j is the value of indicator L at load bus j.
NLB is the number of load buses.

2.4.2 Formulation of OPF with Steady-State Voltage Stability Consideration

Finally, the problem has now been formulated as follows:

$$\begin{array}{ll} \text{Min} & \text{Eq. (2.23)} \\ \text{Subject to} & \text{Eqs. (2.7) – (2.13)} \end{array} \tag{2.24}$$

Please note that the scaling factor expressed in Eq. (2.23) is inserted to give the importance of voltage stability issue with respect to the fuel cost term. The higher the value of scaling factor is, the more the voltage stability issue is concerned. The selection of the value of scaling factor normally is based on the engineer experience and system status. The setting of this scaling factor in this dissertation will be presented and discussed later on.

2.5 OPF with Transient and Voltage Stability Considerations

According to the previous sessions 2.3 and 2.4, the transient and voltage stabilities both are the important issues in power system operation, about which the system operator should concern. Therefore, the OPF problem considering these two vital transient and voltage stability issues is formulated in this session. The transient stability issue introduces the additional constraints, i.e. swing equation and transient stability limit into the conventional OPF problem whereas the voltage stability issue is regarded by inserting a voltage stability index (the indicator L) into the OPF objective function.

2.5.1 Formulation of OPF with Transient and Voltage Stability Considerations

Finally, the problem has now been formulated as follows:

$$\begin{array}{ll} \text{Min} & \text{Eq. (2.23)} \\ \text{Subject to} & \text{Eqs. (2.7) – (2.13)} \\ & \text{Eqs. (2.16) and (2.18)} \end{array} \qquad (2.25)$$

2.6 Constraint Handling Strategies

Since the proposed EP methodology is stochastic search algorithm, it does not take the equality and inequality constraints into account. Therefore, the following section will be used to force both equality and inequality constraints in the OPF problems.

For the equality constraints, power balance equations shown in Eqs. (2.7) and (2.8) are satisfied by power flow calculation (AC load flow) using Newton-Raphson method, and swing equations in Eq. (2.16) are met by time domain simulation.

The inequality constraints expreesed in Eqs. (2.9)−(2.13) and (2.18) will be coped by a penalty function. The penalty function for any variable violating its limits can be expressed mathematically as follows:

$$h(x_i) = \begin{cases} (x_i - x_{i,\max})^2 & if \quad x_i > x_{i,\max} \\ (x_{i,\min} - x_i)^2 & if \quad x_i < x_{i,\min} \\ 0 & if \quad x_{i,\min} \le x_i \le x_{i,\max} \end{cases} \qquad (2.26)$$

where

$h(x_i)$ is the penalty function of variable x_i

$x_{i,\max}$, $x_{i,\min}$ are the upper and lower limits of the variable x_i

x_i is the variable shown in Eqs. (2.9)−(2.13) and (2.18).

By doing so, the objective functions of OPF, TSCOPF, OPF considering steady-state voltage stability and OPF considering both transient and voltage stability problems are now

transformed to unconstrained ones by penalizing all conressponding inequality constraints. The extended objective functions for each OPF-based problem are formed as shown in Eqs. (2.27), (2.28), (2.29), and (2.30) respectively.

$$F_{ext} = \sum_{i=1}^{NG} F_i(P_{Gi}) + K_p\left[h(P_{slack})\right] + K_q \sum_{i=1}^{NG} h(Q_{Gi}) + K_v \sum_{i=1}^{NLB} h(V_{Li}) + K_s \sum_{i=1}^{NL} h(S_{Li}) \tag{2.27}$$

$$F_{ext} = \sum_{i=1}^{NG} F_i(P_{Gi}) + K_p\left[h(P_{slack})\right] + K_q \sum_{i=1}^{NG} h(Q_{Gi}) + K_v \sum_{i=1}^{NLB} h(V_{Li}) + K_s \sum_{i=1}^{NL} h(S_{Li}) + \sum_{i=1}^{NK} K_R \tag{2.28}$$

$$F_{ext} = \sum_{i=1}^{NG} F_i(P_{Gi}) + \alpha \cdot Max(L_j) + K_p\left[h(P_{slack})\right] + K_q \sum_{i=1}^{NG} h(Q_{Gi}) + K_v \sum_{i=1}^{NLB} h(V_{Li}) + K_s \sum_{i=1}^{NL} h(S_{Li}) \tag{2.29}$$

$$\begin{aligned} F_{ext} = & \sum_{i=1}^{NG} F_i(P_{Gi}) + \alpha \cdot Max(L_j) + K_p\left[h(P_{slack})\right] \\ & + K_q \sum_{i=1}^{NG} h(Q_{Gi}) + K_v \sum_{i=1}^{NLB} h(V_{Li}) + K_s \sum_{i=1}^{NL} h(S_{Li}) + \sum_{i=1}^{NK} K_R \end{aligned} \tag{2.30}$$

where, K_p, K_q, K_v, and K_s are penalty weights of active power output of slack bus (P_{slack}), reactive power output of generator bus, load bus voltage magnitude, and line loading respectively; K_R is a penalty constant for transient stability limit; $h(P_{slack})$, $h(Q_G)$, $h(V_L)$, and $h(S_L)$ are the penalty terms of related variables; NK is the number of contingencies; NK will be 1 for the single-contingency consideration.

The active power generation limits of all generator buses except for slack bus, voltage limits of all generator buses, and transformer tap setting limits are not included in the extended objective functions, since these control variables are randomly created within their feasible limits during the process of the proposed methods. In conclusion, Eqs. (2.27), (2.28), (2.29), and (2.30) already considering all inequality constraints will be used as the new objective functions to be evaluated and minimized during the proposed methods.

2.7 Summary

Since the fuel cost minimization is typically used as a main objective in the OPF problem, the input ($/hr)-output (MW) characteristic of a thermal generating unit is mentioned at the beginning of this chapter. Basically, the cost function of a generating unit can be approximated as the simple quadratic function. Nevertheless, when the valve-point loading effects normally occurring in a thermal unit and the combined-cycle nature are taken into consideration, the cost function cannot be simply represented by the quadratic curve anymore. Due to the limitation of the classical optimization techniques in such a way that they can handle only some specific types of cost function, the new types of cost curve need a powerful optimizer to deal with. The proposed EP-based methods can be an answer for this.

After that, the basic concept of the conventional OPF problem is fully described and explained. The objective function and the corresponding constraints in the OPF problem used in this dissertation are formulated. Next, the additional constraints regarding the transient stability issue are mentioned and added into the conventional OPF problem to form the TSCOPF problem. The constraints generally consist of the swing equation and transient stability limit. Some literatures related to the TSCOPF problems are also given. After that, the topic of OPF with steady-state voltage stability consideration is explained. The indicator L, which is widely applied to estimate the voltage stability margin in many applications, is adopted to add the voltage stability issue into the conventional OPF problem. This creates the modified objective function, which is the trade-off between the economical issue and voltage stability issue. The technical meaning and mathematical calculation of indicator L are also expressed. Finally, the OPF with both transient and voltage stability considerations is formulated to make the OPF problem more practical and suitable to the present power system situation.

To handle the constraints in the OPF problem, strategies applied are stated in the last session. For equality constraints, the full AC power flow is run to satisfy the power balance equation and time domain simulation is performed to cope with the swing equation. The penalty function, where its value grows with a quadratic form when the constraints are violated and is 0 in the region where constraints are not violated, is employed to deal with all inequality constraints. Using the above-mentioned strategies, the extended objective functions that include the penalty terms of all inequality constraints are formed and they will be used to evaluate the optimality of each EP individual in the next chapter.

References

[1] J. Wood, B. F. Woollenberg: Power Generation, Operation, and Control, John Wiley & Sons, New York, 1996.

[2] H. T. Yang, P. C. Yang, and C. L. Huang: "Evolutionary Programming Based Economic Dispatch for Units with Non-Smooth Fuel Cost Functions", *IEEE Transactions on Power Systems*, Vol. 11, No. 1, pp. 112–118, 1996.

[3] Y. Yuan, J. Kubokawa, and H. Sasaki: "A Solution of Optimal Power Flow with Multicontingency Transient Stability Constraints", *IEEE Trans. Power Syst*., Vol. 18, No. 3, pp. 1094–1102, 2003.

[4] D. Gan, R. J. Thomas, and R. D. Zimmerman: "Stability-Constrained Optimal Power Flow", *IEEE Trans. Power Syst.*, Vol. 15, No. 2, pp. 535–540, 2000.

[5] L. Chen, Y. Tada, and H. Okamoto: "Optimal Operation Solutions of Power Systems with Transient Stability Constraint", *IEEE Trans. Circuit and Syst.*, Vol. 48, No. 3, pp. 327–339, 2001.

[6] P. Kundur: Power System Stability and Control, McGraw-Hill, Inc., New York, 1994.

[7] P. M. Anderson and A. A. Fouad: "Power System Control and Stability", Iowa, the Iowa State University Press, 1977.

[8] "Voltage Stability of Power Systems: Concepts, Analytical Tools and Industry Experience", IEEE Committee, Vol.IEEE/PES 93TH0358-2-PWR, 1990.

[9] K. Takahashi and Y. Nomura: "The Power System Failure on July 23rd 1987 in Tokyo" CIGRE SC-37 Meeting 37.87(JP)07(E), 1987.

[10] C. Reis and F. P. Maciel Barbosa: "A Comparison of Voltage Stability Indices", in *Proc. Electrotechnical Conference, IEEE MELECON*, pp. 1007–1010, 2006.

[11] P. Kessel and H. Glavitsch: "Estimating the Voltage Stability of a Power System", *IEEE Trans. Power Del*., Vol. PWRD-1, No. 3, pp. 346–354, 1986.

[12] R. Billinton and S. Aboreshaid: "Voltage Stability Consideration in Composite Power System Reliability Evaluation", *IEEE Trans. Power Syst*, Vol. 13, No. 2, pp. 655–660, 1998.

[13] G. M. Huang, N. C. Nair: "An OPF Based Algorithm to Evaluate Load Curtailment Incorporating Voltage Stability Margin Criterion", in *Proc. NAPS Conference*, 2001.

[14] S. Kim, T. Y. Song, M. H. Jeong, B. Lee, Y. H. Moon, J. Y. Namkung, and G. Jang: "Development of Voltage Stability Constrained Optimal Power Flow (VSCOPF)", in *Proc. IEEE PES Summer Meeting*, Vol. 3, pp. 1664–1669, 2004.

CHAPTER 3

Evolutionary Programming (EP)-Based Methods

3.1 Introduction

This chapter will mainly explain all components and procedures of three versions of the proposed EP-based methods for the various types of the OPF problem earlier mentioned in Chapter 2. The proposed EP-based methods include the conventional EP, Improved EP (IEP), and Adaptive EP (AEP). The conventional EP is similar to the EP methods applied to solve the power system optimization problems as reviewed in Chapter 1. The IEP and AEP are developed to enhance the searching process of the conventional EP in terms of the quality of the solution and computational time. These three proposed algorithms are explained as follows:

3.2 Conventional Evolutionary Programming (EP)

EP [1] is an optimization technique in the field of evolutionary computation (EC) similar to Genetic Algorithm (GA) and Particle Swarm Optimization (PSO). It is a stochastic method that searches for the optimal solution by evolving a population of candidate solutions over a number of iterations based on the natural evolution theory; namely mutation and natural selection. It emphasizes on the linkage between parent and its offspring rather than emulating some specific parts of parents as found in GA. The real-valued optimization problems in which the optimization surface possesses many locally optimal solutions are well suited for EP [2]. As revealed in [3], EP tends to provide a more robust method for solving the constrained optimization problems than does GA.

The solution representation and main components of the conventional EP algorithm are stated as follows:

3.2.1 Representation of Solution and Its Coding

An individual in a population represents a candidate of the OPF solution. Each individual consists of OPF control variables coded by real number as shown in Fig. 3.1. The coded control

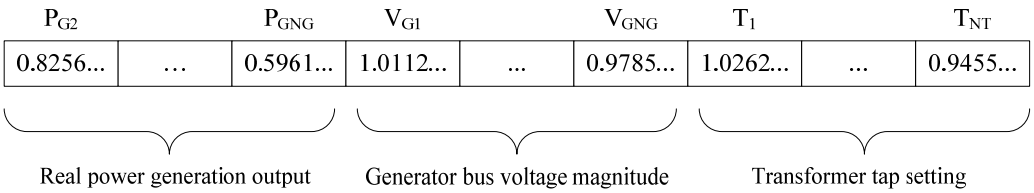

Fig. 3.1 Real number coding solution (individual)

variables employed in the algorithm are real power generation outputs of all generator buses excluding slack bus, voltage magnitudes at all generator buses including slack bus, and tap settings of all variable-tap transformers. Since this real-value coded representation is totally different from that of GA, which treats the candidate solution as the binary code, the encoding and decoding processes usually found in GA are not necessary for the EP method leading to the computational time saving.

The k-th individual in a population is represented by a trial solution vector $S_k = [P_{G2},\ldots,P_{GNG},V_{G1},\ldots,V_{GNG},T_1,\ldots,T_{NT}]$, where NG is the number of generators and NT is the number of variable-tap transformers.

3.2.2 Initialization

The initial population is randomly created using a set of uniform random number distribution ranging over the feasible limits of each control variable. Each element of the trial solution vector S_k, $k = 1, 2, \ldots, P$, where P is the population size, is determined by the following equation:

$$x_i = x_{i,\min} + U \cdot \left(x_{i,\max} - x_{i,\min}\right) \tag{3.1}$$

where

U	is a uniform random number in the interval [0,1].
x_i	is the i-th element of the individual in a population.
$x_{i,\min}$	is the lower limit of the i-th control variable of the individual.
$x_{i,\max}$	is the upper limit of the i-th control variable of the individual.

If the summation of the initialized active power output of all generators is less than the total active power demand, the initialization will be recalculated.

3.2.3 Fitness Calculation

EP is usually designed so as to maximize the fitness function, which is a measure of the quality of each candidate solution. The fitness of all individuals in a population will be calculated to determine their degree of optimality. In this thesis, the objective is to minimize the total fuel cost. Therefore, transformation is needed to convert the cost minimization objective function to an appropriate fitness function to be maximized by EP. A simple function for fitness calculation in the minimization problem is shown as follows:

$$f_k = \frac{1}{F_{ext,k}} \tag{3.2}$$

where

f_k	is the fitness value of the k-th individual.
$F_{ext,k}$	is the extended objective function of the k-th individual.

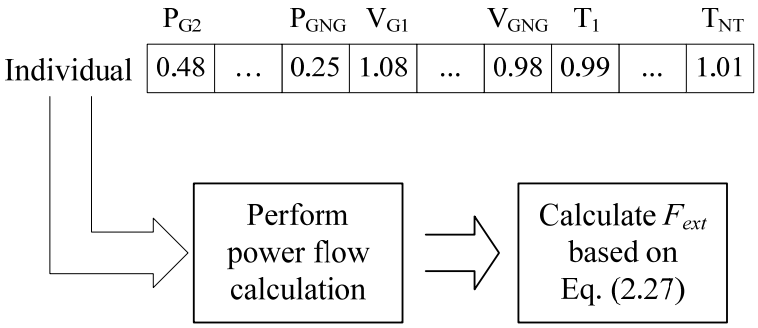

Fig. 3.2 Process for calculating the extended objective function of OPF problem

The following will explain how to calculate the extended objective function (F_{ext}) of each EP individual for the different OPF problems.

OPF Problem

In order to calculate the fitness of each individual, the equality constraints, i.e. power balance equations, have to be forced. A power flow calculation is performed for each individual to come up with all dependent variables, **x,** i.e. generator reactive power, all load bus voltage magnitudes, all bus voltage angles except the angle of slack bus, generator real and reactive power of slack bus, and transmission line flow in each line. These dependent variables are delivered to calculate the penalty terms associated with all inequality constraints. Finally, the extended objective function shown in Eq. (2.27) can be calculated. This process for obtaining F_{ext} can be depicted in Fig. 3.2.

Newton-Raphson (NR) technique is used for obtaining power flow solution. If the power flow of any individual fails to converge, the individual will be removed and replaced by a new randomly created individual.

TSCOPF Problem

In this problem, the equality constraints i.e. power balance equations and swing equation are needed to be forced in the proposed searching process. The power flow calculation by Newton-Raphson method is performed for every individual to come up with all variables in the system. These variables will be sent to calculate the penalty function shown in Eq. (2.26).

After this, the reduced Y_{bus} (before, during, and after the considered contingency) and all necessary values for transient stability analysis can be obtained. Time domain simulation is performed to get the generator rotor angle curve when a fault occurs. In time domain simulation, Newton-Raphson method is applied to solve the implicit function based on Eq. (2.16). At each integration step, if any generator rotor angle with respect to COI is over the transient stability limit, time domain simulation is ended before the maximum simulation time is reached leading to computational time saving. After this, the transient stability status of the power system against the contingency can be known. For the multi-contingency TSCOPF problem (MC-TSCOPF),

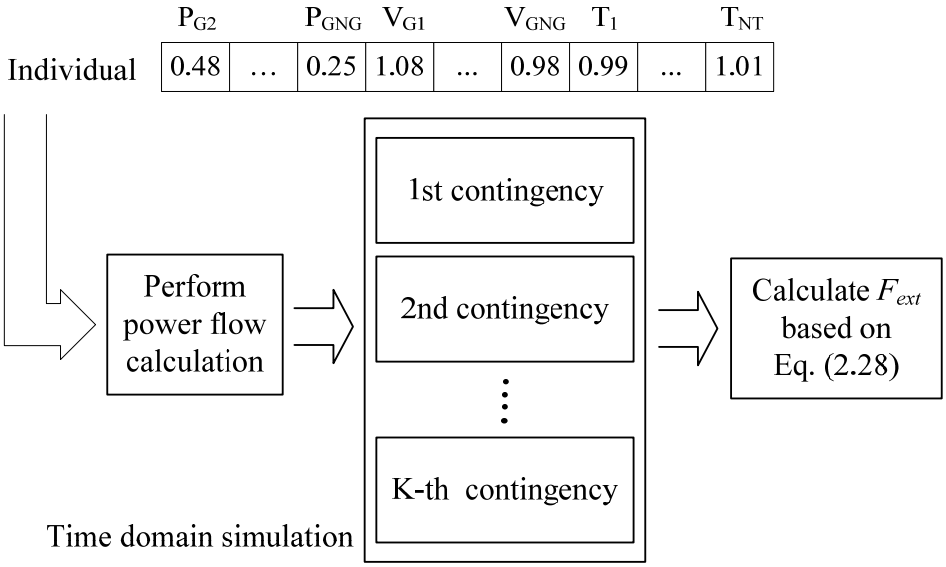

Fig. 3.3 Process for obtaining the extended objective function of TSCOPF problem

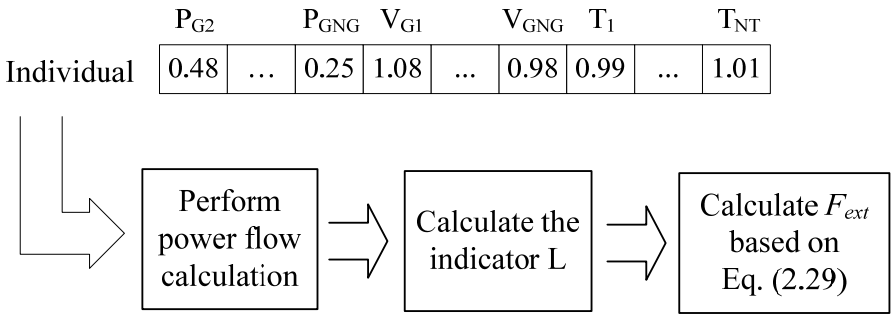

Fig. 3.4 Process for obtaining the extended objective function of OPF with voltage stability consideration

time domain simulation will be performed for every contingency. This process for obtaining the extended objective function of TSCOPF problem can be depicted in Fig. 3.3.

OPF with Steady-State Voltage Stability Consideration

Similar to two previous problems, the power flow calculation by Newton-Raphson method is first performed for every individual to obtain all system variables. Then the indicator L of each load bus is computed based on the power flow solution. At this moment, the weakest bus (the maximum value of indicator L among all load buses) can be identified. This process for obtaining the extended objective function of OPF with steady-state voltage stability consideration can be illustrated in Fig. 3.4.

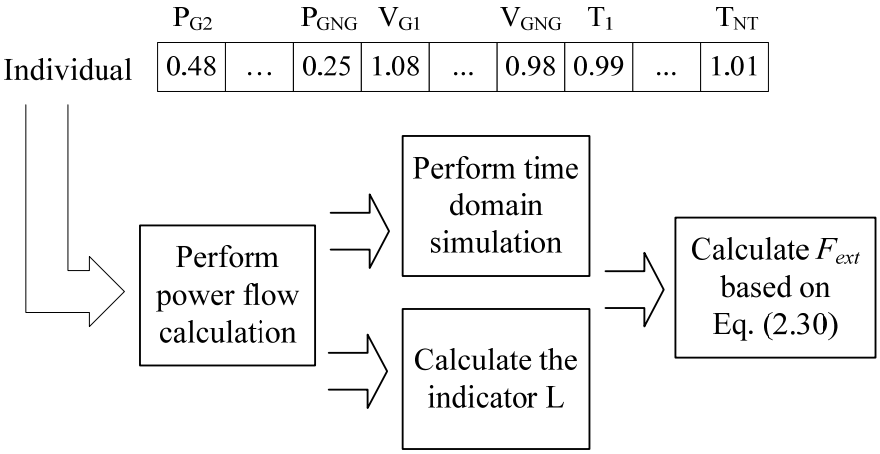

Fig. 3.5 Process for obtaining the extended objective function of OPF with transient and voltage stability considerations

OPF with Transient and Voltage Stability Considerations

In the last OPF problem, the power flow calculation, time domain simulation, and indicator L calculation are implemented respectively to obtain the extended objective function shown in Eq. (2.30). The process for obtaining the extended objective function is depicted in Fig. 3.5.

3.2.4 Mutation

A new or offspring population is produced from the existing or parent population through the mutation operator on a one-by-one basis. Each control variable of the k-th offspring individual is computed as follows:

$$\begin{aligned} x'_{ki} &= x_{ki} + N(0, \sigma_{ki}^2) \\ \sigma_{ki} &= (x_{ki,\max} - x_{ki,\min}) \left(\frac{f_{\max} - f_k}{f_{\max}} + a^g \right) \end{aligned} \tag{3.3}$$

where

x'_{ki} is the value of the i-th control variable of the k-th offspring individual.

x_{ki} is the value of the i-th control variable of the k-th parent individual.

$N(0, \sigma_{ki}^2)$ is a Gaussian random number with a mean of zero and standard deviation of σ_{ki}.

$x_{ki,\max}$, $x_{ki,\min}$ are the upper and lower limits of the i-th control variable of the k-th parent individual.

f_k is the fitness value of the k-th individual.

$f_{\max}$ is the maximum fitness of the parent population.

a is a positive number constant slightly less than one.

g is the iteration counter.

If any control variable mutated by Eq. (3.3) exceeds its corresponding limits, or the summation of the mutated active power output of all generators is less than the total active power demand, the control variable will be recalculated by Eq. (3.3).

The probability of the offspring individual to move far away from the parent individual depends upon the value of standard deviation, σ, or mutation step size. There are two factors that have effect on mutation step size. Firstly, the term a^g in Eq. (3.3) is used to reduce the mutation step size when the iteration counter increases. Consequently, the diversification of EP process will be introduced at the beginning and the intensification will then be introduced when the iteration counter is increased. Secondly, the fitness value of an individual also affects the mutation step size. It can be observed from Eq. (3.3) that an individual, which has a much lower fitness value than $f_{\max}$, will have the higher value of mutation step size. Hence, it will be probably moved further to the better position.

3.2.5 Selection

In this process, the current parent and offspring populations are combined together making the combined population and the new parent population will be selected from this combined population. For optimization to occur or the movement to the global optimum, the fitter or more optimal solutions should have greater chance of selection. The selection technique used is a tournament scheme described in the following

In tournament scheme, each individual in the combined population has to compete with N_t randomly selected individuals on a one-by-one basis. If the fitness value of the individual is greater than that of the selected opponent, the individual scores 1 or wins. Otherwise, it scores 0 or loses. This rule is represented in Eq. (3.4). The total competition score of each individual, s_k, is the summation of competition scores from N_t competitions as shown in Eq. (3.5). The new parent population will be selected based on this total competition score.

$$w_t = \begin{cases} 1 & f_k > f_r \\ 0 & otherwise \end{cases} \tag{3.4}$$

$$s_k = \sum_{t=1}^{Nt} w_t \tag{3.5}$$

where

f_k is the fitness value of the k-th individual in the combined population.

f_r is the fitness value of the r-th opponent randomly selected from the combined population based on $r = \lfloor 2 \cdot P \cdot U + 1 \rfloor$.

$\lfloor x \rfloor$ is the greatest integer less than or equal to x.

U is a uniform random number in the interval [0,1].

P is the population size.

w_t is the competition score.

s_k is the total competition score of the k-th individual.

When all individuals in the combined population get their total competition scores, they will be ranked in descending order according to their score, s_k. After this, the first P individuals with higher total competition score will be transcribed along with their fitness to form the parent population of the next generation.

3.2.6 Termination Criterion

The iteration process is terminated, if the maximum generation number (G_{max}) is reached. Otherwise, the mutation, fitness calculation, and selection process will be performed until the criterion is satisfied.

3.2.7 EP Procedure for Solving OPF Problems

The procedure and flowchart of conventional EP algorithm for the OPF problems are described as follows:

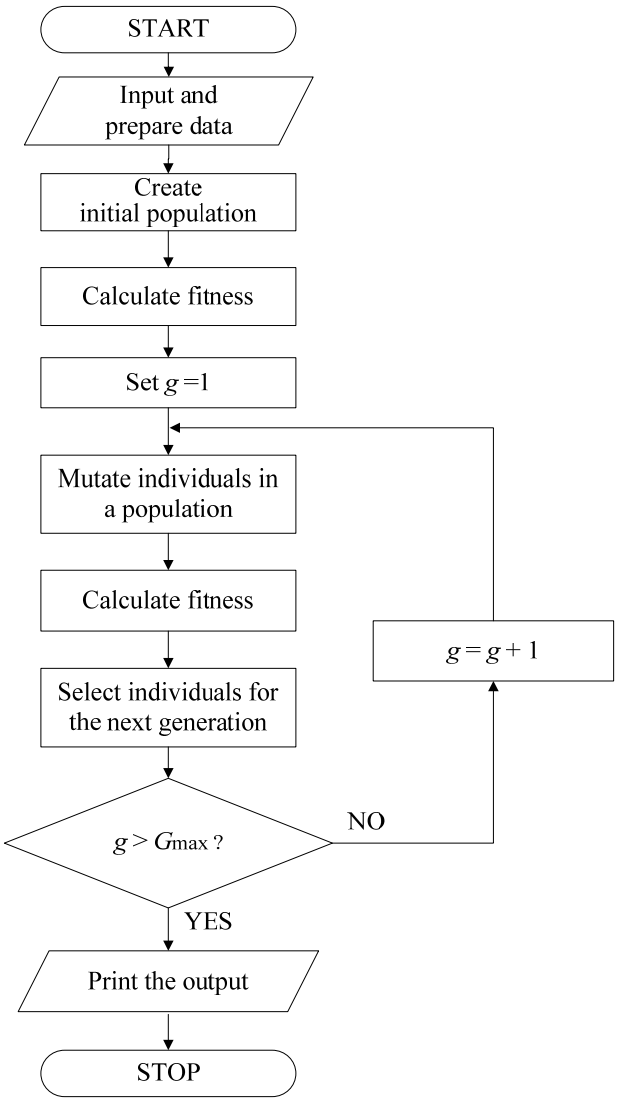

Fig. 3.6 Flowchart of the conventional EP method

Step 1: Read system data and EP parameters.
Step 2: Set $g = 1$.
Step 3: Initialize all individuals in a population by Eq. (3.1).
Step 4: Calculate fitness for all initial individuals by Eq. (3.2).
Step 5: Set best solution (S_b) = the individual with the highest fitness value.
Step 6: Create the offspring population through mutation process by Eq. (3.3).
Step 7: Perform fitness calculation for all individuals in the offspring population.
Step 8: If the fitness value of the fittest individual in the offspring population is greater than that of S_b, set S_b = the fittest individual in the offspring population.
Step 9: Select the new parent population for the next iteration by the tournament scheme.
Step10: If $g < G_{max}$, set $g = g + 1$ and go back to Step 6. Otherwise, terminate the process and S_b is the solution of the OPF problem.

3.3 Improved Evolutionary Programming (IEP)

As noticed from the previous session, the conventional EP generates the offspring by using only mutation process, which moves the control variables by disturbing their value using Gaussian distribution. As a result, the offspring generation can be upgraded in order to increase the chance to obtain the better individuals and reduce the computational time.

The proposed Improved Evolutionary Programming (IEP) is the EP-based optimization algorithm with the addition of crossover techniques. It enhances the offspring generation process by using both the mutation in conventional EP and crossover techniques, normally found in Real Coded Genetic Algorithm (RCGA) [4, 5]. Different from the mutation, the crossover generates the offspring by exchanging some parts of candidate solution (individual) between two selected parents without perturbing their values. Through the processes of EP mutation and RCGA crossover, the offspring is generated either by perturbing its parent on a one-by-one basis or exchanging information between two selected parents. The utilization of the appropriate proportion between mutation and crossover can provide better probability of detecting an optimal solution. If a control variable in an IEP individual is regarded as one characteristic of the individual, the meaning of crossover in IEP can be defined as a process of exchanging characteristics of two individuals.

The individual representation, fitness calculation, selection, and stopping criterion, which are mentioned in the conventional EP, are also applied here in the IEP method.

3.3.1 Offspring Generation Process in IEP

An offspring individual in a population is created by either mutation or crossover operator based on the crossover acceptance rate (M). If $U[0,1]$ (uniform random number between 0 and 1) is higher than M, the offspring will be created by the mutation operator. Otherwise, it will be created by the crossover technique. The offspring generation diagram used in the IEP method can be simply depicted in Fig. 3.7.

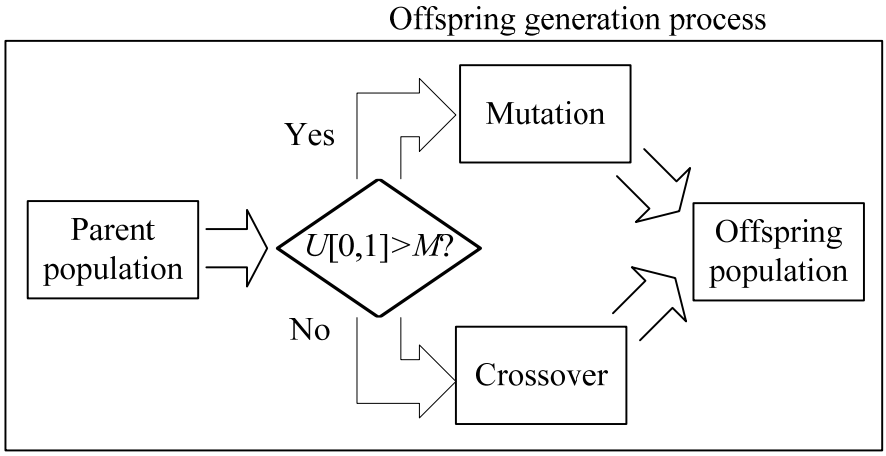

Fig. 3.7 Offspring generation diagram used in IEP

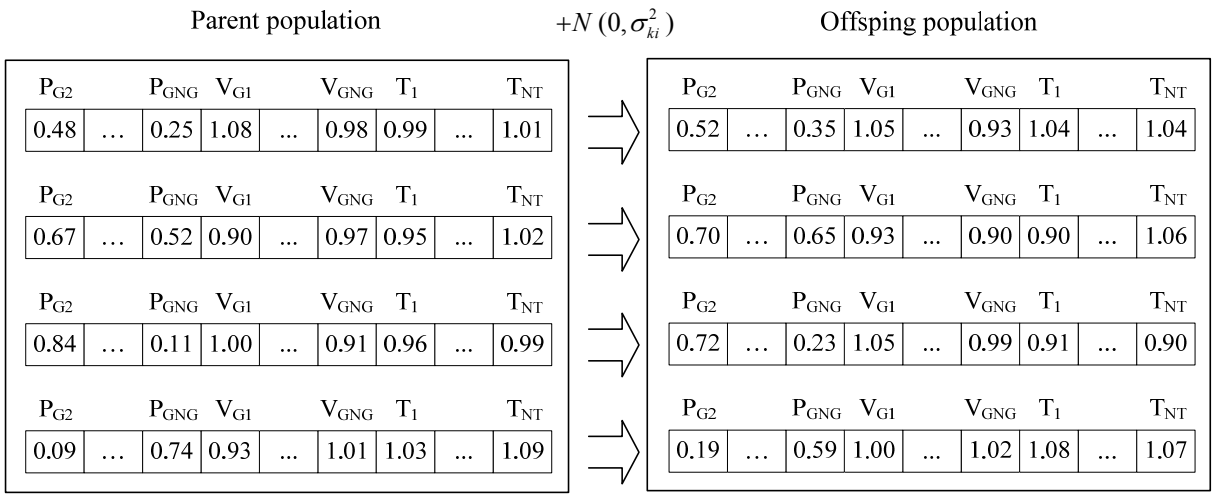

Fig. 3.8 Mutation process for offspring generation

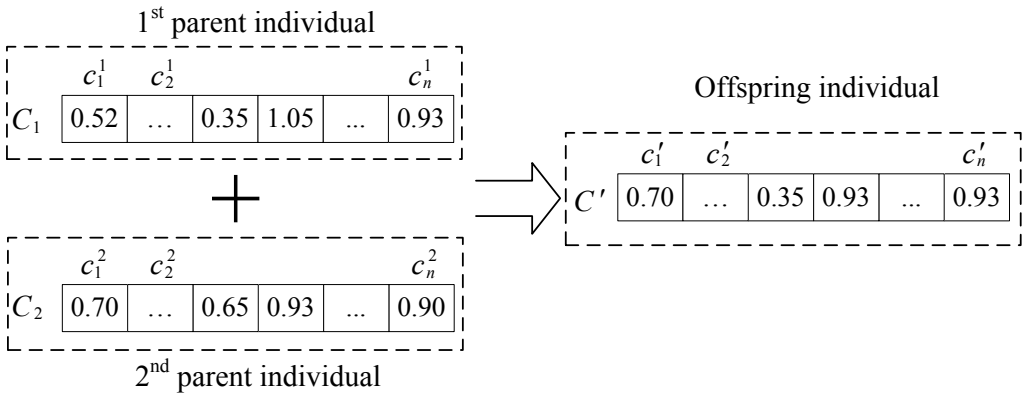

Fig. 3.9 Crossover process for offspring generation

Mutation

The mutation process explained in Chapter 3.2.4 is applied as one of the offspring generation processes. As mentioned, the offspring is produced from its corresponding parent on a one-by-one basis. The information exchange between two different parents cannot be seen from this operator. The mutation process is demonstrated in Fig. 3.8.

Crossover

In this dissertation, various types of crossover techniques shown in [4] are adopted as one of the offspring generation processes to generate new individuals. Suppose that $C_1 = \left(c_1^1, \ldots\ldots, c_n^1\right)$ and $C_2 = (c_1^2, \ldots\ldots, c_n^2)$ are two parent individuals that are randomly selected for crossover and n is

the number of control variables. The offspring $C' = (c_1', ..., c_n')$ is created as shown in Fig. 3.9. The crossover techniques used in the IEP method for the offspring generation are described as follows:

(1) *Flat Crossover*: An offspring indiviudal is created as follows:

$$c_i' = U\left[c_i^1, c_i^2\right] \tag{3.6}$$

In this crossover, the control variable of the offspring individual is obtained from the uniform random number ranging between the corresponding control variables of two chosen parents.

(2) *Simple Crossover*: A position $i \in \{1, 2, ..., n-1\}$ is chosen randomly and the offspring are created as follows:

$$C' = \left(c_1^1, c_2^1, ..., c_i^1, c_{i+1}^2, ..., c_n^2\right) \tag{3.7}$$

In the simple crossover, the offspring is obtained by connecting one part of the first parent with one part of the second parent at the position *i*.

(3) *Arithmetical Crossover*: An offspring individal is created as follows:

$$c_i' = \lambda c_i^1 + (1-\lambda) c_i^2 \tag{3.8}$$

where the value of λ is a constant. In this dissertation, λ is set to 0.5.

In this arithmetical crossover, the control variable of the offspring individual is the middle position of two points, which are the corresponding control variables of the first and second parent individuals.

(4) *BLX-α Crossover*: An offspring individal is created as follows:

$$c_i' = U\left[c_{\min} - I \cdot \alpha, c_{\max} + I \cdot \alpha\right] \tag{3.9}$$

$$c_{\max} = \max\left(c_i^1, c_i^2\right), c_{\min} = \min\left(c_i^1, c_i^2\right) \tag{3.10}$$

$$I = c_{\max} - c_{\min} \tag{3.11}$$

In this dissertation, *BLX-0.25* is examined. In this crossover, the control variable of the offspring individual is obtained from the uniform random number ranging between the corresponding control variables of two chosen parents $\pm\ I \cdot \alpha$. This crossover is similar to the flat crossover, but the range of the generated offspring is wider.

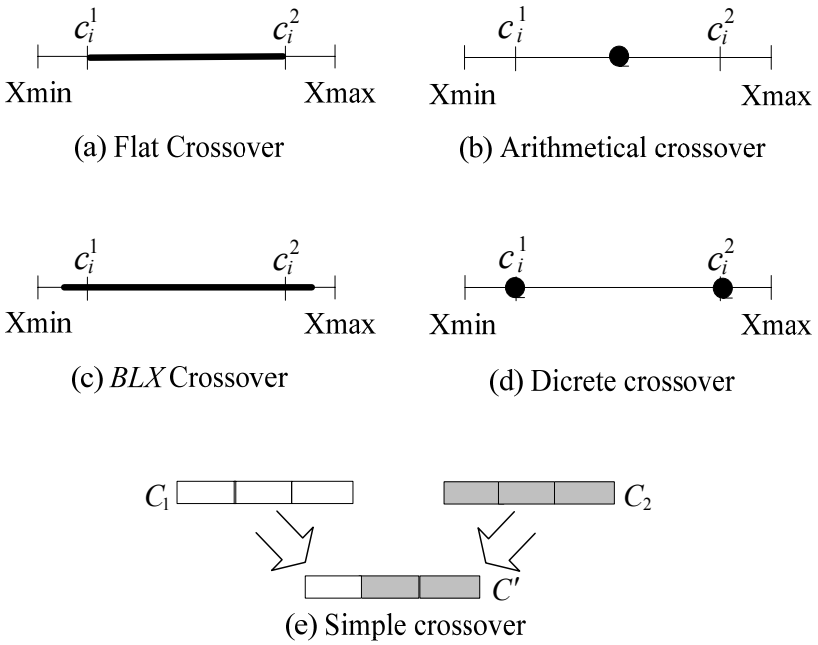

Fig. 3.10 Various types of crossover technique

(5) *Discrete Crossover*: An offspring individual is created as folows:

$$c_i' \in \left\{c_i^1, c_i^2\right\} \tag{3.12}$$

In the discrete crossover, the control variable of the offspring individual is selected from the corresponding control variable of either the first parent or the second parent. This crossover is analogous to the simple crossover. The difference is that the simple crossover is one-point crossover, but the discrete crossover is multiple-point crossover.

(6) *Modified Discrete Crossover*: An offspring individual is created as folows:

$$c_i' = \begin{cases} c_{1i} & if \quad U[0,1] \le f_1/(f_1+f_2) \\ c_{2i} & if \quad U[0,1] > f_1/(f_1+f_2) \end{cases} \tag{3.13}$$

where f_1 and f_2 are the fitness values of the first and second parent individuals respectively.

The modified discrete crossover introduces the fitness value of the parents in the discrete crossover in order to increase the chance to obtain the fitter offspring. The control variable of the parent with a higher fitness value will have more chance to be selected.

Fig. 3.10 depicts the various types of crossover techniques used in IEP. In conclusion, EP employs only mutation to generate the offspring whereas IEP uses both mutation and crossover.

Table 3.1 IEP methods with various crossover techniques

Algorithms	Crossover Technique
IEP1	Flat crossover
IEP2	Simple crossover
IEP3	Arithmetical crossover
IEP4	BLX-0.25 crossover
IEP5	Discrete crossover
IEP6	Modified Discrete crossover

IEP with both mutation and crossover offers the diversification of offspring generation. The offspring individual is generated not only by moving the control variables from a single parent, but also exchange the information from two parents. This will increase the chance of obtaining the optimal solution. In addition, sometimes the offspring generated from the mutation process is required to be re-mutated, because some control variables of that offspring may violate their limits. The recalculation of offspring can occur many times when the control variables of its parent are near their limits. Therefore, the less complicated process of the crossover techniques for offspring generation leads to the overall computational time saving. Table 3.1 shows the abbreviation of the proposed IEP with different crossover techniques.

Based on the proposed IEP method, the differences between the RCGA and IEP are listed as follows:

- In RCGA, the selection is performed first in order to select the good parents, and then crossover and mutation is applied respectively whereas in IEP the selection is performed after crossover and mutation.
- In RCGA, both crossover and mutation are performed for an individual, but in the proposed IEP either crossover or mutation is applied depending on the parameter M.
- In IEP, the mutation is applied by perturbing all control variables of a parent individual. On the other hand, in RCGA only some of control variables in a chromosome are mutated depending upon a mutation rate.

3.3.2 IEP Procedure for Solving OPF Problems

The procedure and flowchart of IEP algorithm for the OPF problems are described as follows:

Step 1: Read system data and IEP parameters.
Step 2: Set $g = 1$.
Step 3: Initialize all individuals in a population by Eq. (3.1).
Step 4: Calculate fitness for all initial individuals by Eq. (3.2).
Step 5: Set best solution (S_b) = the individual with the highest fitness value.
Step 6: Create the offspring population through mutation process by Eq. (3.3) or crossover technique based on the parameter M.
Step 7: Perform fitness calculation for all individuals in the offspring population.

Step 8: If the fitness value of the fittest individual in the offspring population is greater than that of S_b, set S_b = the fittest individual in the offspring population.

Step 9: Select the new parent population for the next iteration by the tournament scheme.

Step10: If $g < G_{max}$, set $g = g + 1$ and go back to Step 6. Otherwise, terminate the process and S_b is the solution of the OPF problem.

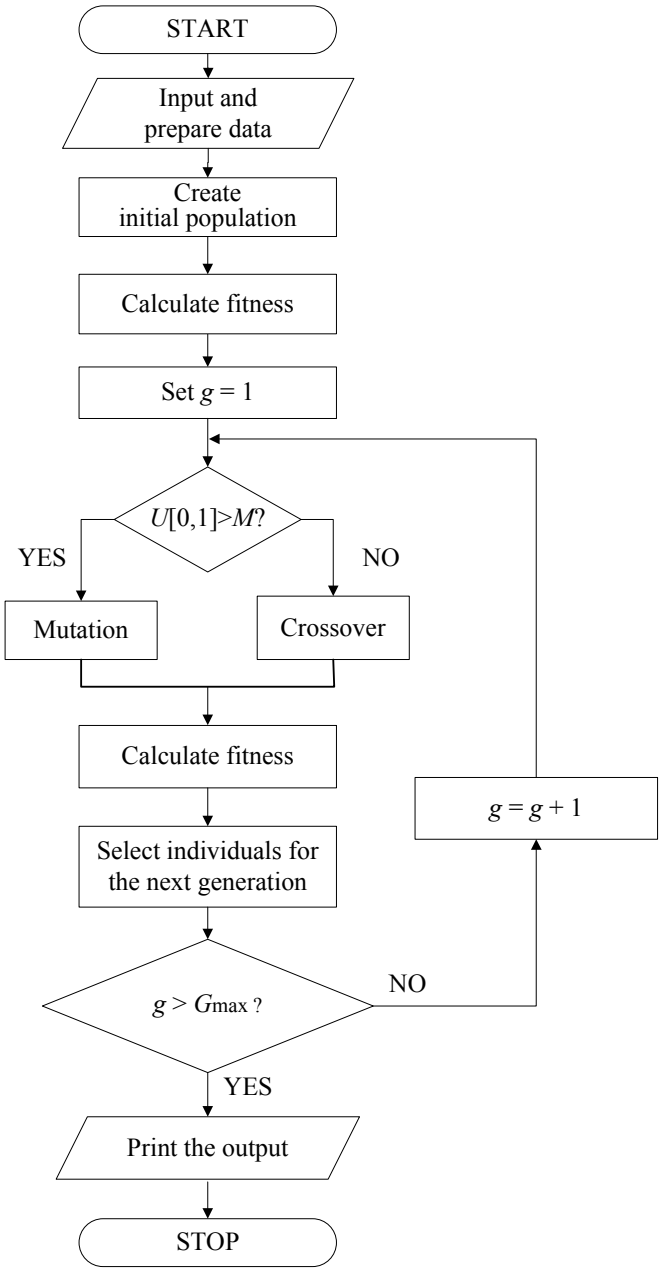

Fig. 3.11 Flowchart of the IEP method

3.4 Adaptive Evolutionary Programming (AEP)

Generally, to apply the Artificial Intelligence (AI)-based methods, main parameters in those methods, e.g. swarm size and inertia weight of PSO, population size, crossover and mutation rates of GA, population size of Differential Evolution (DE) [6] etc., are needed to be predefined. In case of the conventional EP, the main parameters, i.e. population size (P), decaying mutation rate (a), and maximum generation ($G_{\max}$) have to be predefined. Since the efficiency and execution time of the proposed EP method are strongly influenced by these parameters, especially P, the selection of the suitable population size in order to get the good result is a difficult task and relies on the time-consuming trials and errors with different parameter sets.

3.4.1 Population Adaptation Rule

In this dissertation, an adaptive evolutionary programming (AEP), which starts with a single-individual population and then changes the population size adaptively, is proposed. The population size of AEP is automatically adjusted based on the quality of the population (*good* or *bad*). The population adaptation rule is based on the idea of removing or adding a particle in TRIBES PSO [7].

As shown in Fig. 3.12, the concept is that a population that has many *good* individuals (*good* population) can benefit from the removal of the weakest individual, since it already possesses many good candidate solutions. On the other hand, a population that has many *bad* individuals (*bad* population) can benefit from the addition of a new individual to increase the possibility of improvement. Please note that in the case of a single-individual population, even the population has a single *good* individual, the removal will be voided. An individual is said to be *good*, if it has the higher fitness than its parent, and vice versa. Let P_i and G_i be the population size and the number of *good* individuals of the i-th generation respectively. The adaptation rule for adding or removing an individual can be described as follows:

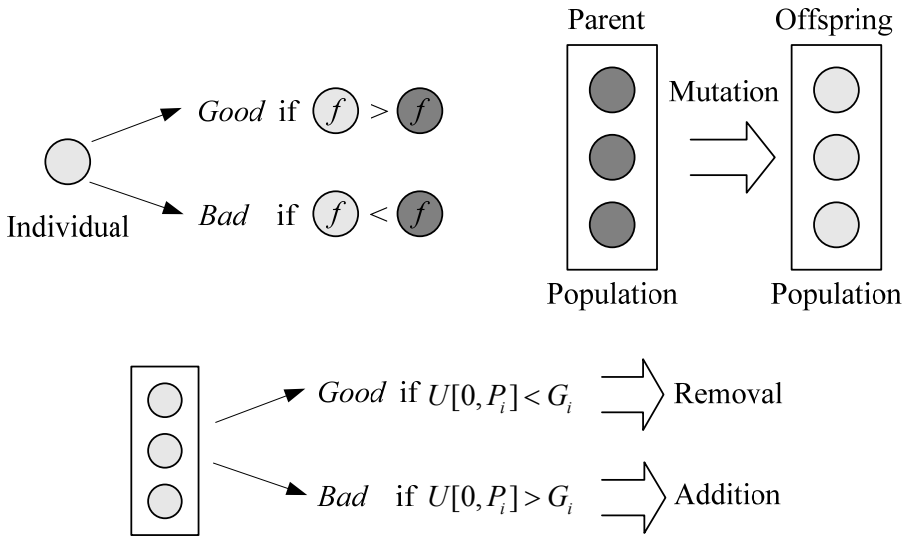

Fig. 3.12 Definitions of quality of individual and population

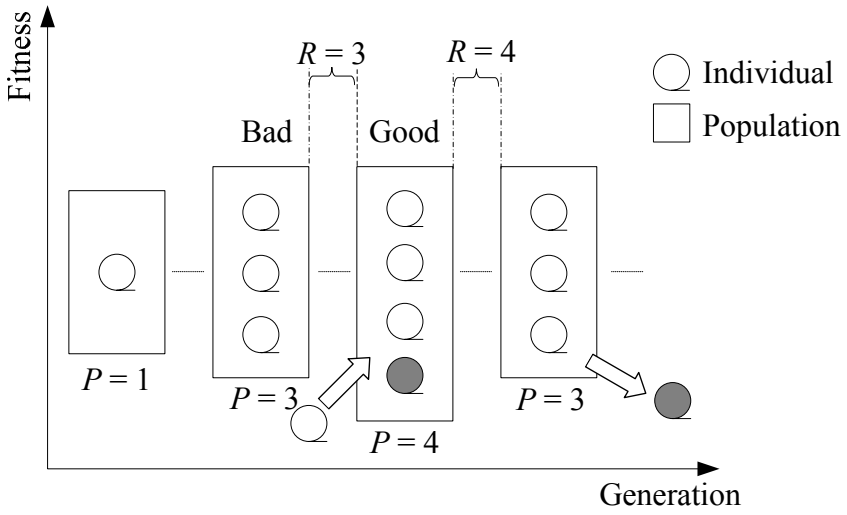

Fig. 3.13 Adaptation process of population size in AEP

$$P_{i+1} = \begin{cases} P_i + 1 & if \quad U[0, P_i] > G_i \\ P_i - 1 & if \quad U[0, P_i] < G_i \end{cases} \tag{3.14}$$

where

P_{i+1} is the population size of the $(i+1)$-th generation.

$U[0, P_i]$ is a uniform distribution ranging between 0 and P_i .

G_i is the number of *good* individuals of the i-th generation.

The removal will be applied to the *good* population by taking out the individual having the lowest fitness among all individuals in the population. On the other hand, the addition will be applied to the *bad* population by adding a new randomly-created individual. The new individual will be generated using Eq. (3.1).

The adaptation rule will not take place at every generation, since the individuals should be allowed to search the solution for some time. In this research, the population size will be modified after P generations. For example, if right now the population size is 4, this population will be allowed to search for the optimal solution for 4 generations and after that the adaptation rule will be performed. This means that the larger the population size is the longer the time between two adaptations will be. At the beginning, the population size will change quite frequently and when the population size becomes large, the adaptation rule will be rarely applied. Fig. 3.13 depicts the concept of adaptation process of population size in the AEP method. Note that R shown in Fig. 3.13 is the number of iterations since the last population's adaptation and P is the dynamic population size of the g-th iteration (generation).

The individual representation, fitness calculation, mutation, selection, and stopping criterion, which are mentioned in the conventional EP, are also applied here in the AEP method.

3.4.2 AEP Procedure for Solving OPF Problems

The procedure and flowchart of AEP algorithm for the OPF problems can be summarized as follows:

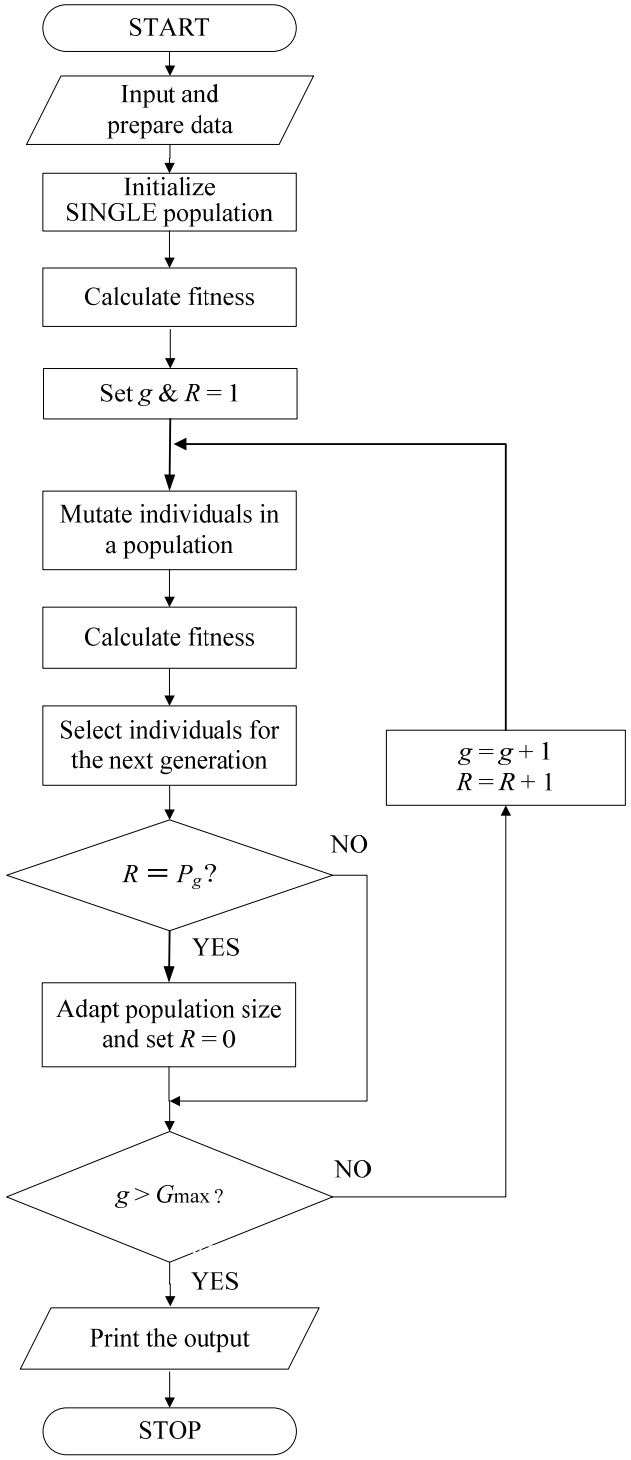

Fig. 3.14 Flowchart of the AEP method

Step 1: Read system data and AEP parameters.
Step 2: Set g and $R = 1$.
Step 3: Initialize a SINGLE individual in a population by Eq. (3.1).
Step 4: Calculate fitness for an initial individual by Eq. (3.2).
Step 5: Set best solution (S_b) = the individual with the highest fitness value.
Step 6: Create the offspring population through mutation process by Eq. (3.3).
Step 7: Perform fitness calculation for all individuals in the offspring population.
Step 8: If the fitness value of the fittest individual in the offspring population is greater than that of S_b, set S_b = the fittest individual in the offspring population.
Step 9: Select the new parent population for the next iteration by the tournament scheme.
Step 10: If $R = P_g$, modify the population size by Eq. (3.14) and set $R = 0$. Otherwise, the population size is the same.
Step11: If $g < G_{max}$, set $g = g + 1$, $R = R + 1$, and go back to Step 6. Otherwise, terminate the process and S_b is the solution of the OPF problem.

Please note that P_g is the dynamic population size of the g-th generation.

3.5 Summary

The process and procedure of the conventional EP method used to solve the various types of the OPF problems are firstly elaborated. The power flow calculation, time domain simulation, and indicator L calculation are respectively carried out in order to evaluate the fitness of each individual in the EP population. Only mutation process is performed to generate the offspring individuals. The tournament scheme which compares the fitness of individual with others in the combined population is adopted to select the promising individuals for the next generation. In the conventional EP, the presetting of three parameters, i.e. population size, decaying mutation rate and maximum generation is required.

To enhance the offspring generation process, six types of crossover techniques, flat crossover, simple crossover, arithmetical crossover, *BLX-* α crossover, discrete and modified discrete crossovers are introduced. These six crossover operators are borrowed from RCGA. Both mutation and crossover are applied to generate the offspring individuals based on the crossover acceptance rate (*M*). The mutation puts emphasis on perturbing the control variables of a parent individual whereas the crossover techniques focus on the information exchange between two parent individuals. The crossover provides the simpler operator for creating offspring and the diversification to the search template. In Addition, the differences between the proposed IEP method and RCGA are mentioned. In IEP, the presetting of four parameters, i.e. population size, decaying mutation rate, maximum generation, and crossover acceptance rate is needed.

The final version of the EP-based methods, AEP, is suggested to reduce the parameters required to pre-define when the EP method is selected to solve the OPF problem. The reduced parameter is the population size, which normally plays a crucial role on the quality of solution and execution time. In AEP, the presetting of only decaying mutation rate and maximum generation is necessary. The population size starts with one single individual at the beginning and then it will change adaptively according to the adaptation rule adopted from an idea in TRIBES PSO. The idea is that the population having a large amount of potential individuals will remove one weakest individual to save the computational time whereas the population having a small amount of potential individuals will add one new individual to increase the chance to find the optimal solution. The adaptation rule will be applied when the number of iterations since the last population's adaptation is equal to the population size of that generation.

These three proposed EP-based methods will be applied to solve the OPF problems earlier formulated in Chapter 2.

References

[1] J. Yuryevich and K. P. Wong: "Evolutionary Programming Based Optimal Power Flow Algorithm", *IEEE Trans. Power Systems*, Vol. 14, No. 4, pp. 1245–1250, 1999.

[2] L. L. Lai: "Intelligent System Applications in Power Engineering: Evolutionary Programming and Neural Networks", John Wiley & Sons, New York, 1998.

[3] D. B. Fogel: "A Comparison of evolutionary programming and genetic algorithms on selected constrained optimization problems", *Simulation*, Vol. 64, No. 6, pp. 397–404, 1995.

[4] F. Herrera, M. Lozano, and J. L. Verdegay: "Tackling Real-Coded Genetic Algorithms: Operators and Tools for Behavioral Analysis", *Artificial Intelligence Review*, Vol. 12, No. 4, pp. 265–319, 1998.

[5] G. Zwe-Lee and H. Hou-Sheng: "Real-coded mixed-integer genetic algorithm for constrained optimal power flow", in *Proc. 2004 IEEE TENCON Conf.*, Vol. 3, pp. 323–326, 2004.

[6] H. R. Cai, C. Y. Chung, and K. P. Wong: "Application of Differential Evolution Algorithm for Transient Stability Constrained Optimal Power Flow", *IEEE Trans. Power Systems*, Vol. 23, No. 2, pp. 719–728, May 2008.

[7] Y. Cooren, M. Clerc, and P. Siarry: "Initialization and Displacement of the Particles in TRIBES, a Parameter-Free Particle Swarm Optimization Algorithm", *Adaptive and Multilevel Metaheuristics*, Springer Berlin / Heidelberg, pp. 199–219, 2008.

CHAPTER 4

ARTIFICIAL NEURAL NETWORK (ANN) FOR TRANSIENT STABILITY ASSESSMENT

4.1 Introduction

To evaluate the transient stability of a power system, the several methods have been widely applied. The three main methods are time domain simulation [1], transient energy function (TEF) method [2], and artificial neural network. Even though time domain simulation of course provides the accurate results of transient stability assessment in which the detailed models of generator, loads, and relative controls can be included, it suffers from a great deal of computational time. The convergence property when solving for the controlling unstable equilibrium point and limitation in modeling capacity of power system components are major impediments for using TEF method. To alleviate the above problem, this dissertation proposes the combination of time domain simulation and neural network to evaluate the system transient stability. The examples of researches on transient stability assessment using a neural network can be found in [3, 4]. In [3], a selection method of input parameters and their sensitivity analysis for neural network application to transient stability assessment are presented. In [4], transmission power margin (TMAR) is proved to be a significant input parameter to reduce the error of the neural network output. This chapter will mainly show the proposed artificial neural network for transient stability assessment in the TSCOPF problem.

The basic model of feed-forward neural network is shown in Fig. 4.1. The network consists of *NR* input neurons in the input layer, *NO* output neurons in the output layer, and *NS* neurons in one or more hidden layers. Once such network is trained with the prepared input and output vectors, it can estimate the unknown output from new input vector without the need of detailed analysis. With the help of the network, the transient stability degree can be roughly evaluated.

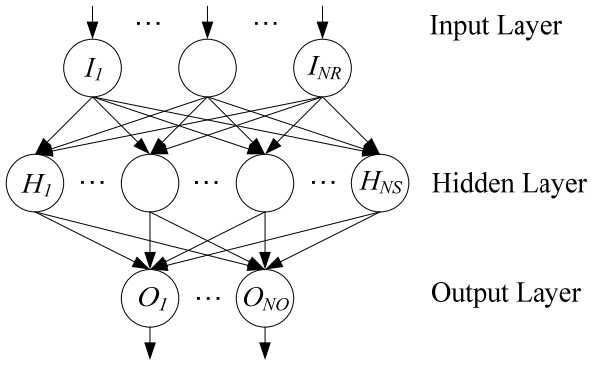

Fig. 4.1 Three-layer feed-forward neural network

4.2 Proposed Artificial Neural Network

Rather than using only time domain simulation to evaluate the transient stability in the TSCOPF problem as depicted in Fig. 3.3, the neural network, which is less time-consuming, is first used to classify the individual into three regions, namely *stable*, *unstable*, and *critical* regions using pre-set thresholds and then time domain simulation will be performed with only individual classified in the *critical* region. Instead of directly evaluating the system in terms of only *stable* and *unstable* regions, the thresholds are introduced in order to account for the inherent error of the neural network.

The architecture, inputs and output of the proposed network are depicted in Fig. 4.2. The proposed feed-forward network consists of inputs, one or more hidden layers, and one output layer. The inputs are the EP individual and P_{slack}. The hidden layers consist of neurons with the tan-sigmoid transfer function whereas the output layer consists of a single neuron with the log-sigmoid transfer function. A single output of the network signifies the stability degree of the individual. The stability degree is simply measured by the 0.05-gain sigmoid function $[(Sigmf\ (X\ )]$ of the difference between δ_{MAX} and maximum rotor angle deviation among all generators $(\delta_{MAXdiv}\,)$ as shown in Fig. 4.3. If δ_{MAXdiv} is lower than δ_{MAX}, the value of X will be a positive number, and vice versa. The individual that leads to very high degree of stability (high positive X) or instability (high negative X) will have the output near 1 or 0 respectively. When δ_{MAXdiv} is exactly equal to δ_{MAX}, the output will assign the value of 0.5. The criterion to perform time domain simulation is determined by the output of the neural network. Namely, if the output is between the thresholds L_1 and L_2 (*critical* region), time domain simulation is performed for the individual to scrutinize the transient behavior. Otherwise, the transient stability is estimated without time domain simulation i.e. output < L_1 means *unstable* and output > L_2 means *stable*.

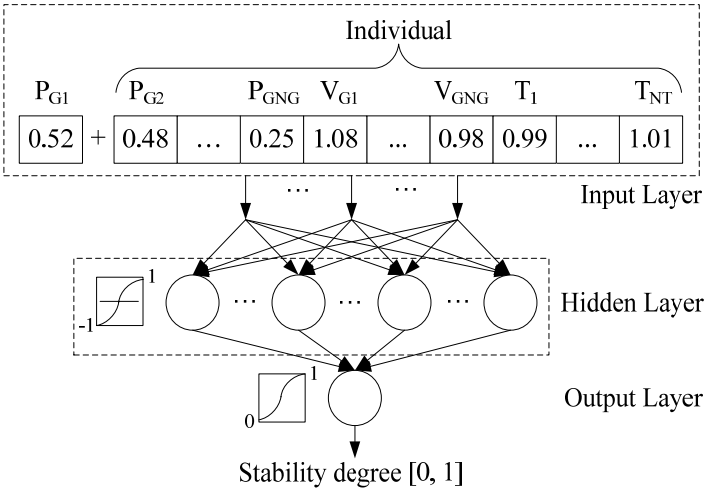

Fig. 4.2 Architecture of the proposed neural network

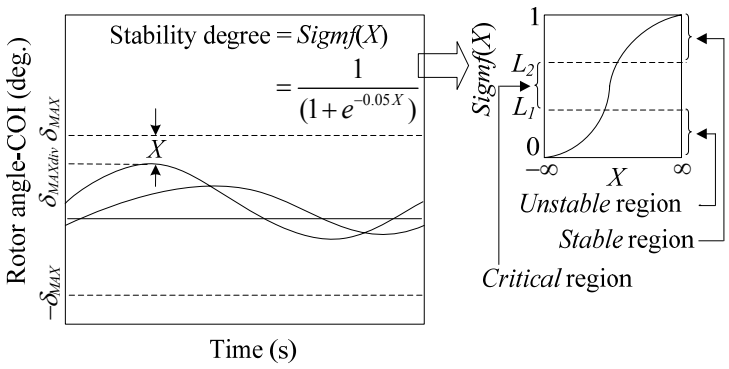

Fig. 4.3 Output of the proposed neural network

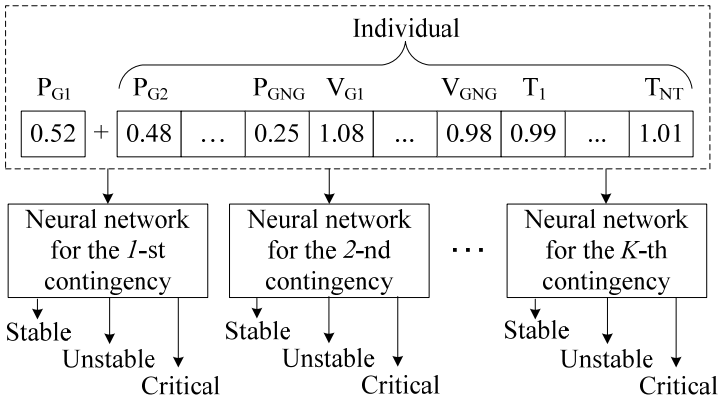

Fig. 4.4 Strategy for handling multi-contingency constraints

Fig. 4.4 illustrates the proposed strategy for dealing with multi-contingency constraints. The neural network is individually trained for each contingency and it will evaluate the transient stability of the individual against the corresponding contingency. The thresholds for each contingency may be different depending on the performance of the trained neural network.

4.3 Study of Proposed Artificial Neural Network

The IEEE 30-bus system consisting of 41 transmission lines, 6 generators, and 4 tap-changing transformers is used as the test system. The single-line diagram of the system is depicted in Fig. 4.5. The bus and line data of the system can be found in [5]. The operating range of each transformer is set between 0.9 and 1.1. In this section, the results of the proposed neural network will be discussed. The inputs of the network illustrated in Fig. 4.2 contain 6 active power generations and 6 voltage magnitudes of all generator buses, as well as 4 transformer-tap settings, totally 16 inputs (NR = 16). The selection of critical inputs for the neural network is beyond the scope in this study, but it is important for a large power system where the number of generators and transformers is very high. A single output (NO = 1) is transient stability degree represented by the sigmoid function of X shown in Fig. 4.3. Six single contingencies at points A, B, C, D, E, and F shown in Fig. 4.5 are considered in the simulation. Each contingency is a three-phase grounding fault at t = 0 s and cleared by removing the line at t = 0.35 s. For time-domain simulation, the integration time step is 0.01 s, T_s is 1.5 s, and δ_{MAX} is 120 degrees.

Modified from Newton's method, Levenberg-Marquardt algorithm is chosen to train the proposed network. The inputs are randomly generated within their feasible operating range. The maximum growth factor is set to 2. The performance of the trained network is measured by the mean sum squares of the network errors (MSE) as follows:

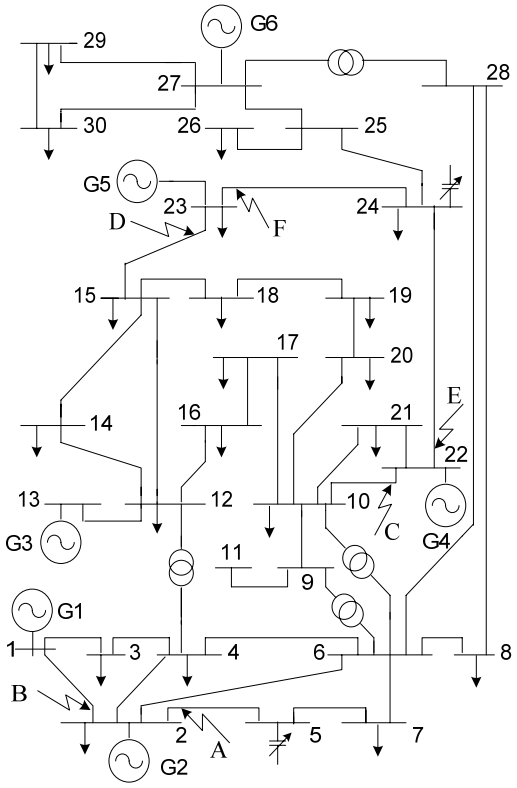

Fig. 4.5 Single-line diagram of IEEE 30-bus system

$$MSE = \frac{1}{N}\sum_{i=1}^{N}(t_i - a_i)^2 \tag{4.1}$$

where

t_i is the i-th actual output.

a_i is the i-th output value from the neural network.

N is the total number of patterns in the corresponding sets (training or testing sets).

One of the problems that occur during neural network training is so called overfitting. As known, even though the number of neurons in the hidden layer should be large enough to model the complex function, the too large number of neurons can cause overfitting leading to degradation of network generalization. Besides, the error on the training sets is driven to a very small value, but when new data is presented to the network, the error becomes very large. The network has memorized the training patterns, but it is not learned to generalize to the new patterns. To alleviate this problem, the early stopping [6] is adopted in the training process. In this technique, the available data is divided into two subsets. The first subset is the training set, which is used for computing the gradient and updating the weights and biases of the network. The second subset is the validation set. The error on the validation sets is monitored during the training process. The validation error normally decreases during the initial phase of training, as does the training set error. However, when the network begins to overfit the data, the error on the validation sets typically begins to rise. When the validation error increases for a specified number of iterations, the training is stopped, and the weights and biases at the minimum of the validation error are returned.

The mechanism of the conventional training and the training with early stopping can be shown in Fig. 4.6. The following section will show the results of the proposed neural network based on the training process with and without the validation sets.

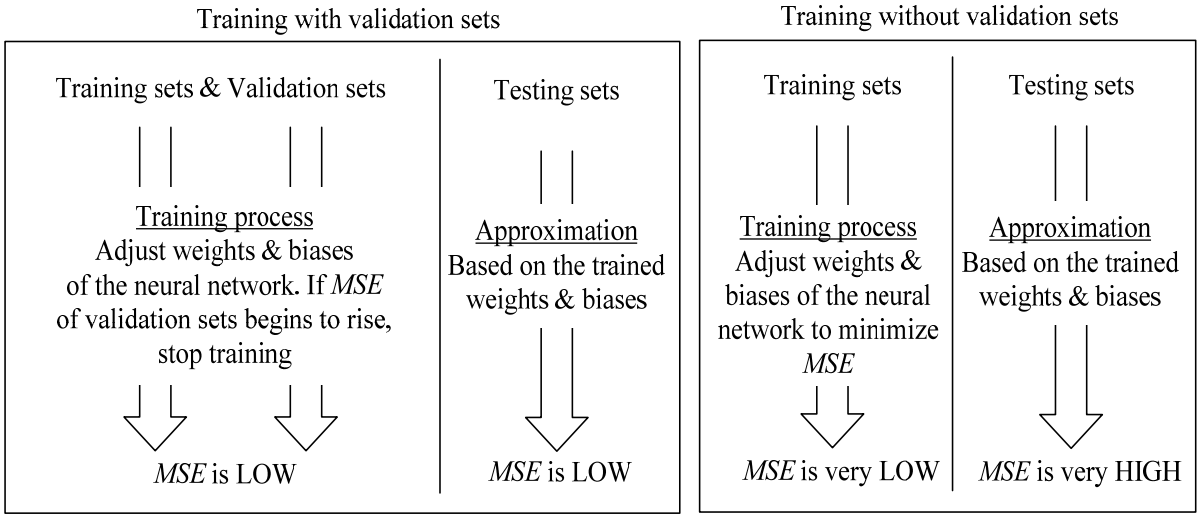

Fig. 4.6 Mechanism of the training with and without the validation sets

Table 4.1 Performance of the proposed network without validation sets

Architecture	$MSE \times 10^{-3}$	
	Training (3000 sets)	Testing (1000 sets)
16/25/1	0.0146	8.17
16/30/1	0.0125	13.60
16/35/1	0.00970	5.78
16/40/1	0.00815	4.10
16/45/1	0.00419	9.09

Table 4.2 Performance of the proposed network with validation sets

Architecture	$MSE \times 10^{-3}$			The number of MIs	
	Training	Validation	Testing	Without thresholds	With thresholds
16/20/5/1	0.303	1.440	1.619	61	9
16/25/5/1	0.445	1.607	1.555	68	15
16/30/5/1	0.095	1.470	1.550	31	6
16/35/5/1	0.568	1.834	1.664	73	25
16/40/5/1	0.435	1.448	1.619	57	19

4.3.1 Single contingency

Only contingency *A* at the end of line 2-5 is considered. The inertia constants (*H*) of all generators are set to 10 s for G1 and 13 s for G3 and 3 s for G2 and G4–G6.

Training without validation sets

The early stopping is not used in this section. The proposed network is trained with 3000 training sets for the contingency *A*. After that, 1000 testing sets are used to evaluate the error of the trained network. The number of epochs is set to 1000. In this section, five different network architectures are trained to observe the performance of the neural network. The architecture 16/25/1 means that there are 16 input neurons, 25 neurons in a hidden layer and one neuron of the output. Please note that in this training, a single hidden layer provides the better performance than two hidden layers.

Table 4.1 shows the performance (*MSE*) of five different numbers of neurons. The *MSE* of the training sets drops when the number of neurons becomes larger. The lowest number of neurons of 25 has the highest error during training but has the moderate performance for testing sets. On the contrary, the largest number of neurons of 45 provides the smallest *MSE* for training sets but the second worst for testing sets. These results indicate that too high number of neurons overfits the training sets and degrades the generalization of the network while too small number of neurons cannot model the difficult function. In addition, from the table the difference of *SME* of the training sets and testing sets is significant. Obviously, without the early stopping, the trained network has the overfitting problem as mentioned earlier.

Training with validation sets (Early stopping)

The early stopping is used in this section to avoid the mentioned overfitting problem. Different from the previous section, in this training two hidden layers are selected in the architecture of the proposed neural network since the two hidden layers provide the better performance than a single hidden layer.

Table 4.2 shows the *MSE* of the five different network architectures trained with 3000 training and 1000 validation sets when the contingency *A* is considered. Moreover, the *MSE* of the independent 1000 testing sets, which are not used during the training process, is given to compare the performance of different architectures. Besides, out of 5000 sets (training + validation + testing), the number of misclassified individuals (MIs), i.e. the individual actually leads to *stable* case but the neural network classifies it into the *unstable* region, and vice versa, is given for both with and without the threshold cases. The thresholds L_1 and L_2 are here set to 0.45 and 0.55. The architecture 16/20/5/1 means that there are 16 input neurons, 20 neurons in the first hidden layer, 5 neurons in the second hidden layer, and one neuron of the output.

From the table, the architecture 16/30/5/1, which offers the smallest *MSE* for both training and testing sets and the smallest number of MIs, is chosen to estimate the transient stability in the next session of TSCOPF results. Note that the 6 misclassified individuals are 0 from training sets, 4 from validation sets and 2 from testing sets. The overall percentage of misclassification of the selected network is 0.12%. In addition, all 6 misclassifications are safe for system operator, since all of them are the case that the system is *stable* but the neural network classifies it into the *unstable* region. It is very harmful if the system is *unstable* but the neural network classifies it into the *stable* region.

Comparing between Tables 4.1 and 4.2, the early stopping helps improving the performance of the proposed network (good network generalization). In the training process without validation sets, even though the *SME* of the training sets is driven to a very small value, but the *SME* of testing sets (new sets) is very high. On the other hand, in the training process with validation sets, the *SME* of the testing sets is quite low for all architectures.

4.3.2 Multi-contingencies

Six single contingencies at points *A*, *B*, *C*, *D*, *E*, and *F* shown in Fig. 4.5 are considered in the simulation. The inertia constants (*H*) are set to 4 s for G1 and 5.2 s for G3 and 1.2 s for G2 and G4–G6. The early stopping is applied in the training process.

Table 4.3 shows the *MSEs* of the 12 different network architectures trained with 6000 training and 2000 validation sets when the contingency *A* is considered. Moreover, the *MSEs* of the independent 2000 testing sets, which are not used during the training process, are given to compare the performance of different architectures. From the table, although most of the architectures with two hidden layers provide the smaller *MSE* for the training sets than do ones with one hidden layer, they are not accurate for the testing sets. Here the architecture 16/25/1, which offers the smallest *MSEs* for both validation and testing sets, is chosen to estimate the transient stability for all contingencies.

Table 4.3 Comparison of *MSEs* of 12 different architectures

Architecture	Training	Validation	Testing
16/15/1	0.00156	0.00224	0.00267
16/15/5/1	0.00124	0.00236	0.00247
16/20/1	0.00131	0.00213	0.00263
16/20/5/1	0.00118	0.00226	0.00258
16/25/1	0.00145	0.00205	0.00196
16/25/5/1	0.00108	0.00251	0.00336
16/30/1	0.00142	0.00279	0.00270
16/30/5/1	0.00183	0.00236	0.00298
16/35/1	0.00139	0.00257	0.00258
16/35/5/1	0.00192	0.00298	0.00361
16/40/1	0.00145	0.00273	0.00299
16/40/5/1	0.00126	0.00270	0.00352

Table 4.4 *MSEs* and the number of MIs for all contingencies

Contingency	*MSE*			The number of MIs	
	Training	Validation	Testing	Without thresholds	With thresholds
A	0.00145	0.00205	0.00196	117	39
B	0.00072	0.00174	0.00183	68	34
C	0.00020	0.00049	0.00076	38	7
D	0.00024	0.00070	0.00042	53	4
E	0.00016	0.00025	0.00020	29	1
F	0.00015	0.00028	0.00031	48	0

Based on the chosen architecture, Table 4.4 gives *MSEs* of 6000 training, 2000 validation and 2000 testing sets for all contingencies after training. Out of 10000 individuals, the number of misclassified individuals (MIs) is also given for both with and without the threshold cases. The thresholds L_1 and L_2 are set to 0.4 and 0.6 for contingency A and 0.45 and 0.55 for contingencies B–F. Obviously, the introduced thresholds can greatly decrease the number of MIs. Besides, the percentage of misclassification after setting the thresholds is less than 0.5% for all contingencies, e.g. 0.39% for the contingency *A* (39 out of 10000 individuals). The trained neural networks here will be used for the MC-TSCOPF problem.

4.4 EP-Based Methods & Proposed ANN for TSCOPF

To calculate the fitness value of individual during the search process of the proposed EP methods for TSCOPF problem, each individual is needed to perform power flow calculation and transient stability assessment by time domain simulation as earlier described in Chapter 3.2.3. From Fig. 3.3, the more the number of contingencies is considered, the more frequent the time domain simulation is performed. It can be imagined how huge the computational load will be when the EP-based methods are applied to solve MC-TSCOPF problem.

To alleviate the mentioned problem, the proposed neural network will be inserted into the fitness evaluation process of the EP-based methods to reduce the utilization of time domain simulation while the accuracy of transient stability evaluation is still maintained at an acceptable level. When the proposed neural network is incorporated into the EP-based methods, the transient stability assessment will change as shown in Fig. 4.7. First, the individual will be sent to perform AC power flow calculation to obtain all variables in the system including the active power generation at the slack bus (P_{G1}). Please note that in IEEE 30-bus system, bus no. 1 is the slack bus. Next, each individual and its corresponding active power at slack bus will be used as the input of the proposed neural network already trained for each contingency. The output (stability degree) of the proposed neural network with the predefined thresholds L_1 and L_2 for each

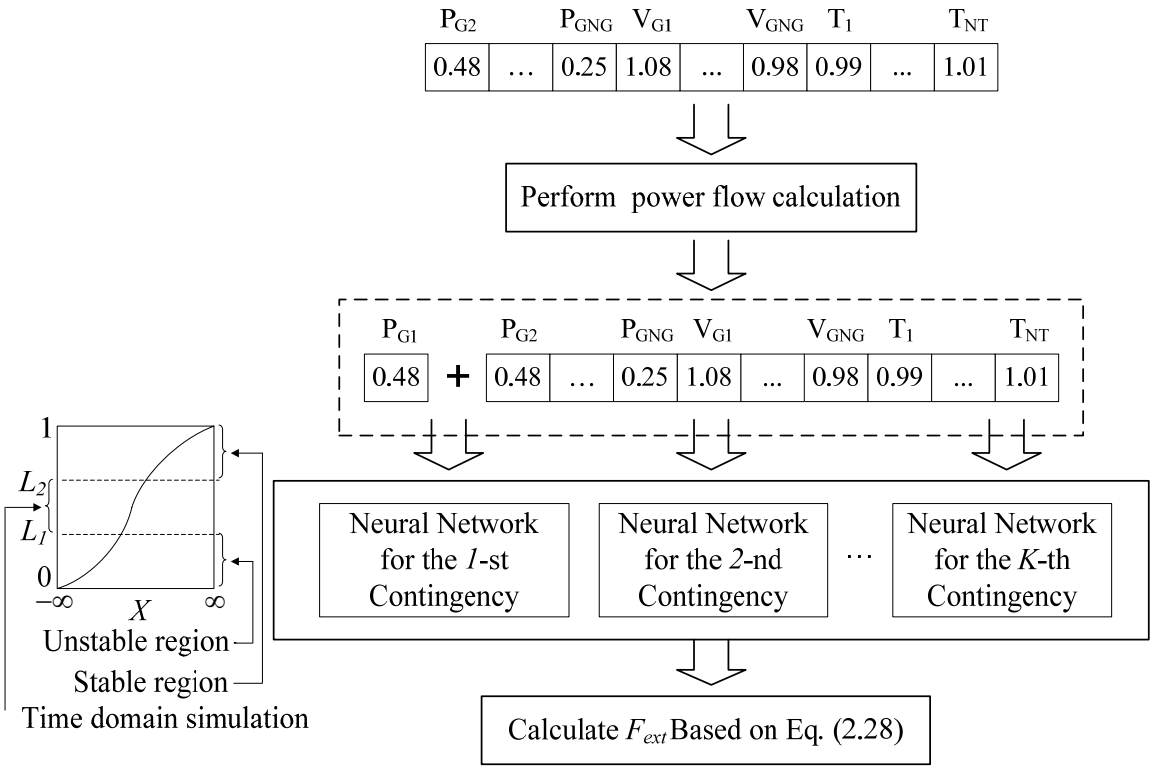

Fig. 4.7 The fitness evaluation process when the neural network is equipped into EP-based methods

contingency is then known. If the output is classified in *stable* or *unstable* region, the stability status is immediately identified without the help of time domain simulation. On the other hand, if the output is classified in *critical* region, time domain simulation is performed to trace the generator rotor angle because the stability degree is ambiguous.

To calculate the fitness of the individual, In case of *unstable* evaluated by either the neural network or time domain simulation, since the transient stability limit is considered as the severe constraint, the objective function is penalized by the large number K_R as appeared in Eq. (2.28). Using different values of K_R for different contingencies can give a high or low priority to the particular contingency.

Based on the proposed scheme for transient stability evaluation, it can be expected that the computational time of the EP-based methods for TSCOPF problem can be decreased. This is because even if the approximation time of the neural network is necessary, it is very small compared to the execution time of time domain simulation. In the next chapter, the contribution of the proposed neural network will be elaborated when the EP-based methods incorporating the neural network are applied to solve TSCOPF and MC-TSCOPF problems.

4.5 Summary

This chapter mainly presents the proposed artificial neural network for transient stability assessment in the TSCOPF problem. The input of the network is the individual of the EP-based methods and the active power at the slack bus whereas the output is the stability degree determined by the difference between the maximum rotor angle deviation and transient stability limit. The neural network is combined with time domain simulation to assess whether the system is stable or not after the contingency. The thresholds are set to account for the inherent error of the neural network. Any individual falling into the thresholds (critical region) has to perform time domain simulation to clarify its transient stability status. The advent of the neural network will definitely reduce the computational time of the EP-based methods for TSCOPF, since most of the individuals will be evaluated their stability status immediately by the proposed neural network rather than the time-consuming time domain simulation.

To avoid the overfitting problem normally found during the training process, the early stopping is adopted to terminate the training process when the error of validation sets begins to increase. The performance of the proposed network is tested on the IEEE 30-bus system. The results are categorized into two parts, i.e. training with validation sets (early stopping) and training without validation sets. The results without validation sets show that the more the number of the neurons is, the smaller the *SME* of the training sets will be. However, this can lead to the increase in the *SME* of the testing sets. This trend of the results can be regarded as the overfitting problem. On the other hand, the results with validation sets indicate that even though the error of the training sets is not as small as that obtained by training without validation sets, the error of the testing sets is acceptable. It can be said that the early stopping provides the better network generalization. In addition, the contribution of the thresholds is remarked. From the results, the thresholds can substantially decrease the number of the misclassified individuals. In other words, it can improve the performance of the neural network.

Equipped with the EP-based methods, the trained neural network with the chosen architecture in this chapter will be used in the fitness calculation for the TSCOPF problem. The impacts of the neural network on the TSCOPF solution in terms of computational time and the quality of solution will be reported in the Chapter 5.

References

[1] P. Kundur: Power System Stability and Control, McGraw-Hill, Inc., New York, 1994.

[2] A. A. Fouad and V. Vittal; Power System Transient Stability Analysis Using the Transient Energy Function Method, Englewood Cliffs, NJ: Prentice-Hall, 1992.

[3] A. G. Bahbah and A. A. Girgis, "Input feature selection for real-time transient stability assessment for artificial neural network (ANN) using ANN sensitivity analysis", in *Proc. IEEE Power Industry Computer Applications (PICA) Conf.*, pp. 295-300, 1999.

[4] K. K. Sanyal, "Transient stability assessment using artificial neural network", in *Proc. IEEE Electricity Utility Deregulation, Restructuring and Power Technologies*, 2004.

[5] R. Zimmerman, E. Murillo-Sánchez, and D. Gan: "MATPOWER: a MATLAB Power System Simulation Package", 2006.

[6] Neural Network Toolbox User's Guide*,* the MathWorks, Inc., 2007.

CHAPTER 5

NUMERICAL RESULTS AND DISCUSSION

5.1 Introduction

Three proposed EP-based methods, i.e. the conventional EP, Improved EP (IEP) and Adaptive EP (AEP) explained in Chapter 3 are applied to solve the various types of OPF problems formulated in Chapter 2. The WSCC 9-bus system and IEEE 30-bus system are used as the test systems. The single-line diagrams of the WSCC 9-bus system and IEEE 30-bus system are depicted in Fig. 5.1 and Fig. 5.2. The bus data, line data, generator data, and cost coefficients of the two systems can be found in [1] and [2] respectively. The operating range of all transformers is set between 0.9 and 1.1. Moreover, to demonstrate the effectiveness of the algorithms, three different types of generator fuel cost curve i.e. quadratic cost curve (F_q), piecewise quadratic cost curve (F_p), and quadratic cost curve superimposed by sine component (F_s) are considered. All cost curves are mathematically expressed as follows:

$$F_{qi}(P_{Gi}) = a_i + b_i P_{Gi} + c_i P_{Gi}^2 \tag{5.1}$$

$$F_{pi}(P_{Gi}) = \begin{cases} a_{1i} + b_{1i} P_{Gi} + c_{1i} P_{Gi}^2 & if \;\; P_{Gi,\min} \le P_{Gi} \le P_{Xi} \\ a_{2i} + b_{2i} P_{Gi} + c_{2i} P_{Gi}^2 & if \;\; P_{Xi} < P_{Gi} \le P_{Gi,\max} \end{cases} \tag{5.2}$$

$$F_{si}(P_{Gi}) = a_i + b_i P_{Gi} + c_i P_{Gi}^2 + \left| d_i \sin(e_i (P_{Gi,\min} - P_{Gi})) \right| \tag{5.3}$$

The generator data and cost coefficients represented by Eq. (5.1) of the WSCC 9-bus system can be found in Table 5.1. In this system, the *2*-nd generator (G2) is also modeled by Eq. (5.2) and Eq. (5.3) to represent the combined-cycle unit and valve-point loading effects of the

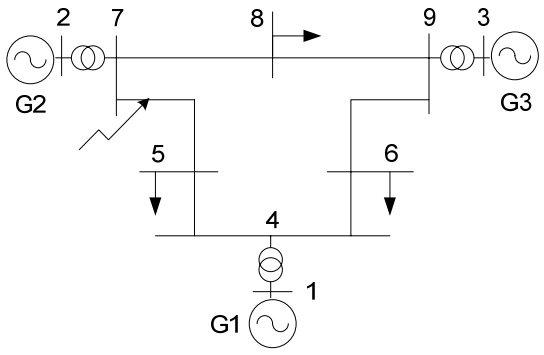

Fig. 5.1 Single-line diagram of WSCC 9-bus system

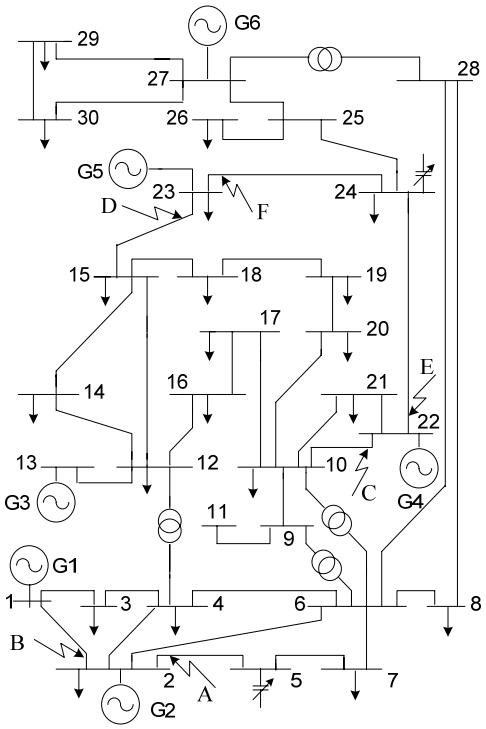

Fig. 5.2 Single-line diagram of IEEE 30-bus system

Table 5.1 The generator data and cost coefficients of WSCC 9-bus system represented by quadratic curve

Bus No.	Active power generation		Cost coefficient		
	Min (MW)	Max(MW)	a ($/hr)	b ($/MW/hr)	c ($/MW^2/hr)
1	10	250	150	5.0	0.1100
2	10	300	600	1.2	0.0850
3	10	270	335	1.0	0.1225

thermal unit respectively [3, 4]. The cost coefficients of the *2*-nd generator when it is modeled by Eq. (5.2), i.e. a_{12}, b_{12}, c_{12}, a_{22}, b_{22}, c_{22}, and P_{x2} are 500, 1, 0.05, 2500, 1.1, 0.065, and 175 respectively. The cost coefficients of the *2*-nd generator when it is modeled by Eq. (5.3), i.e. a_2, b_2, c_2, d_2, and e_2 are 500, 5, 0.05, 700, and 0.036 respectively.

For the IEEE 30-bus system, the generator data and cost coefficients represented by Eq. (5.1) can be found in Table 5.2. In this system, the *2*-nd and *3*-rd generators (Bus no. 2 and 13) are also modeled by Eq. (5.2) and Eq. (5.3). The cost coefficients of the *2*-nd and *3*-rd generators when they are modeled by Eq. (5.2) are given in Table 5.3, and when they are modeled by Eq. (5.3) are given in Table 5.4.

All of the penalty constants, i.e. K_p, K_q, K_v, K_s and K_R which employ to force the related inequality constraints for both systems are set to 1000. The prototype program is developed on MATLAB environment and implemented on a personal computer with Intel Pentium IV 3.8-GHz processor and 512 MB memory.

Table 5.2 The generator data and cost coefficients of IEEE 30-bus system by quadratic curve

Bus No.	Active power generation		Cost coefficient		
	Min (MW)	Max (MW)	*a* ($/hr)	*b* ($/MW/hr)	*c* ($/MW^2/hr)
1	0	80	0	2.00	0.02000
2	0	80	0	1.75	0.01750
13	0	40	0	3.00	0.02500
22	0	50	0	1.00	0.06250
23	0	30	0	3.00	0.02500
27	0	55	0	3.25	0.00834

Table 5.3 Cost coefficients of *2*-nd and *3*-rd generators represented by piecewise quadratic curve

Bus no.	Active power generation		Cost coefficient		
	Min (MW)	Max (MW)	*a* ($/hr)	*b* ($/MW/hr)	*c* ($/MW^2/hr)
2	0	40	0	1.5	0.005
	40	80	0	2	0.02
13	0	20	0	2.0	0.01
	20	40	0	3.5	0.03

Table 5.4 Cost coefficients of *2*-nd and *3*-rd generators represented by quadratic curve with sine component

Bus no.	Active power generation		Cost coefficient				
	Min (MW)	Max (MW)	*a*	*b*	*c*	*d*	*e*
2	0	80	0	2.5	0.01	35	0.118
13	0	40	0	3.7	0.022	21	0.236

5.2 Study of Parameters Used in the EP-Based Method

The IEP6 (mutation and modified discrete crossover) described in Chapter 3.3 is selected to investigate the sensitivity of the parameters of IEP method on the IEEE 30-bus system. The fuel cost function of all generators is represented by the quadratic curve as shown in Eq. (5.1). The generator data and cost coefficients can be found in Table 5.2. Three main parameters of the IEP algorithm, i.e. population size (P), crossover acceptance rate (M), and decaying mutation rate (a), are tuned when the conventional OPF problem is considered. The maximum generation number (G_{max}) is fixed to 200. Table 5.5 shows the IEP6-based OPF results as the IEP6 parameters are varied. The results consist of best, average, worst costs, average run time and standard deviation of 20 independent runs.

From the Table 5.5, It indicates that when the population size increases, the quality of the obtained solutions is improved i.e. lower fuel cost (the best, worst and average costs) and smaller standard deviation. When P increases beyond 4, both fuel cost and standard deviation are improved slightly whereas the computational time is increased considerably. It implies that the value of P equal to 4 is sufficient to get the acceptable solution for the problem. The increase in the computational time is observed to be linearly proportional to the enlargement of the population size. The optimal value of M is found to be 0.4. This number indicates the suitable proportion between mutation and crossover utilization against the OPF problem. The larger the value of M is, the shorter the computational time will be. This emphasizes that the proposed crossover technique takes less processing time than the mutation. Even if the high reliance on the crossover contributes to computational time saving, the solution is degraded (increases in the fuel

Table 5.5 Study of tuning IEP parameters

Parameter		Best cost ($/hr)	Avg. cost ($/hr)	Worst cost ($/hr)	Avg. time (s)	Standard deviation
P when (M = 0.4, a = 0.97, G_{max} = 200)	2	575.31	576.40	579.93	9.95	1.09
	4	574.77	575.35	575.81	19.92	0.25
	8	574.52	575.05	575.45	41.12	0.23
	12	574.45	574.96	575.31	83.47	0.20
M when (P = 4, a = 0.97, G_{max} = 200)	0.2	575.03	575.33	575.92	20.85	0.25
	0.4	574.77	575.35	575.81	19.92	0.25
	0.6	575.10	575.72	577.26	18.07	0.62
	0.8	576.02	577.24	579.93	16.05	1.30
a when (P = 4, M = 0.4, G_{max} = 200)	0.9	576.42	582.32	597.47	13.33	6.12
	0.94	576.04	578.22	590.43	16.51	2.99
	0.97	574.77	575.35	575.81	19.92	0.25
	0.99	576.16	581.65	587.08	23.45	3.13

Table 5.6 Comparison of OPF results among different algorithms

Result	IEP	EP	GA	PSO
Avg. cost ($/hr)	575.35	575.46	576.75	576.69
Worst cost ($/hr)	575.81	575.89	576.91	576.87
Best cost ($/hr)	574.77	575.02	576.64	576.63
Avg. run time (s)	19.92	21.71	-	-

cost and standard deviation) as shown in the table. Therefore, the value of M should be carefully selected in order to prevent too high reliance on the crossover technique. The suitable tuning of M can lead to better or almost the same quality of the solution as the conventional EP with less computational time. At the fixed value of G_{max}, i.e. 200, the value of a, which provides the lowest fuel cost and smallest standard deviation is found to be 0.97. As appeared in Eq. (3.3), the value of a partially impacts the convergence rate of the proposed algorithm. At the specific value of G_{max}, too small value of a leads to the premature of the solution because the distance that an offspring can be moved far away from its parent decreases too rapidly as iteration counter increases. On the other hand, too high value of a results in the slow convergence rate because the solution does not converge smoothly to the local or global optimum. Since the computational time is strongly related to the convergence rate, the high value of a is more time-consuming than the low one as shown in the table. Basically, the problem of too high value of a can be handled by appropriately tuning the value of $G_{\max}$ to guarantee a proper convergence of the solution. In other words, $G_{\max}$ should be increased to avoid the termination of the algorithm before the intensified search is implemented. However, with the increase of $G_{\max}$, longer computational time is required.

In summary, the large value of P always provides the better quality of the solution in terms of the best, worst and average costs and standard deviation of the solution. Nevertheless, the longer computational time is unavoidable. For parameter M, the proper setting is necessary to reduce the simulation time while maintaining the quality of the solution. Lastly, the value of a should be tuned simultaneously with $G_{\max}$ to introduce the diversification at the beginning and then the intensification when the iteration counter is increased.

After the parameter tuning, for the IEEE 30-bus system, the IEP parameters are set as follows: the values of P, M, a, G_{max} are 4, 0.4, 0.97, and 200 respectively. The conventional EP parameters are set as follows: the values of P, a, G_{max} are 4, 0.97, and 200 respectively. The AEP parameters are set as follows: the values of a, G_{max} are 0.97, and 200 respectively.

To investigate the effectiveness of the proposed algorithm, Table 5.6 shows a comparison of OPF results solved by IEP and those solved by the conventional EP, Genetic Algorithm (GA) and Particle Swamp Optimization (PSO). The proposed algorithm can obtain the lower fuel cost than the others. Besides, the computational time of IEP is less than that of EP. Note that the results solved by GA and PSO are reported in [5] and for the reason that GA and PSO are run on the different CPU, the run time of those methods is not inserted in the table.

5.3 Results of the Conventional OPF

The EP-based algorithms are tested on the IEEE 30-bus system. The numerical examples are divided into three cases as follows:

Case 1: The cost curves of all generators in the IEEE 30-bus system are represented by Eq. (5.1). The generator data and cost coefficients can be found in Table 5.2.

Case 2: The cost curves of *2*-nd and *3*-rd generators are replaced by Eq. (5.2). The cost coefficient of *2*-nd and *3*-rd generators can be found in Table 5.3.

Case 3: The cost curves of *2*-nd and *3*-rd generators are replaced by Eq. (5.3). The cost coefficient of *2*-nd and *3*-rd generators can be found in Table 5.4.

The OPF results of Case 1 solved by the conventional EP, IEPs (referred to Table 3.1) and sequential quadratic programming (SQP) are tabulated in Table 5.7. They consist of the average, worst, best solutions in terms of the total generator fuel cost, standard deviation of cost and average computational time from 20 runs without any limit violation. The results show that the conventional EP and the IEP methods can obtain the better OPF solution (even the worst cost) than SQP, but as expected the EP and IEP methods require more computational time. Note that the solution of OPF problem by SQP is solved by MATPOWER software [2] which is capable of handling only the quadratic cost function. From the table, it is obvious that all IEP-based methods require less computational time than the conventional EP. In term of the best cost, the total fuel costs of IEP1, IEP2, IEP4, IEP5, and IEP6 are slightly cheaper than EP where IEP6 provides the cheapest cost of 574.77 $/hr. Moreover, the IEP6 can obtain the better result than that of PSO and GA, both of which are also based on the evolutionary computation. The optimal solutions of 576.63 and 576.64 $/hr solved by PSO and GA respectively are reported in [5]. The standard deviation and average cost of IEP6 are the lowest among all algorithms except for SQP. IEP3 is the fastest heuristic method, but it has the worst performance in obtaining the optimal solution.

Table 5.8 shows the OPF results from 20 runs without any limit violation in Case 2. It is also evident that all IEP-based techniques are faster than the conventional EP similar to the results reported in Case 1. In terms of the best cost, the performances of all IEP methods are slightly better than EP. In Case 2, IEP5 can find the lowest fuel cost of 526.52 $/hr and has the best performance in terms of the average cost. IEP3 still becomes the fastest algorithm but it has the poorest quality of the solution among the IEP methods.

Table 5.7 OPF results of IEEE 30-bus system with various methods in Case 1

Results	SQP	EP	IEP1	IEP2	IEP3	IEP4	IEP5	IEP6
Avg. cost ($/hr)	-	575.46	575.70	575.64	575.83	575.87	575.63	575.35
Worst cost ($/hr)	-	575.89	576.59	576.63	576.39	576.65	576.36	575.81
Best cost ($/hr)	576.89	575.02	574.93	574.94	575.15	574.87	574.88	574.77
Standard deviation	0.00	0.27	0.40	0.37	0.35	0.48	0.42	0.25
Avg. run time (s)	3.73	21.71	19.77	19.88	19.42	19.93	20.01	19.92

Table 5.8 OPF results of IEEE 30-bus system with various methods in Case 2

Results	EP	IEP1	IEP2	IEP3	IEP4	IEP5	IEP6
Avg. cost ($/hr)	528.87	527.87	528.00	527.86	527.69	527.63	527.72
Worst cost ($/hr)	529.68	529.67	529.20	528.72	529.70	529.29	528.63
Best cost ($/hr)	527.91	526.67	526.95	527.01	526.68	526.52	526.96
Standard deviation	0.49	0.85	0.78	0.47	0.76	0.79	0.48
Avg. run time (s)	22.33	20.39	20.34	19.90	20.60	20.56	20.41

Table 5.9 OPF results of IEEE 30-bus system with various methods in Case 3

Results	EP	IEP1	IEP2	IEP3	IEP4	IEP5	IEP6
Avg. cost ($/hr)	606.89	606.48	606.33	606.87	606.05	606.48	606.38
Worst cost ($/hr)	609.90	609.01	609.00	609.29	609.69	609.07	608.86
Best cost ($/hr)	604.85	604.61	604.70	605.06	604.23	604.55	604.75
Standard deviation	1.45	1.06	1.29	1.06	1.45	1.18	1.17
Avg. run time (s)	22.23	19.89	20.00	19.53	20.05	20.14	20.18

Table 5.9 shows the OPF results from 20 runs without any limit violation in Case 3. It is similar to Cases 1 and 2 that all IEP-based techniques are faster than the conventional EP. In terms of the best, averagre, and worst costs, the performances of all IEP methods except for IEP3 are slightly better than EP. In Case 3, IEP4 can obtain the lowest fuel cost of 604.23 $/hr and has the best performance in terms of the average cost. IEP3 still has the poorest performance but it is the fastest algorithm among IEP methods.

Based on the results in Tables 5.7, 5.8 and 5.9, it can conclude that almost all of the IEP-based methods except for IEP3 (Arithmetical Crossover) outperform the conventional EP in terms of both computational time and the quality of the solution (the best cost) when applied to solve OPF with convex and non-convex objective functions. The reduction in calculation time of IEP algorithms comes from the fact that the crossover operators used to generate offspring are simpler than the mutation operator. The difference of computational time between EP and IEP will be significant when P and G_{max} are increased, because the possibility of using crossover techniques instead of mutation operator is augmented. In IEP2, IEP5, and IEP6, the created offspring is the combination of control variables from two selected parents without moving their values whereas the crossovers used in IEP1, IEP3, IEP4 introduce more flexible search template in IEP i.e. sometimes the offspring is created without the guidance of parent fitness value and iteration counter. This can prevent the premature of the solutions and avoid to be trapped in to a local optimum.

The optimal operating points of the best OPF solution solved by IEP6 in Case 1, IEP5 in Case 2, and IEP4 in Case 3 are shown in Table 5.10.

Table 5.10 Optimal operating points based on OPF results in all cases

	Case 1 (IEP6)	Case 2 (IEP5)	Case 3 (IEP4)
P_{G1} (MW)	43.56	45.58	46.47
P_{G2} (MW)	57.17	39.99	53.24
P_{G3} (MW)	16.76	20.00	13.32
P_{G4} (MW)	23.10	23.52	24.32
P_{G5} (MW)	16.22	18.49	18.03
P_{G6} (MW)	34.87	44.15	36.54
V_{G1} (p.u.)	1.04	1.02	1.03
V_{G2}(p.u.)	1.04	1.01	1.02
V_{G3} (p.u.)	1.06	1.08	1.05
V_{G4} (p.u.)	1.02	1.03	1.04
V_{G5} (p.u.)	1.03	1.04	1.05
V_{G6}(p.u.)	1.04	1.06	1.06
T_1 (bus 6-9)	1.01	0.93	0.96
T_2 (bus 6-10)	0.95	0.99	1.03
T_3 (bus 4-12)	1.00	1.02	1.04
T_4 (bus 28-27)	1.09	1.08	1.08
Total fuel cost ($/hr)	574.77	526.52	604.23

Table 5.11 Comparison of OPF results solved by AEP and EP

Result	Case 1		Case 3	
	AEP	EP	AEP	EP
Avg. cost ($/hr)	575.00	575.05	605.94	605.63
Worst cost ($/hr)	575.28	575.45	607.58	608.63
Best cost ($/hr)	574.41	574.52	603.92	604.33
Standard deviation	0.22	0.23	0.93	1.13
Avg. population size	5.43	8	6.10	8
Avg. run time (s)	31.11	41.12	35.10	43.84

Next, the results of OPF solved by the conventional EP and AEP will be compared. Table 5.11 shows the OPF results of 20 independent runs solved by AEP. Here, only results in Case 1 and Case 3 are investigated. To show the effectiveness of AEP, the OPF results solved by the conventional EP with $P = 8$ are also given. The results show AEP can obtain the cheaper fuel cost and requires the shorter computational time than does EP in both cases. The reason why AEP spends less computational time than EP is because the average population size of AEP is smaller than that of EP.

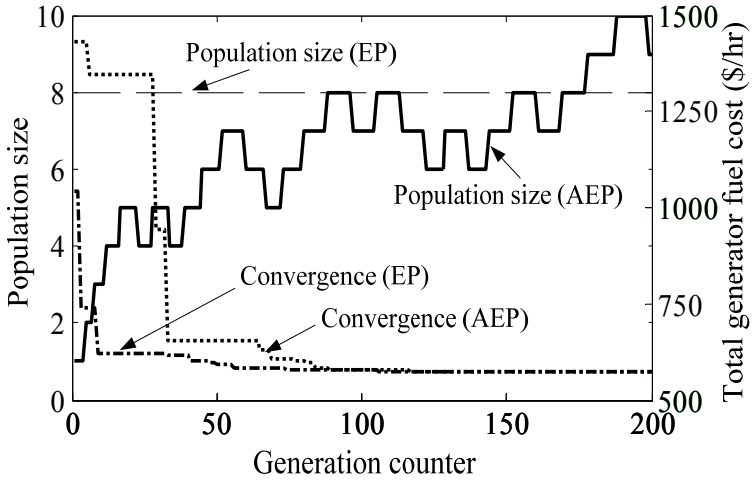

Fig. 5.3 Population size and convergence of EP and AEP in Case 1

Based on the AEP and EP best solutions in Case 1, the population size and convergence are plotted in Fig. 5.3. From the figure, it can be observed that AEP converges to the optimal solution slower than EP, since the population size of AEP is much smaller than that of EP during the first 100 generations. Nevertheless, after 200 generations, AEP can provide the lower fuel cost than does EP.

From the OPF results based on the conventional EP, IEP, and AEP, It can be seen that the new versions of EP methods, AEP and IEP, outperform the conventional EP in both locating the optimal solution and saving the computational time, especially AEP where the population size does not have to predefine. In the following sections, the effectiveness of IEP and AEP will be clarified again by the more complicated optimization problems, i.e. TSCOPF.

5.4 Results of Transient Stability Constrained OPF (TSCOPF)

5.4.1 TSCOPF on WSCC 9-Bus System

Firstly, the WSCC 9-Bus system depicted in Fig. 5.1 is used as the simple test system. The control variables for this system are active power generation outputs of all generator buses excluding slack bus (bus 1) and voltage magnitudes of all generator buses. The numerical examples are divided into three cases as follows:

Case 1.1: The cost curves of all generators in WSCC 9-bus system are represented by Eq. (5.1). The generator data and cost coefficients can be found in Table 5.1.

Case 1.2: The cost curve of *2*-nd generator is replaced by Eq. (5.2).

Case 1.3: The cost curve of *2*-nd generator is replaced by Eq. (5.3).

A single contingency with three-phase grounding fault near bus 7 at the end of the line 5-7 at t = 0 s is considered. The fault is cleared at t = 0.27 s for Case 1.1, 0.19 s for Cases 1.2 and 0.16 s for Case 1.3. To observe the rotor oscillation with two swings, the maximum integration period used is 2 s. The integration time step is 0.01 s and δ_{MAX} is 100 degrees. For this system, the EP parameters are set as follows: P, a, G_{max} are 4, 0.99, and 800 respectively.

The conventional EP is applied to solve TSCOPF problem on this system. The EP-based OPF and TSCOPF results of all cases consisting of the average, worst, best solutions in terms of the total generator fuel cost, and average run time from 20 runs without any limit violation including stability limit are tabulated in Table 5.12. The control variables and cost differences based on the best solution between TSCOPF and OPF are also shown. Besides, the OPF results by a conventional method (SQP) are given to compare with EP-based OPF results in Case 1.1. From Table 5.12, the proposed EP algorithm can obtain the same the OPF solution (the best solution) as the conventional method, but as expected it requires longer computational time. The

Table 5.12 EP-based TSCOPF and OPF results of WSCC 9-bus system in Cases 1.1–1.3

	Case 1.1			Case 1.2		Case 1.3	
	SQP	OPF	TSCOPF	OPF	TSCOPF	OPF	TSCOPF
P_{G1} (MW)	89.80	89.80	96.06	68.62	73.91	63.80	73.81
P_{G2} (MW)	134.32	134.32	127.32	175.00	168.71	184.53	184.53
P_{G3} (MW)	94.19	94.19	94.76	75.57	76.36	71.20	61.15
V_{G1} (p.u.)	1.10	1.10	1.09	1.10	1.09	1.09	1.04
V_{G2} (p.u.)	1.10	1.10	1.10	1.10	1.10	1.09	1.10
V_{G3} (p.u.)	1.09	1.09	1.09	1.09	1.09	1.09	1.10
Avg. cost ($/hr)	-	5297.00	5306.81	4328.47	4338.68	5072.54	5100.49
Worst cost ($/hr)	-	5298.55	5307.99	4330.87	4339.67	5075.25	5103.76
Best cost ($/hr)	5296.69	5296.69	5305.82	4327.48	4337.88	5069.22	5097.68
Cost diff. ($/hr)	-	-	9.13	-	10.39	-	28.46
Avg. run time (s)	1.77	9.04	429.03	9.25	465.03	9.21	466.07

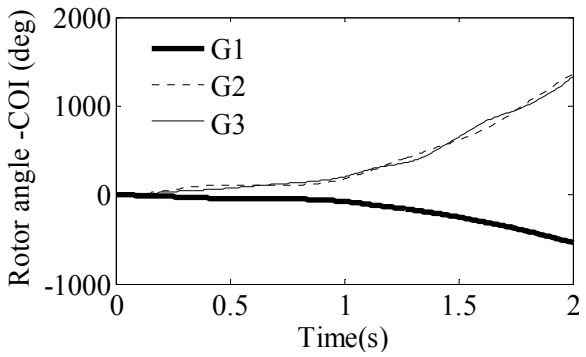

Fig. 5.4 Rotor angle curves based on OPF solution in Case 1.1 on WSCC 9-bus system

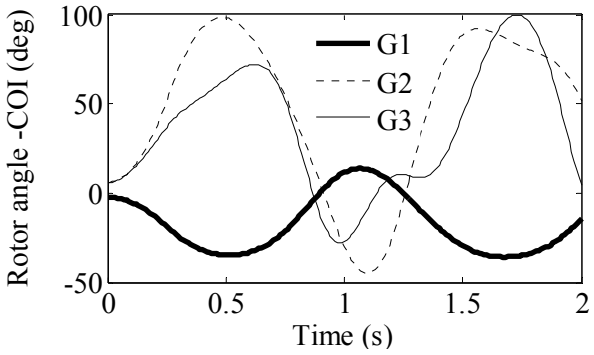

Fig. 5.5 Rotor angle curves based on TSCOPF solution in Case 1.1 on WSCC 9-bus system

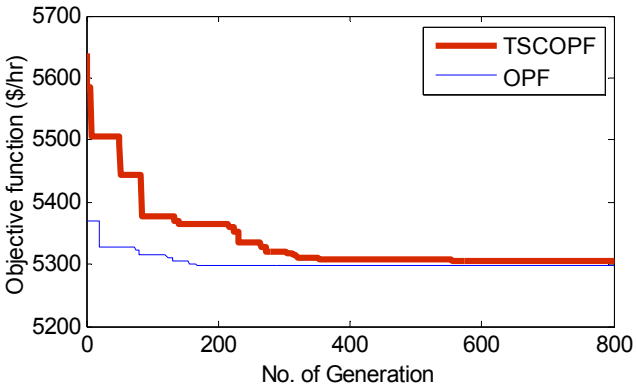

Fig. 5.6 Convergence comparison of TSCOPF and OPF solutions in Case 1.1

difference between the best and worst costs of both TSCOPF and OPF is significant in Case 1.3 compared to Cases 1.1 and 1.2, because in Case 1.3 there are many local optimums in optimization problem introduced by the sine component whereas in Cases 1.1 and 1.2, the cost curve is smooth and convex.

The rotor angles with respect to COI of all generators based on OPF and TSCOPF solutions in Case 1.1 are plotted in Figs. 5.4 and 5.5. It is obvious that the operating point from OPF can not maintain transient stability. In order to guarantee transient stability after the contingency, the

operating points have to shift from OPF to TSCOPF solutions leading to the additional costs of 9.13 $/hr, 10.39 $/hr, and 28.46 $/hr in Cases 1.1, 1.2, and 1.3 respectively. The computational times for TSCOPF highly increase from OPF, since the time domain simulation is performed for every individual during EP iterations. The rotor angles of all generators based on OPF and TSCOPF solutions in Cases 1.2 and 1.3, which are not shown here, behave the same as Case 1.1.

The convergence characteristics of EP for Case 1.1 when it is applied to solve TSCOPF and OPF are shown in Fig. 5.6. From the figure, the convergence speed for TSCOPF is much slower than that for OPF. This comes from the transient stability constraints that introduce the complexity in the problem.

5.4.2 TSCOPF on IEEE 30-Bus System

The IEEE 30-bus system is used as the practical test system to test the proposed EP-based methods. The single-line diagram of the IEEE 30-bus system is depicted in Fig. 5.2. The control variables are active power generation outputs of all generator buses excluding slack bus (bus 1), voltage magnitudes of all generator buses, and tap setting of all transformers. The numerical examples for this system are divided into three cases as follows:

Case 2.1: The cost curves of all generators in the IEEE 30-bus system are represented by Eq. (5.1). The generator data and cost coefficients can be found in Table 5.2.

Case 2.2: The cost curves of *2*-nd and *3*-rd generators are replaced by Eq. (5.2). The cost coefficient of *2*-nd and *3*-rd generators can be found in Table 5.3.

Case 2.3: The cost curves of *2*-nd and *3*-rd generators are replaced by Eq. (5.3). The cost coefficient of *2*-nd and *3*-rd generators can be found in Table 5.4.

Single Contingency

A single contingency (A) with three-phase grounding fault near bus 2 at the end of the line 2-5 at t = 0 s is considered. The fault is cleared at t = 0.35 s for all cases. To observe the rotor oscillation with two swings, the maximum integration period is 1.5 s. The integration time step is 0.01 s and δ_{MAX} is 120 degrees. The inertia constants (H) of all generators are set to 10 s for G1 and 13 s for G3 and 3 s for G2 and G4–G6.

Firstly, the conventional EP is applied to solve TSCOPF problem on this system. Table 5.13 shows the average, worst, best solutions in terms of the total generator fuel cost, and average run time from 20 runs without any limit violation. The control variables and cost differences based on the best solution between TSCOPF and OPF are also given. From this table, The EP algorithm can obtain the better OPF solution (Case 2.1) in terms of the total generator fuel cost than the conventional method (SQP). The trend of the solutions is quite similar with that of WSCC 9-bus test system. With the complicated cost curve (Case 2.3), the difference between the best and worse solutions for both OPF and TSCOPF is quite high. The increases of total generator fuel cost of 10.13 $/hr, 3.39 $/hr, and 20.49 $/hr in Cases 2.1, 2.2, and 2.3 respectively are needed in order to maintain the transient stability in the system after the contingency. The computational times of TSCOPF greatly rise up due to time domain simulation.

Table 5.13 EP-based TSCOPF and OPF results of IEEE 30-bus system in Cases 2.1–2.3

	Case 2.1			Case 2.2		Case 2.3	
	SQP	OPF	TSCOPF	OPF	TSCOPF	OPF	TSCOPF
P_{G1} (MW)	41.54	43.70	50.25	45.88	54.15	43.67	58.44
P_{G2} (MW)	55.40	57.28	38.86	39.97	38.49	53.26	26.69
P_{G3} (MW)	16.20	17.04	17.96	19.99	19.90	13.30	13.32
P_{G4} (MW)	22.74	23.16	27.33	22.63	22.11	24.32	28.56
P_{G5} (MW)	16.27	16.55	20.29	19.52	18.43	18.90	23.36
P_{G6} (MW)	39.91	34.01	37.25	44.07	38.89	38.57	41.58
T_1 (bus 6-9)	1.00	0.93	1.02	1.07	1.00	0.92	0.98
T_2 (bus 6-10)	1.00	1.03	0.99	0.94	1.00	0.92	0.98
T_3 (bus 4-12)	1.00	1.02	0.97	0.93	1.02	0.97	0.95
T_4 (bus 28-27)	1.00	1.06	1.04	1.10	1.04	1.09	1.05
Avg. cost ($/hr)	-	575.46	585.83	528.87	532.41	606.89	628.45
Worst cost ($/hr)	-	575.89	586.86	529.68	534.63	609.90	630.91
Best cost ($/hr)	576.89	575.02	585.15	527.91	531.30	604.85	625.34
Cost diff. ($/hr)	-	-	10.13	-	3.39	-	20.49
Avg. run time (s)	3.73	21.71	451.18	22.33	459.60	22.23	459.34

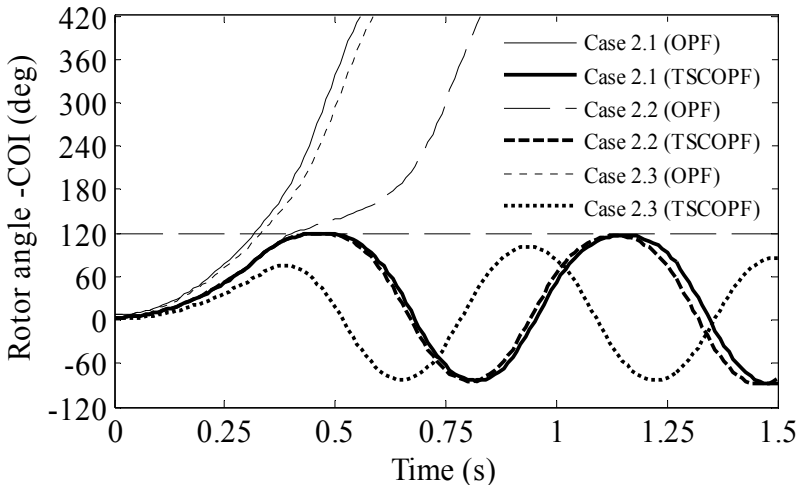

Fig. 5.7 Rotor angle curves with the EP-based OPF and TSCOPF solutions of all cases for IEEE 30-bus system

The rotor angles with respect to COI of only the generator with the largest swing (*2*-nd generator) in all cases based on TSCOPF and OPF solutions are plotted in Fig. 5.7. It is clear that the TSCOPF solution is indispensable. The convergence characteristics of EP based on the best solution for three cases when it is applied to solve both TSCOPF and OPF are plotted in Fig. 5.8. The convergence of EP for OPF is faster for all cases when compared to that of TSCOPF in which additional constraints related to the stability issue are included.

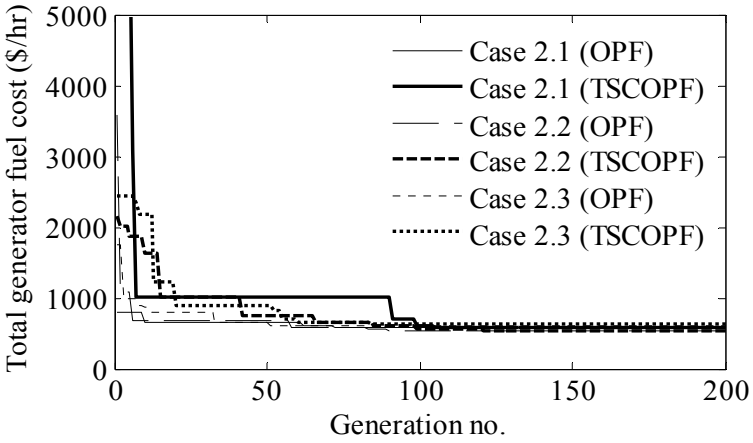

Fig. 5.8 EP convergence comparison of OPF and TSCOPF for all cases

Table 5.14 TSCOPF results of IEEE 30-bus system with three types of cost curves by EP and IEP

	Case 2.1		Case 2.2		Case 2.3	
	EP	IEP	EP	IEP	EP	IEP
P_{G1} (MW)	50.25	48.27	54.15	52.39	58.44	57.46
P_{G2} (MW)	38.86	38.50	38.49	39.22	26.69	26.67
P_{G3} (MW)	17.96	19.72	19.90	19.95	13.32	13.45
P_{G4} (MW)	27.33	25.88	22.11	26.82	28.56	28.84
P_{G5} (MW)	20.29	20.39	18.43	14.97	23.36	23.61
P_{G6} (MW)	37.25	39.02	38.89	38.66	41.58	41.76
T_1 (bus 6-9)	1.02	0.98	1.00	0.97	0.98	0.98
T_2 (bus 6-10)	0.99	0.97	1.00	1.04	0.98	0.98
T_3 (bus 4-12)	0.97	1.01	1.02	1.04	0.95	0.99
T_4 (bus 28-27)	1.04	1.03	1.04	1.05	1.05	1.02
Avg. cost ($/hr)	585.83	584.90	532.41	531.79	628.45	628.01
Worst cost ($/hr)	586.86	586.11	534.63	533.95	630.91	629.78
Best cost ($/hr)	585.15	584.13	531.30	530.50	625.34	625.23
Standard deviation	0.50	0.52	0.99	0.94	1.85	1.23
Avg. run time (s)	451.18	445.20	459.60	450.24	459.34	452.29

Next, IEP with modified discrete crossover (IEP6) is applied to solve TSCOPF when contingency *A* is considered. The TSCOPF results solved by IEP are tabulated in Table 5.14. The results of EP are also provided in the same table for comparison. From the table, IEP can locate the lower objective function than EP for all cases. The standard deviation of IEP in Cases 1 and 2 is almost the same as that of EP whereas the standard deviation of IEP in Case 3 is smaller than that of EP. This implies that IEP works well with the complicated objective function. In addition, IEP can find the optimal solution with shorter computational time than EP.

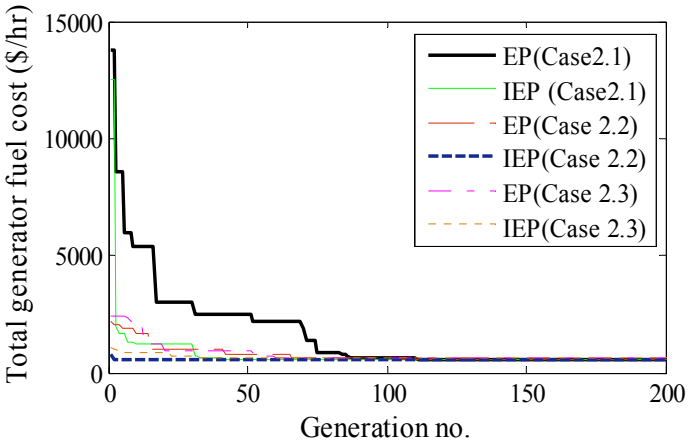

Fig. 5.9 Convergence speed comparison of EP and IEP for TSCOPF problem

The convergence speeds of EP and IEP for TSCOPF in all cases are drawn in Fig. 5.9. Evidently, IEP converges to the solution faster than EP in all cases. The fast convergence of IEP emphasizes the superiority of IEP over the conventional EP.

From the results of IEP and EP, the quality of solution of TSCOPF in terms of the difference between the best and worst cost is slightly worse than that of OPF. Besides, the computational time of TSCOPF exponentially increases from that of OPF due to time domain simulation needed. The maximum integration periods for time domain simulation, which are 2 s in WSCC 9-bus system and 1.5 s in IEEE 30-bus system, play an important role on this issue. The implementation of the EP-based methods on parallel computers is a good option to alleviate the computation load in TSCOPF.

The two main parameters i.e. G_{max} and P have great effects on both the quality of solution and computational time. With high values of the parameters, although the quality is improved, the computational load is heavily augmented. The value of G_{max} in the WSCC system (G_{max} = 800) is set higher than that in the IEEE system (G_{max} = 200), due to the very large search space of control variables (Limits of active power generation output) in the WSCC system. The penalty constants i.e. K_p, K_q, K_v, K_s and K_R for forcing all related inequality constraints to the objective function should be selected based on the value of the objective function. If the values of the penalty constants are too high, then the real objective function being minimized will be distorted. On the other hand, if the values are too low, then solutions with limit violations will occur.

From the TSCOPF results in the previous session, the computational time for TSCOPF is quite high because time domain simulation is implemented to evaluate the transient stability status for each individual. To alleviate this computational load, the EP is equipped with the proposed artificial neural network explained in Chapter 4 to screen out some individuals, which have very high degrees of stability and instability. Only few individuals having unclear stability degree will be sent to perform time domain simulation. This method is so called Evolutionary Programming incorporating Neural Network (EPNN). When the contingency A is considered, the TSCOPF results in all cases solved by the proposed EPNN and the conventional EP without

Table 5.15 Comparison of TSCOPF results solved by EP and EPNN

	Case 2.1		Case 2.2		Case 2.3	
	EP	EPNN	EP	EPNN	EP	EPNN
Avg. cost ($/hr)	585.83	585.84	532.41	533.12	628.45	628.80
Worst cost ($/hr)	586.86	586.73	534.63	534.39	630.91	630.93
Best cost ($/hr)	585.15	585.12	531.30	531.32	625.34	625.43
Avg. run time (s)	451.18	220.17	459.60	265.55	459.34	206.66
Avg. number of individuals classified in *stable* or *unstable*	-	513	-	438	-	526
Avg. number of individuals classified in *critical*	-	287	-	362	-	274
Total no. individuals	800	800	800	800	800	800
% Time reduction	-	51.20	-	42.22	-	55.01

neural network (reported in Table 5.14) are tabulated in the Table 5.15. All results in the table have no any limit violation.

Table 5.15 confirms that EPNN can lessen the computational burden in EP without loss of the ability to locate the optimum. The 51.20%, 42.22%, and 55.01% decreases of computational time in Cases 2.1, 2.2, and 2.3 can be gained when the neural network is incorporated into the conventional EP. Please note that the total number of individuals of both EP and EPNN is 800, since the population size and maximum generation of them are set to 4 and 200 respectively. From independent 20 runs, the average number of individuals that perform time domain simulation (classified in *critical* region) and do not perform time domain simulation (classified in *stable* or *unstable* region) is also given. The percentage of reduction in computational time directly depends on the number of individuals classified in *stable* or *unstable* region. The number of individuals classified in *stable* or *unstable* region can be increased by setting L_1 and L_2 near the value of 0.5 (Please referred to Chapter 4.2). However, by doing so the obtained solution may violate the transient stability constraint due to the inherent error of the artificial neural network.

Next, to confirm again that the proposed neural network contributes the decrease in the computational time without degrading the quality of the solution, the TSCOPF results solved by AEP will be investigated in the following session. For Cases 2.1 and 2.3, the TSCOPF solutions of 20 independent runs solved by AEP with the neural network (AEPNN) and AEP without neural network are tabulated in Table 5.16. The percentage of utilization of time domain simulation (U_{TDS}) for transient stability assessment and the average population size are also given. The more frequent the time domain simulation is run, the longer the computational time will be. With the help of the neural network, the computational time is decreased around 60 % in Case 2.1 and up to 89 % in Case 2.3 without degrading the quality of the solution. This confirms

Table 5.16 Comparison of TSCOPF results solved by AEPNN and AEP

	Case 2.1		Case 2.3	
	AEPNN	AEP	AEPNN	AEP
Avg. cost ($/hr)	585.00	585.15	625.54	625.76
Worst cost ($/hr)	585.91	585.95	627.71	628.40
Best cost ($/hr)	584.16	584.19	624.21	624.18
Avg. population size	6.48	5.98	6.99	6.69
% U_{TDS}	38.65	100	3.28	100
Avg. run time (s)	235.88	577.73	79.50	711.29
% Time reduction	59.17	-	88.82	-

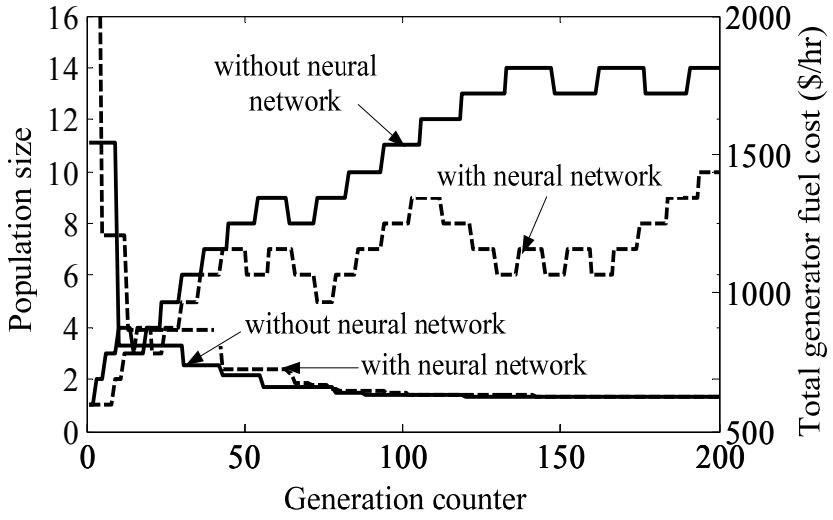

Fig. 5.10 Population size and convergence of AEP of TSCOPF results in Case 2.3

that AEP with the neural network can greatly lessen the computational burden regarding the transient stability constraints without loss of the ability to locate the optimal solution.

Based on the best TSCOPF solutions in Case 2.3, the population size and convergence of AEP with and without the neural network are plotted in Fig. 5.10. From the figure, the convergence speed of both cases is similar, because the population size of both methods is comparatively the same at the first 100 generations.

After the contingency *A*, the rotor angles with respect to COI of the *2*-nd generator (the largest swing) in Cases 2.1 and 2.3 based on the best AEP-based OPF solutions (Table 5.11) and AEPNN-based TSCOPF solutions (Table 5.16) are plotted in Fig. 5.11. It is clear that the neural network applied does not harm the transient stability of the obtained results.

The proposed neural network proves that it can substantially reduce the computational load caused by the transient stability constraints. The EP-based algorithm with the proposed neural

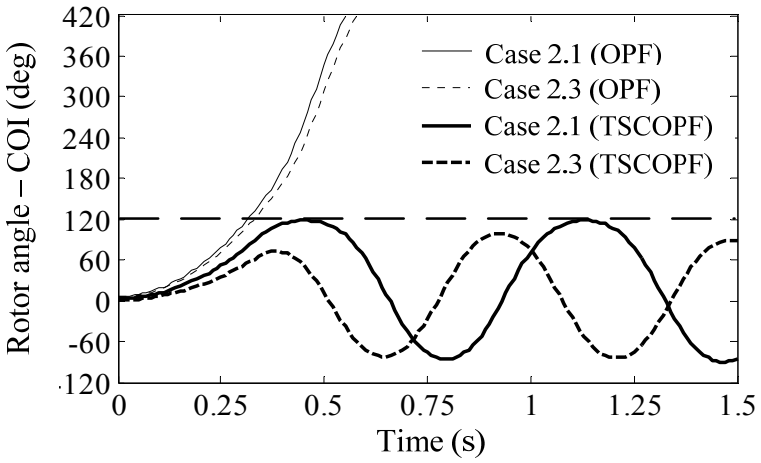

Fig. 5.11 Rotor angle curves based on the best AEP-based OPF and AEPNN-based TSCOPF solutions

network is proved to be a promising method for TSCOPF problem. The following session will investigate the applicability of the proposed EP-based method incorporating the neural network for a multi-contingency TSCOPF (MC-TSCOPF) problem.

Multi-Contingencies

Six single contingencies at points *A*, *B*, *C*, *D*, *E*, and *F* shown in Fig. 5.2 are considered in the simulation. Each contingency is the three-phase grounding fault at t = 0 s and cleared at t = 0.35 s. The maximum integration time is 1.5 s, and δ_{MAX} is 120 degrees. Note that the inertia constants of all generators in the IEEE 30-bus system are modified. The inertia constants (H) are set to 4 s for G1 and 5.2 s for G3 and 1.2 s for G2 and G4–G6. Case 2.1 and Case 2.3 are considered to show the effectiveness of the proposed method in this session.

The IEP6 (mutation and modified discrete crossover) incorporating the proposed neural network (IEPNN) is applied to obtain the MC-TSCOPF solutions. Table 5.17 tabulates the results of OPF, single-contingency TSCOPF, and MC-TSCOPF solved by the IEPNN method in Case 2.1. The results consist of the average, worst, best solutions, average computational times from independent 20 runs, and the control variables of the best solution. Moreover, the average numbers of individuals that perform time domain simulation (classified in *critical* region) and do not perform time domain simulation (classified in *stable* or *unstable* region) against each contingency are given. Note that the column "*A*" in single contingency TSCOPF means the TSCOPF considering only contingency *A* and the column "*A* + *C*" in MC-TSCOPF means TSCOPF considering both the contingencies *A* and *C*. It can be observed that when more contingencies are included in TSCOPF, the fuel cost is increased. The active power output of the generator near the faulted line should be decreased to prevent the transient instability. For example, the active power output of G2 in case "*A*" drops from 57.17 MW of OPF case to 8.61 MW of TSCOPF (*A*) case, since G2 at bus 2 is the closest generator to the contingency *A*. It is also found that the more the individuals are classified in *stable* or *unstable* region, the shorter the

Table 5.17 OPF, single-contingency TSCOPF, and MC-TSCOPF results by IEPNN for Case 2.1

	OPF	Single-contingency TSCOPF						MC-TSCOPF	
		A	*B*	*C*	*D*	*E*	*F*	*A+C*	*A+C+F*
P_{G1} (p.u.)	43.56	71.00	56.32	44.58	43.31	45.07	44.22	72.08	76.58
P_{G2} (p.u.)	57.17	8.61	14.26	59.22	57.96	59.58	59.01	8.97	13.30
P_{G3} (p.u.)	16.76	29.24	30.16	18.18	17.35	17.65	18.41	29.64	34.43
P_{G4} (p.u.)	23.10	28.05	26.55	18.05	23.25	16.80	23.60	17.98	16.67
P_{G5} (p.u.)	16.22	13.11	18.52	16.99	13.94	17.87	11.99	19.39	12.27
P_{G6} (p.u.)	34.87	41.96	46.10	34.98	36.00	34.96	34.65	44.21	39.40
V_{G1} (p.u.)	1.04	1.00	0.99	1.00	1.01	1.01	1.00	1.00	0.98
V_{G2} (p.u.)	1.04	0.99	0.99	0.99	1.01	1.01	0.99	0.99	0.96
V_{G3} (p.u.)	1.06	1.07	1.04	1.09	1.08	1.08	1.07	1.07	1.06
V_{G4} (p.u.)	1.02	1.01	1.01	1.02	1.03	1.03	1.02	1.00	1.01
V_{G5} (p.u.)	1.03	1.03	1.03	1.04	1.04	1.04	1.02	1.02	0.99
V_{G6} (p.u.)	1.04	1.04	1.05	1.03	1.05	1.06	1.03	1.02	1.03
Avg. cost ($/hr)	575.35	641.25	621.66	577.87	575.79	578.73	576.44	643.82	649.74
Worst cost ($/hr)	575.81	642.98	622.91	578.97	576.25	579.69	577.39	645.88	652.96
Best cost ($/hr)	574.77	640.18	620.11	577.15	575.42	577.74	576.02	641.76	645.37
Avg. run time (s)	19.92	214.59	150.53	177.08	110.57	188.32	187.99	375.20	497.71
Avg. number of individuals classified in *stable* or *unstable*	-	475.85	591.80	526.65	651.00	507.70	516.25	477.20(*A*) 587.80(*C*)	478.40 (*A*) 634.15 (*C*) 688.95 (*F*)
Avg. number of individuals classified in *critical*	-	324.15	208.20	273.35	149.00	292.30	283.75	322.80(*A*) 212.20(*C*)	321.60 (*A*) 165.85 (*C*) 111.05 (*F*)

computational time is required. Since the parameters of the proposed method are kept the same for all simulations, the difference between the best and worst solutions in multi-contingency cases is more significant than that in single-contingency or OPF cases.

To compare the performance in terms of computational time, the results of single-contingency TSCOPF and MC-TSCOPF solved by IEP without the proposed neural network are provided in Table 5.18. From Tables 5.17 and 5.18, it is obvious that with the help of the neural network, the computational time is substantially decreased without the degradation of the quality of the solution (average, worst, and best solutions). This again confirms that IEPNN can lessen the computational burden regarding the transient stability constraints without loss of the ability to locate the optimal solution.

Table 5.18 Single-contingency TSCOPF, and MC-TSCOPF results by IEP for Case 2.1

	Single-contingency TSCOPF						MC-TSCOPF	
	A	*B*	*C*	*D*	*E*	*F*	*A+C*	*A+C+F*
Avg. cost ($/hr)	641.34	621.19	578.07	575.82	578.70	576.61	643.99	649.22
Worst cost ($/hr)	642.81	622.96	579.07	576.70	579.72	577.57	645.97	652.68
Best cost ($/hr)	640.10	620.23	577.05	575.48	577.88	576.01	641.53	645.03
Avg. run time (s)	456.62	414.51	423.57	453.43	415.34	435.71	883.31	1254.83

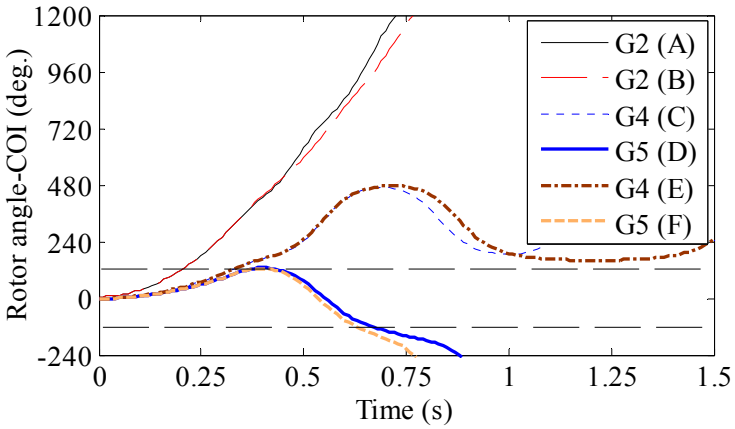

Fig. 5.12 The rotor angle deviation based on OPF solution after the contingencies *A–F*

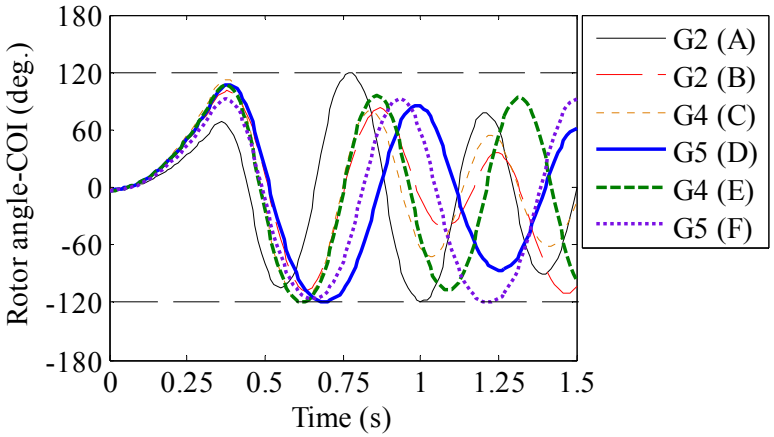

Fig. 5.13 The rotor angle deviation based on TSCOPF solution after the corresponding contingencies *A–F*

Fig. 5.12 sketches the rotor angles with respect to COI based on the OPF solution after the contingencies *A–F*. The rotor angles plotted are only the generator with the largest swing when the corresponding contingencies occur. Fundamentally, the generator, which is closest to the contingency, will deviate from COI with the largest swing. For instance, since the contingency *A*

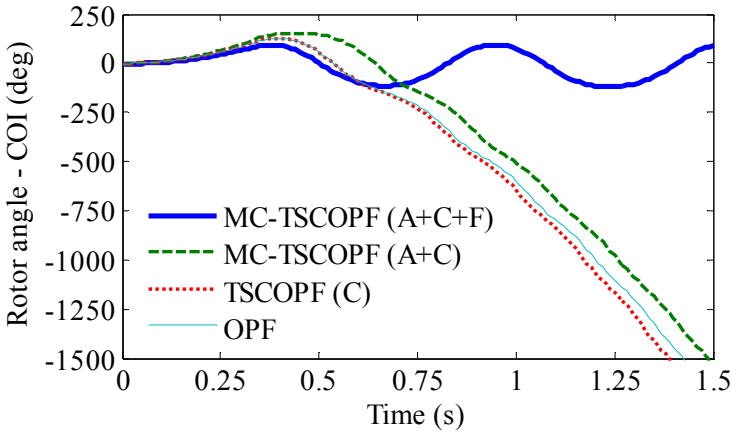

Fig. 5.14 The rotor angle deviation after contingency *F* in Case 2.1

Table 5.19 OPF, single-contingency TSCOPF, and MC-TSCOPF results by IEPNN for Case 2.3

	OPF	TSCOPF	MC-TSCOPF	
		A	*A*+*C*	*A*+*C*+*F*
Avg. cost ($/hr)	606.38	671.91	679.69	700.32
Worst cost ($/hr)	608.86	673.81	681.87	704.42
Best cost ($/hr)	604.75	668.78	676.83	696.85
Avg. run time (s)	20.18	159.06	286.19	391.25
Avg. number of individuals classified in *stable* or *unstable*	-	617.05	614.95(*A*) 580.85(*C*)	666.00(*A*) 597.80(*C*) 682.70(*F*)
Avg. number of individuals classified in *critical*	-	182.95	185.05(*A*) 219.15(*C*)	134.00(*A*) 202.20(*C*) 117.30(*F*)

is close to generator no. 2 (G2), G2 will have the largest swing among all generators. It is comprehensible from this figure that transient stability after the contingencies cannot be expected from the OPF solution. Fig. 5.13 sketches the rotor angles of the largest swing generator with respect to COI based on the single-contingency TSCOPF solutions (cases *A*–*F*) after the corresponding contingency. It indicates that TSCOPF can guarantee the transient stability after the pre-considered contingency.

Fig. 5.14 sketches the rotor angles with respect to COI of only the generator with the largest swing (G5) based on the MC-TSCOPF (*A*+*C*+*F*), MC-TSCOPF (*A*+*C*), TSCOPF (*C*) and OPF after the contingency *F* in Case 2.1. The figure shows that only MC-TSCOPF (*A*+*C*+*F*) can maintain the transient stability against the contingency *F* whereas others cannot. This is because the contingency *F* is not considered in MC-TSCOPF (*A*+*C*), TSCOPF (*C*) and OPF.

Next, Table 5.19 gives the results of OPF, single-contingency TSCOPF, and MC-TSCOPF solved by IEPNN in Case 2.3. To compare the results, Table 5.20 gives the results of single-

Table 5.20 Single-contingency TSCOPF, and MC-TSCOPF results by IEP for Case 2.3

	TSCOPF	MC-TSCOPF	
	A	*A+C*	*A+C+F*
Avg. cost ($/hr)	671.20	679.71	700.48
Worst cost ($/hr)	672.78	682.66	704.81
Best cost ($/hr)	668.96	676.17	696.58
Avg. run time (s)	462.54	860.28	1273.42

contingency TSCOPF and MC-TSCOPF solved by IEP without the neural network. Similar to Case 2.1, IEPNN can greatly reduce the computational time of TSCOPF problem. To give an example, IEPNN can decrease the simulation time from 1273.42 s to 391.25 s leading to approximately 70 % execution time saving for MC-TSCOPF (*A+C+F*). Besides, it can be noticed that the difference between the best and worst costs of OPF, TSCOPF and MC-TSCOPF is significant in Case 2.3 compared to Case 2.1, because in Case 2.3 there are many local optimums in optimization problem introduced by the sine component.

In conclusion, the incorporation of the proposed neural network into IEP can enhance the search temple by cutting the unnecessary execution time of time domain simulation. Moreover, the results show the robustness of the proposed method for solving MC-TSCOPF problem with both smooth (Case 2.1) and non-smooth (Case 2.3) objective functions.

Fig. 5.15 and Fig. 5.16 sketch the rotor angles with respect to COI of only the generator with the largest swing based on the MC-TSCOPF (*A+C+F*), MC-TSCOPF (*A+C*), TSCOPF (*A*) and OPF in Case 2.3 after the contingencies *A* and *F* respectively. When the contingency *A* occurs, almost all solutions except for OPF can maintain the transient stability. On the other hand, only MC-TSCOPF (*A+C+F*) solution can maintain the transient stability after the

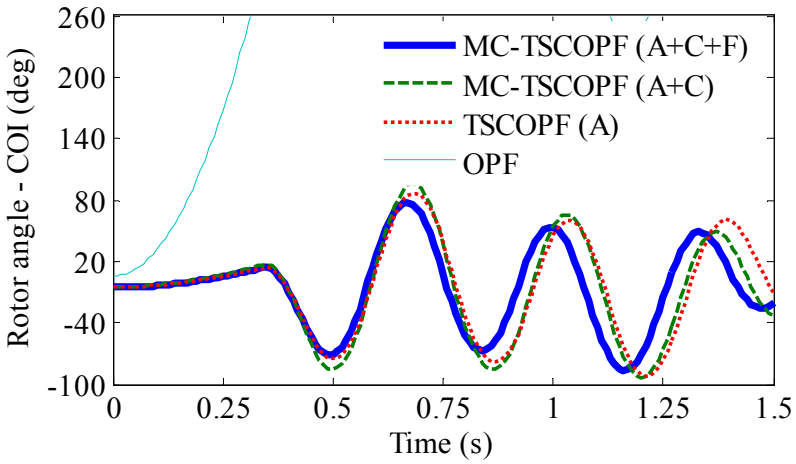

Fig. 5.15 The rotor angle deviation after contingency *A* in Case 2.3

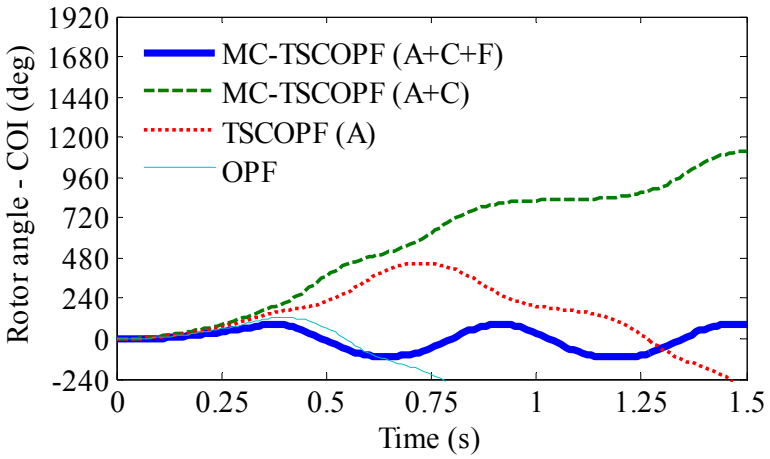

Fig. 5.16 The rotor angle deviation after contingency *F* in Case 2.3

contingency *F*. The results confirm that MC-TSCOPF is indispensable to guarantee the transient stability against the possible multi-contingencies that may happen in the system.

5.5 Results of OPF with Steady-State Voltage Stability Consideration

The EP-based algorithms are tested on the IEEE 30-bus system. The scaling factor (α) used in Eq. (2.23) is set to 5000 in the simulation. The numerical examples are divided into four cases as follows:

Case 1: The cost curves of all generators in the IEEE 30-bus system are represented by Eq. (5.1). The generator data and cost coefficients can be found in Table 5.2.

Case 2: The cost curves of *2*-nd and *3*-rd generators are replaced by Eq. (5.2). The cost coefficient of *2*-nd and *3*-rd generators can be found in Table 5.3.

Case 3: The cost curves of *2*-nd and *3*-rd generators are replaced by Eq. (5.3). The cost coefficient of *2*-nd and *3*-rd generators can be found in Table 5.4.

Case 4: The objective function shown in Eq. (2.23) is modified to minimize only the indicator L at the weakest bus regardless of the economic fuel cost term.

Table 5.21 tabulates the results in all cases consisting of control variables, and their corresponding fuel cost, computational time, and indicator L at bus 8. It is important to note that bus 8 is the weakest bus in the test system owing to its largest load demand and the fuel cost of Case 4 is calculated based on the data of the cost function in Case 3. For Cases 1-3, the fuel costs of OPF with voltage stability consideration (α = 5000) slightly rise up from OPF (α = 0) problem. The additional costs of 1.13 $/hr, 1.61 $/hr, and 2.40 $/hr are required in Cases 1, 2 and 3 respectively to increase the voltage stability degree, which is indicated by the lower value of indicator L. For example, in case 1 the value of indicator L decreases from 0.051 to 0.049 when the voltage stability issue is considered in the OPF problem. Because of indicator L's calculation, the voltage stability-considered case consumes the run time slightly longer than OPF case does. Case 4 provides the smallest value of indicator L among all cases, implying that the operating point obtained by Case 4 possesses the largest voltage stability margin. However, at the same fuel cost data, the fuel cost of Case 4 is significantly more expensive than that of Case 3. This can be realized as the trade-off problem between the economic and system security points of view.

The reason why the value of indicator L in Case 4 is not notably different from other cases can be explained as the following. Based on Eq. (2.21), to reduce the value of indicator L, the voltage magnitude of generator buses and transformer tap setting near the weakest bus should be lifted up since the indicator L is influenced by voltages (both magnitude and angle) at generator buses and sub-matrix F_{LG}. In other words, if the voltages of generator buses are set higher and transformer-tap setting is adjusted properly, the value of indicator L will drop. This can be noticed in Table 5.21 that the voltage magnitudes of the cases with voltage stability consideration are set higher than those of the OPF cases. However, the over-increase in voltage magnitudes may cause line overloading and also bring out overvoltage at load buses. In addition, the adjusting of active power generation, which mainly changes the voltage angles of generator buses, has a minor impact on the value of indicator L. Therefore, it is quite difficult to improve the voltage stability by lowering indicator L when the operating point from the OPF has already set the voltage magnitudes of generator buses at a high value or near their upper limits.

Table 5.21 OPF and OPF considering steady-state voltage stability results solved by IEP in all cases

	Case 1		Case 2		Case 3		Case 4
	$\alpha = 0$	$\alpha = 5000$	$\alpha = 0$	$\alpha = 5000$	$\alpha = 0$	$\alpha = 5000$	
P_{G1} (p.u.)	43.56	43.19	48.93	50.30	48.15	46.76	24.46
P_{G2} (p.u.)	57.17	56.60	40.00	39.95	53.26	53.29	35.51
P_{G3} (p.u.)	16.76	18.67	19.99	19.95	13.30	13.32	33.44
P_{G4} (p.u.)	23.10	22.83	22.99	26.56	24.93	27.75	30.41
P_{G5} (p.u.)	16.22	12.84	18.29	11.31	16.91	9.31	17.09
P_{G6} (p.u.)	34.87	37.70	41.68	43.67	35.46	41.41	50.47
V_{G1} (p.u.)	1.04	1.05	1.00	1.02	1.02	1.05	1.05
V_{G2} (p.u.)	1.04	1.05	1.00	1.02	1.02	1.05	1.05
V_{G3} (p.u.)	1.06	1.10	1.06	1.09	1.02	1.07	1.09
V_{G4} (p.u.)	1.02	1.06	0.99	1.05	1.01	1.04	1.06
V_{G5} (p.u.)	1.03	1.04	1.01	1.04	1.02	1.05	1.07
V_{G6} (p.u.)	1.04	1.05	1.02	1.06	1.02	1.07	1.05
Best cost ($/hr)	574.77	575.90	526.96	528.57	604.75	607.15	693.96
Run time (s)	19.92	21.91	20.41	21.86	20.18	21.39	20.75
Indicator L at bus 8	0.051	0.049	0.055	0.052	0.053	0.050	0.048

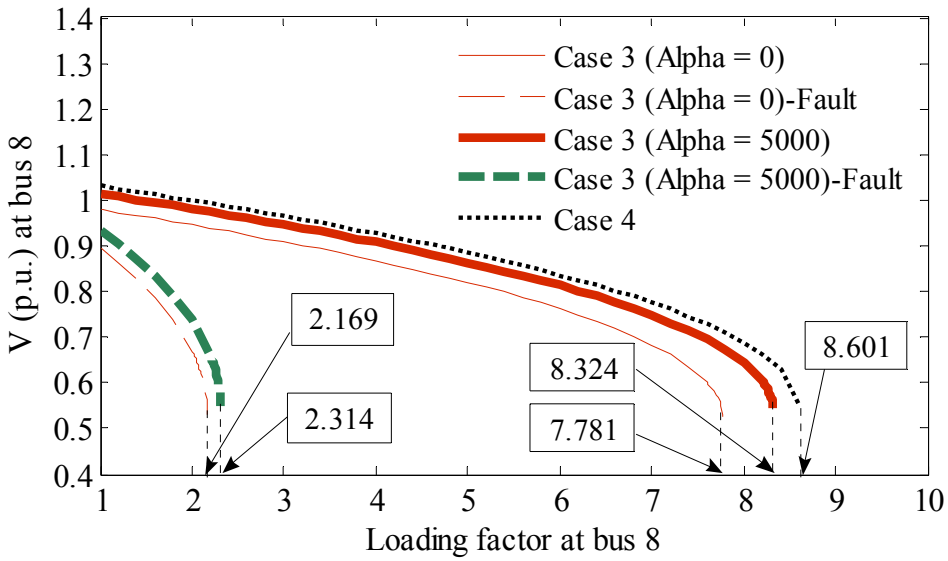

Fig. 5.17 P-V curves in Case 3 and Case 4

The P-V curves at bus 8 based on solutions of Cases 3 and 4 with pre- and post-faults are sketched in Fig. 5.17. The fault is three-phase grounding at line 6-8 and it is cleared by opening the faulted line. From Fig. 5.17 and Table 5.21, the lower the value of indicator L is, the larger

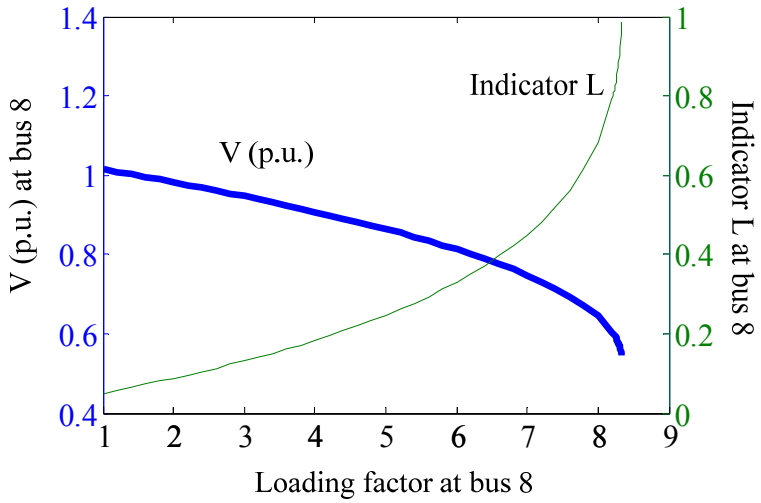

Fig. 5.18 Voltage magnitude and indicator L at bus 8

maximum loading factor will be, and the removal of line 6-8 greatly degrades the system voltage stability. Compared to the OPF case ($\alpha = 0$), the OPF with voltage stability consideration ($\alpha =$ 5000) can increase the maximum loading factor of roughly 7.0 % under pre-fault and 6.7 % under post-fault. Even though, under pre-fault, the 10.5 % increase (from 7.781 to 8.601) of the maximum loading factor from the OPF case can be achieved in Case 4, this improvement leads to very expensive fuel cost as earlier shown in Table 5.21 (from 604.75 to 693.96).

Fig. 5.18 shows the relationship between the voltage magnitude and indicator L at bus 8 based on the solution of OPF considering voltage stability ($\alpha = 5000$) in Case 3 under pre-fault condition. From the figure, with the increase in the loading factor, the voltage at bus 8 drops but the value of indicator L rises. As the voltage becomes collapse at the loading factor equal to 8.324, the value of indicator L approaches 1. In addition, the value of indicator L increases exponentially at the proximity of the voltage collapse point.

Table 5.22 shows an impact of the scaling factor (α) on the fuel cost and indicator L's value in Case 3. When the value of α is beyond 5000, the fuel cost greatly rises up while the indicator L is slightly improved. This signifies that too large value of α results in the unnecessary additional cost without the satisfactory increase in the voltage stability margin. The value of α equal to 5000 seems to be the appropriate scaling factor for the IEEE 30-bus system. The appropriate scaling factor will be different from this number, if the system characteristic and generator data are modified.

To emphasize the robustness of the proposed algorithm against the highly non-convex optimization problem, a comparison of the obtained results in Case 3 ($\alpha = 5000$) between IEP and conventional EP algorithms is shown in Table 5.23. It is obvious that the proposed algorithm (IEP6) outperforms the conventional EP in both finding the optimal solution and saving the computational time. This again supports the idea that the combination of mutation and crossover can enhance the performance of the EP method.

Table 5.22 Results of different values of α in Case 3

Value of α	Fuel cost ($/hr)	Indicator L at bus 8	Max. Loading Factor at bus 8
0	604.75	0.0534	7.781
500	605.40	0.0529	7.844
2500	606.09	0.0510	8.149
5000	607.15	0.0497	8.324
50000	630.97	0.0495	8.426
100000	658.03	0.0492	8.477
Case 4	693.96	0.0485	8.601

Table 5.23 Comparison between IEP and EP results in Case 3

Result	IEP	EP
Worst cost ($/hr)	611.51	627.64
Avg. cost ($/hr)	609.03	625.97
Best cost ($/hr)	607.15	624.48
Avg. run time (s)	21.39	24.66
Indicator L at bus 8	0.050	0.050

5.6 Results of OPF with Transient and Voltage Stability Considerations

The EP-based algorithm is tested on the IEEE 30-bus system as illustrated in Fig. 5.2. The scaling factor (α) used in Eq. (2.23) is set to 5000 in the simulation. First, the cost curves of all generators in the IEEE 30-bus system are represented by quadratic curve expressed in Eq. (5.1). The generator data and cost coefficients can be found in Table 5.2. The numerical examples are divided into four cases as follows:

Case 1a: The conventional OPF
Case 1b: The OPF considering voltage stability
Case 1c: The OPF considering transient stability (TSCOPF)
Case 1d: The OPF considering voltage and transient stabilities

A single contingency (A) with three-phase grounding fault near bus 2 at the end of the line 2-5 at t = 0 s is considered. The fault is cleared at t = 0.35 s. The maximum integration period is 1.5 s. The integration time step is 0.01 s and δ_{MAX} is 120 degrees.

The conventional EP is applied to solve the problem. The results of Cases 1a-d using the proposed method are tabulated in Table 5.24. The results consist of the average, worst, best solutions in terms of the total generator fuel cost, cost differences with respect to Case 1a, average computational time from 20 runs, all control variables, indicator L and maximum loading factor at bus 8 based on the best cost. It is important to note that bus 8 is the weakest bus in the test system due to its heaviest load demand.

From the Table 5.24, the fuel cost of Cases 1b–d, especially in Case 1d, increases from Case 1a due to the consideration of voltage and transient stability issues respectively. Case 1b provides the smallest value of indicator L among all cases, implying that the operating point obtained from Case 1b possesses the largest voltage stability margin, i.e. the obtained maximum loading factor of 8.28. It can be noticed that the voltage magnitudes of the cases that consider voltage stability (Case 1b and Case 1d) are set larger than those of the cases that do not consider voltage stability (Case 1a and Case 1c). This is because, based on Eq. (2.21), to reduce the value of indicator L, the voltage magnitudes of generator buses should be lifted up since the indicator L is mainly influenced by voltages at generator buses. From Cases 1a–d, when the transient stability constraints are included into the conventional OPF, it degrades the degree of steady-state voltage stability. For instance, the maximum loading factor of Case 1c (7.52) is smaller than that of Case 1a (8.06). Case 1d requires the longest computational time because both time domain simulation (to check the transient stability) and indicator L's calculation (to estimate the voltage stability margin) are carried out during the EP search.

The rotor angles with respect to COI of only the generator with the largest swing (*2*-nd generator) in Cases 1a-d after the contingency A are plotted in Fig. 5.19. It is obvious that the operating points obtained from Case 1c and Case 1d can maintain transient stability after the considered contingency whereas Case 1a and Case 1b cannot. Even though Case 1b offers the largest voltage stability margin, it cannot provide the transiently stable operating point. This emphasizes the importance of transient stability consideration.

Table 5.24 Results of the proposed method in Cases 1a–d

	Case 1a	Case 1b	Case 1c	Case 1d
P_{G1} (p.u.)	43.70	43.19	50.25	53.86
P_{G2} (p.u.)	57.28	53.92	38.86	38.04
P_{G3} (p.u.)	17.04	15.14	17.96	17.08
P_{G4} (p.u.)	23.16	23.52	27.33	28.08
P_{G5} (p.u.)	16.55	18.25	20.29	10.29
P_{G6} (p.u.)	34.01	37.82	37.25	44.53
V_{G1} (p.u.)	1.04	1.04	0.99	1.02
V_{G2} (p.u.)	1.03	1.04	0.99	1.02
V_{G3} (p.u.)	1.04	1.09	1.02	1.09
V_{G4} (p.u.)	1.03	1.05	0.99	1.04
V_{G5} (p.u.)	1.04	1.04	1.01	1.03
V_{G6} (p.u.)	1.06	1.06	1.04	1.06
T_1 (bus 6-9)	0.93	0.98	1.02	0.98
T_2 (bus 6-10)	1.03	0.97	0.99	0.97
T_3 (bus 4-12)	1.02	1.09	0.97	0.98
T_4 (bus 28-27)	1.06	1.07	1.04	1.04
Avg. cost ($/hr)	575.46	576.46	585.83	589.92
Worst cost ($/hr)	575.89	577.50	586.86	590.98
Best cost ($/hr)	575.02	576.07	585.15	588.32
Cost diff. ($/hr)	-	1.05	10.13	13.30
Indicator L at bus 8	0.051	0.050	0.055	0.052
Max. loading factor	8.06	8.28	7.52	7.99
Avg. run time (s)	21.71	22.72	451.18	458.62

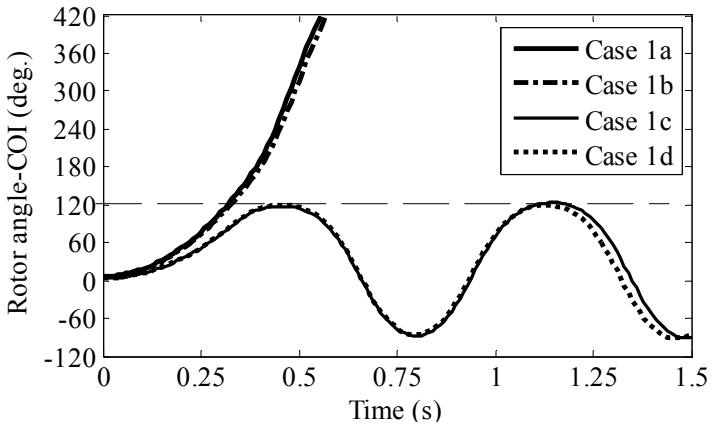

Fig. 5.19 Rotor angle curves (*2*-nd generator) after contingency *A* of Cases 1a-d

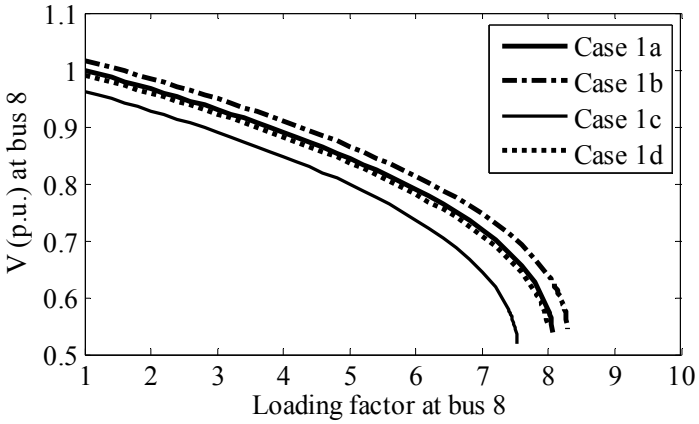

Fig. 5.20 P-V curves at bus 8 of Cases 1a-d

The P-V curves at bus 8 based on the best solutions obtained from Cases 1a-d are depicted in Fig. 5.20. When the voltage stability issue is considered by adding the value of indicator L in the objective function, i.e. Case 1b and Case 1d, their degree of voltage stability increases compared with the cases where voltage stability issue is not regarded, i.e. Case 1a and Case 1c. The increase in voltage stability degree is expressed by the larger value of the maximum loading factor of those cases.

Next, the cost curves of *2*-nd and *3*-rd generators (bus no. 2 and 13) of IEEE 30-bus system used in Cases 1a-d are replaced by quadratic function superimposed by sine component to model the effects of valve-point loading in a thermal unit. Similar to Cases 1a-d, the following four problems are formulated as follows:

Case 2a: The conventional OPF
Case 2b: The OPF considering voltage stability
Case 2c: The OPF considering transient stability (TSCOPF)
Case 2d: The OPF considering voltage and transient stabilities

The results of Cases 2a-d using the proposed EP method are tabulated in Table 5.25. Similar to Cases 1a-d, when the transient and voltage stabilities are considered into the conventional OPF, the additional cost and computational time are unavoidable, especially when transient stability is considered. In this type of cost curve, Case 2d provides the largest voltage stability margin signified by the largest maximum loading factor whereas Case 2a provides the smallest voltage stability margin among all cases. Besides, the computational burden is the heaviest in Case 2d. To alleviate the computational load, the implementation of EP on parallel computing can be a good option or the proposed neural network used in the previous session can be applied. The difference between the best and worst costs of Cases 2a-d is significant compared to Cases 1a-d. This is because in Cases 2a-d the optimization problem has many local optimums introduced by the sine component whereas in Cases 1a-d the problem is less complicated due to the smooth and convex objective function. In Cases 2a-d, when the transient stability constraints are included into the conventional OPF, it improves the degree of steady-state voltage stability.

Table 5.25 Results of the proposed method in Cases 2a–d

	Case 2a	Case 2b	Case 2c	Case 2d
P_{G1} (p.u.)	43.67	58.01	58.44	48.08
P_{G2} (p.u.)	53.26	26.69	26.69	26.63
P_{G3} (p.u.)	13.30	13.33	13.32	26.61
P_{G4} (p.u.)	24.32	28.57	28.56	26.40
P_{G5} (p.u.)	18.90	23.25	23.36	14.49
P_{G6} (p.u.)	38.57	41.90	41.58	49.58
V_{G1} (p.u.)	0.99	1.05	1.02	1.05
V_{G2} (p.u.)	0.99	1.04	1.02	1.04
V_{G3} (p.u.)	1.06	1.09	1.07	1.08
V_{G4} (p.u.)	1.01	1.05	1.03	1.05
V_{G5} (p.u.)	1.03	1.06	1.04	1.03
V_{G6} (p.u.)	1.02	1.06	1.06	1.06
T_1 (bus 6-9)	0.92	0.97	0.98	1.03
T_2 (bus 6-10)	0.92	1.02	0.98	0.93
T_3 (bus 4-12)	0.97	1.03	0.95	0.99
T_4 (bus 28-27)	1.09	1.05	1.05	1.05
Avg. cost ($/hr)	606.89	625.97	628.45	631.80
Worst cost ($/hr)	609.90	627.64	630.91	633.55
Best cost ($/hr)	604.85	624.48	625.34	630.53
Cost diff. ($/hr)	-	19.63	20.49	25.68
Indicator L at bus 8	0.056	0.050	0.052	0.050
Max. loading factor	7.44	8.33	7.95	8.39
Avg. run time (s)	22.23	24.66	459.34	479.57

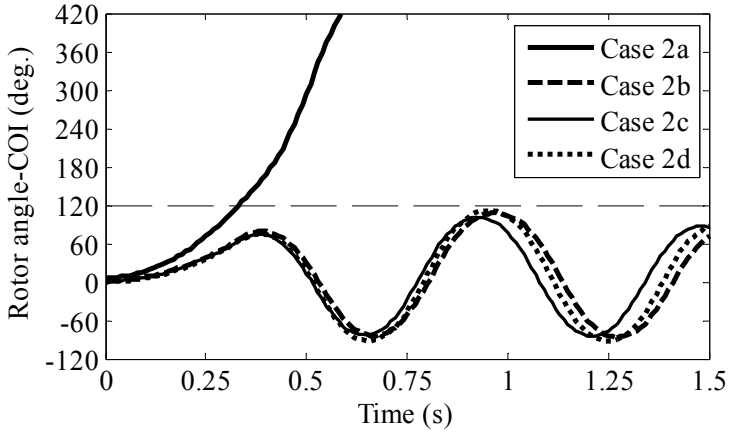

Fig. 5.21 Rotor angle curves (*2*-nd generator) after contingency *A* of Cases 2a-d

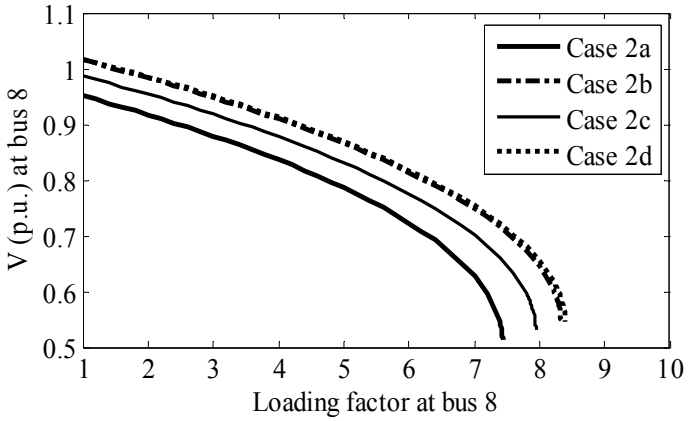

Fig. 5.22 P-V curves at bus 8 of Cases 2a-d

The rotor angles with respect to COI of only the generator with the largest swing (2-nd generator) in Cases 2a-d after the contingency *A* are plotted in Fig. 5.21. From the figure, the operating points obtained from not only Case 2c and Case 2d but also Case 2b can guarantee the transient stability of the power system after the contingency *A*. In this case, it can be said that the voltage stability consideration does not harm the transient stability of the system.

The P-V curves at bus 8 of Cases 2a-d are sketched in Fig. 5.22. Here, Case 2d provides the largest maximum loading factor, which is slightly higher than that of Case 2b. It is seemingly difficult to improve the voltage stability by lowering indicator L when the voltage magnitudes of generator buses are set at a high value or near their upper limits. Case 2a, which does not consider transient and voltage stability issues, has the lowest maximum loading factor and cannot guarantee the transient stability of the system after the contingency. The necessity of consideration of transient and voltage stabilities into the conventional OPF problem is manifested by the above-elaborated results.

5.7 Summary

The effectiveness of three versions of the EP-based methods is demonstrated by the results of four OPF problems, i.e. conventional OPF, TSCOPF, OPF considering steady-state voltage stability, and OPF considering transient and voltage stabilities. The WSCC 9-bus system and IEEE-30 bus system are used as test platforms. Three types of cost functions are considered to represent the approximated cost model and detailed cost model of a thermal unit.

First, the suitable parameters i.e. population size, decaying mutation rate, and crossover acceptance rate of IEP6 are selected based on the conducted experiment. The IEP6 with the selected parameters can obtain the better solution than SQP (one of the classical optimization techniques), the conventional EP, GA, and PSO. In addition, IEP requires the shorter computational time than does EP.

The six different IEP methods (IEP1–IEP6) are used to solve the conventional OPF problem with three types of cost curves. All versions of IEP method except for IEP3 can obtain the lower fuel cost and require the shorter computational time than the conventional EP. After that, AEP is applied to solve the OPF problem. The results show that AEP also performs better than the conventional EP. The smaller average population size of AEP leads to the shorter required computational time than EP. Even though the convergence speed of AEP is slower than that of the conventional EP at the beginning, the final solution is satisfactory. The difference between the best and worst costs (the standard deviation) of the case, where the sine component is introduced to the quadratic curve, is significant compared to the case where the cost curve is smooth and convex. The explanation is that the sine component brings the non-convexity to the problem resulting in many local optimums. Due to the mentioned reason, AEP, which changes its population size adaptively according to the performance in each generation, needs a large population size to obtain the solution in the case of quadratic cost curve with sine component.

The conventional EP, IEP and AEP are applied to obtain the solution of TSCOPF. It is shown that the performance of IEP and AEP is also superior to the conventional EP for this problem. The TSCOPF solution proves that it can guarantee the transient stability against the pre-considered contingency at the expense of the increasing fuel cost. It is also found that the convergence speed of the TSCOPF is slower than that of the conventional OPF. Due to very huge computational time of TSCOPF, the proposed neural network is incorporated into the EP-based methods. The advent of the neural network improves the computational speed without degradation of the quality of solution. Next, IEP combined with the proposed neural network is applied to solve MC-TSCOPF problem. Without the neural network, the computational time of MC-TSCOPF is very extensive. This extensive computational time is alleviated by the proposed neural network. More than 50% of computational time saving in all cases can be witnessed from the simulation as the contribution of the neural network. The solution of MC-TSCOPF confirms that it can guarantee transient stability after all pre-considered contingencies whereas the conventional OPF and single-contingency TSCOPF cannot.

Next, IEP is applied to obtain the solution of OPF with steady-state voltage stability consideration. The solution from this problem can increase the voltage stability margin compared to that from the conventional OPF. However, the significant increase in the stability margin

cannot be seen from the solution, since the solution of OPF already sets the voltage magnitudes of generator buses at a high value and there are the load-bus voltage limits involved. The impact of the scaling factor on the fuel cost term and indicator L term is discussed. Too high value of the scaling factor can cause the excessive rising of fuel cost with a small improvement in the stability margin. The results of IEP are also compared with those of EP in this problem. The superiority of IEP over the conventional EP is again demonstrated.

Lastly, the EP method is applied to solve the OPF with transient and voltage stability considerations. The solution of this problem is compared with that of the conventional OPF, TSCOPF, and OPF with steady-state voltage stability consideration. The results indicate that the consideration of voltage stability alone cannot guarantee the transient stability even though it provides very large voltage stability margin. Likewise, the consideration of transient stability alone can result in a small voltage stability margin. Accordingly, the consideration of both transient and voltage stability issues is clearly necessary in the power system operation.

References

[1] P. M. Anderson and A. A. Fouad: “Power System Control and Stability”, Iowa, the Iowa State University Press, 1977.

[2] R. Zimmerman, E. Murillo-Sánchez, and D. Gan: “MATPOWER: a MATLAB Power System Simulation Package”, 2006.

[3] M. A. Abido: “Optimal Power Flow Using Tabu Search Algorithm”, *Electric Power System Components and Systems*, Vo. 30, pp. 469–483, 2002.

[4] J. Yuryevich and K. P. Wong: “Evolutionary Programming Based Optimal Power Flow Algorithm”, *IEEE Trans. Power Systems*, Vol. 14, No. 4, pp. 1245–1250, 1999.

[5] N. Mo, Z. Y. Zou, K. W. Chan, and T. Y. G. Pong: “Transient stability constrained optimal power flow using particle swarm optimization”, *IET Generation Transmission and Distribution*, Vol. 1, No. 3, pp. 476-483, May 2007.

CHAPTER 6
CONCLUSIONS

This dissertation proposes an efficient method based on evolutionary programming (EP) for Optimal Power Flow (OPF) with transient and voltage stability considerations. The contribution of this dissertation can be categorized into three parts i.e. the formulation of OPF with transient and voltage stability considerations, the application of EP-based methods on various types of the OPF problems, and the development of the novel EP-based methods, i.e. Improved EP (IEP) and Adaptive EP (AEP). All of these three contributions and the conclusions of the obtained results will be described in the following paragraphs.

The conventional OPF, which normally considers only statistic constraints, is firstly formulated. In the OPF problem, the objective function is to minimize the total generator fuel cost. After that the transient stability and voltage stability issues, which play an important role on blackouts in many countries around the world, are taken in considerations. In this dissertation, the transient stability issue is treated as the additional constraints of the conventional OPF. The additional constraints are the swing equation, which describes the transient behavior of a synchronous generator, and transient stability limit, which is used to evaluate the stability status of the system. This problem is called Transient Stability Constrained OPF (TSCOPF). The swing equation is quite difficult to handle, since it consists of a set of differential equations. Time domain simulation based on the trapezoidal rule is adopted to cope with this swing equation. When the number of the considered contingency is more than 1, the problem is called Multi-Contingency TSCOPF (MC-TSCOPF). The voltage stability issue is considered by adding the value of indicator L into the objective function of the conventional OPF. The indicator L, which is widely used in many applications due to its simplicity of calculation and accuracy, is selected to estimate the voltage stability margin of the system. The larger the indicator L is, the closer the system is to the voltage collapse point. The indicator L at the weakest bus is used as the voltage stability indicator of the whole system. Therefore, the objective function now changes to minimize both indicator L of the weakest bus and the fuel cost simultaneously. The scaling factor is used to weight the importance of voltage stability issue and fuel cost term. This factor can be set according to the experience of the system operator. The modified objective function brings about the trade-off problem between the financial issue and system security issue. Finally, OPF with transient and voltage stability considerations is formulated by considering the transient stability issue as the additional constraints and voltage stability issue as one of the objective functions to be minimized apart from the fuel cost term.

Since the objective function used in the OPF problem is the fuel cost minimization, the cost function of the thermal unit is needed to be accurately modeled in order to obtain the optimal or near optimal solutions of OPF. The approximated quadratic cost function normally found in the OPF problem may be not accurate enough. The models of a combined-cycle unit and a thermal unit with valve-point loading effect are therefore introduced in this dissertation. The model of the

combined-cycle unit is represented by the piecewise quadratic curve and the model of the thermal unit with valve-point loading effect is represented by the quadratic curve with sine component. Since these accurate models cannot be handled by the classical optimization techniques such as linear programming or quadratic programming, the EP method is proposed to solve the OPF problems with these types of cost function.

The conventional EP is very popular for solving the optimization problems because of its simple algorithm, flexibility, and good convergence. However, the long execution time and pre-setting of EP parameters (population size, decaying mutation rate, and maximum generation) are the main disadvantages of this technique. The first attempt to enhance the conventional EP is done by introducing the crossover techniques, generally found in Real Coded Genetic Algorithm (RCGA), to the offspring generation process. This new EP-based method is called Improve EP (IEP). IEP employs both mutation of the conventional EP and crossover of RCGA to generate the offspring individuals while other components of conventional EP are still used in IEP. The mutation is performed to perturb the control variables whereas the crossover is performed to exchange the control variables between two parents. The crossover acceptance rate is the criterion to choose either mutation or crossover for generating the offspring. This criterion results in an additional parameter needed to be defined before applying IEP. The second attempt is made by proposing Adaptive EP (AEP), which adjusts its population size adaptively according to the quality of population. The quality of population is determined by the idea that the population having many improved individuals can reduce its size whereas the population having few improved individuals should increase its size. From this idea, it can be realized that AEP reduces the number of parameters needed to pre-define, i.e. population size.

It is found that the computational time required for TSCOPF problem is very extensive due to the execution of time domain simulation for transient stability assessment. To alleviate the problem, the neural network is proposed to handle the transient stability constraints. First, the output of the proposed neural network will classify the individuals into stable, unstable, and critical regions based on the preset thresholds. Only individuals classified in critical region will perform time domain simulation. Others classified in stable or unstable region will trust the output of the neural network. To train the neural network, the early stopping is adopted to avoid the overfitting problem. The result shows that the performance of the trained network against the new input is improved when the early stopping is used. The selection of a suitable architecture of the proposed neural network is studied. The selected architecture will be equipped into the fitness evaluation process of the EP-based methods to handle the transient stability constrains.

The results of the EP-based methods on four types of OPF problems can be divided into 2 issues, i.e. a comparison of solutions of the different OPF problems and a comparison of performance of the proposed EP-based methods.

First the comparison of solutions of the different OPF problems will be discussed. The solution from the conventional OPF problem provides the cheapest operating point among all OPF problems. However, it cannot guarantee the transient stability after some possible contingencies and it provides a small margin of steady-state voltage stability. The computational time of the conventional OPF problem is very short compared to other OPF problems. On the other hand, the solution from TSCOPF can guarantee transient stability after a considered

contingency. Certainly, increases in fuel cost and computational time are unavoidable. Similarly, the solution from MC-TSCOPF can guarantee transient stability after the considered contingencies with the significant increases in fuel cost and computational time. Next, the solution from OPF considering voltage stability provides the larger voltage stability margin than that from the conventional OPF. The increase in stability margin is gained by setting the voltage magnitudes of generator buses at a high value. The computational time of this problem is not as long as that of TSCOPF. The reason is that the calculation time of indicator L is much shorter than time domain simulation. Lastly, the solution from OPF considering transient and voltage stabilities can provide both transiently-stable operating point and a satisfactory voltage stability margin. As expected, the fuel cost and computational time of this problem are the most significant among all OPF problems.

Secondly, the comparison of performance of the proposed EP-based methods will be discussed. For almost all OPF problems, IEP and AEP can obtain the better solutions with the shorter computational time than the conventional EP. When the neural network is incorporated into the EP-based methods, the computational time of TSCOPF and MC-TSCOPF is dramatically reduced while the quality of solution (average, worst, best costs) is almost the same as the methods without the neural network. The neural network is here proved to be the potential tool to handle the transient stability constraints. When the EP-based methods are applied to solve the OPF problems with the more accurate models of cost function, the difference between the best and worst costs is large. This is because the more accurate models create many local optimums in the OPF problems.

In the future, the formulated OPF problems can be added with other important topics, for example gas emission constraints etc., to make the problem more and more practical. It is important to note that in this dissertation the voltage stability issue is simply considered as one of the objective functions to be minimized, because the test system (IEEE 30-bus system) possesses very high degree of voltage stability. In other words, even the contingency, e.g. a line outage, occurs in the system, the OPF operating point can still maintain the voltage stability. For other systems, treating the voltage stability issue as an objective function may not be suitable. Considering the voltage stability issue as an additional constraint (Similar to transient stability issue) in the conventional OPF problem will be a better way. The constraint can formulate in such a way that if there is any contingency occurring, the solution from OPF considering voltage stability can still guarantee the voltage stability.

Moreover, the proposed EP-based methods can be improved by adding some new operators for obtaining the better solution and reducing the computational time. Regarding the AEP method, the adaptation rules of not only population size but also the other parameters should be developed in order to enhance the flexibility of the algorithm.

APPENDIX

DATA OF TEST SYSTEMS

The data of the two test systems, WSCC 9-bus system and IEEE 30-bus system, are provided in the following 2 sections.

1. Data of the WSCC 9-bus system
2. Data of the IEEE 30-bus system

A.1 Data of WSCC 9-bus system

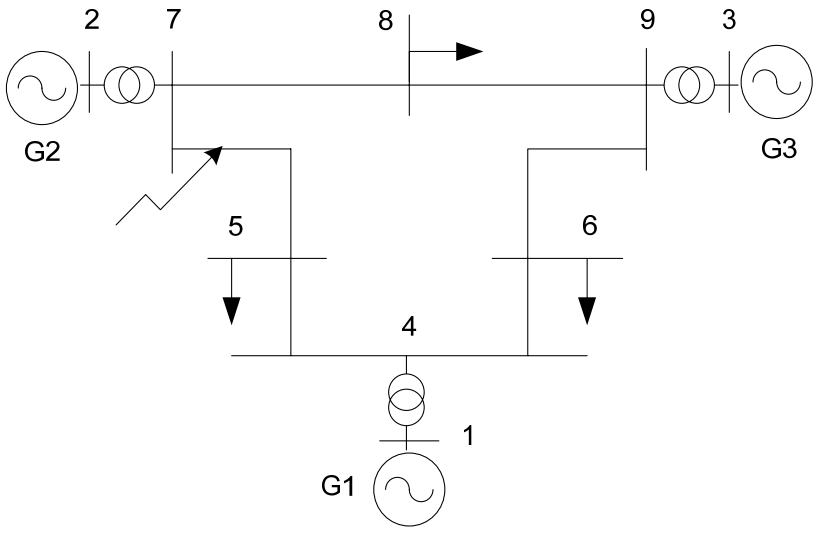

Fig. A.1 WSCC 9-bus test system

Table A.1 Branch data of the WSCC 9-bus system

Branch no.	Node		Branch data (p.u.)			
	From	To	*R*	*X*	*B*	Rating (MVA)
1	1	4	0	0.0576	0	100
2	2	7	0	0.0625	0	100
3	3	9	0	0.0586	0	100
4	4	5	0.0100	0.0850	0.1760	100
5	4	6	0.0170	0.0920	0.1580	100
6	5	7	0.0320	0.1610	0.3060	100
7	6	9	0.0390	0.1700	0.3580	100
8	7	8	0.0085	0.0720	0.1490	100
9	8	9	0.0119	0.1008	0.2090	100

Table A.2 Load data and bus voltage limit data of the WSCC 9-bus system

Bus No.	Load data		Bus voltage limits	
	P_D (MW)	Q_D (MVAR)	V^{min} (p.u.)	V^{max} (p.u.)
1	0.0	0.0	0.95	1.05
2	0.0	0.0	0.95	1.10
3	0.0	0.0	0.95	1.05
4	0.0	0.0	0.95	1.05
5	125	50	0.95	1.10
6	90	30	0.95	1.05
7	0.0	0.0	0.95	1.05
8	100	35	0.95	1.10
9	0.0	0.0	0.95	1.05

Table A.3 The generator data and cost coefficients of the WSCC 9-bus system

Bus No.	Active power generation		Reactive power generation		Cost coefficient		
	Min (MW)	Max (MW)	Min (MVAR)	Max (MVAR)	a ($/hr)	b ($/MW/hr)	c ($/MW^2/hr)
1	10	250	-300	300	150	5.0	0.1100
2	10	300	-300	300	600	1.2	0.0850
3	10	270	-300	300	335	1.0	0.1225

Table A.4 Generator parameters of the WSCC 9-bus system

	G1	G2	G3
X'_d	0.0608	0.1198	0.1813
H (s)	23.64	6.4	3.01

A.2 Data of IEEE 30-Bus System

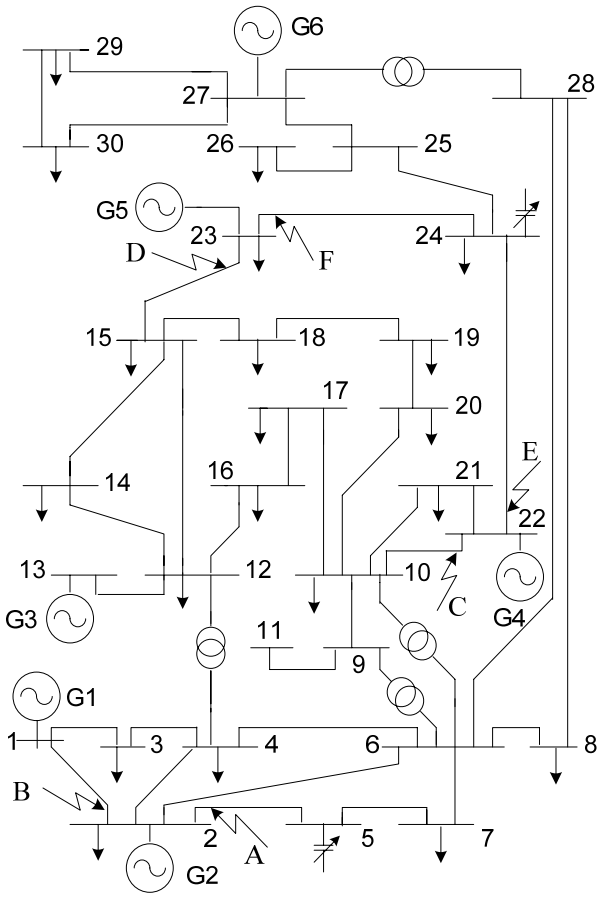

Fig. A.2 IEEE 30-Bus test system

Table A.5 Branch data of the 30-bus IEEE test system

Branch no.	Node		Branch data (p.u.)			
	From	To	*R*	*X*	*B*	Rating (MVA)
1	1	2	0.02	0.06	0.03	130
2	1	3	0.05	0.19	0.02	130
3	2	4	0.06	0.17	0.02	65
4	3	4	0.01	0.04	0	130
5	2	5	0.05	0.2	0.02	130
6	2	6	0.06	0.18	0.02	65
7	4	6	0.01	0.04	0	90
8	5	7	0.05	0.12	0.01	70
9	6	7	0.03	0.08	0.01	130
10	6	8	0.01	0.04	0	32
11	6	9	0	0.21	0	65
12	6	10	0	0.56	0	32
13	9	11	0	0.21	0	65
14	9	10	0	0.11	0	65
15	4	12	0	0.26	0	65
16	12	13	0	0.14	0	65
17	12	14	0.12	0.26	0	32
18	12	15	0.07	0.13	0	32
19	12	16	0.09	0.2	0	32
20	14	15	0.22	0.2	0	16
21	16	17	0.08	0.19	0	16
22	15	18	0.11	0.22	0	16
23	18	19	0.06	0.13	0	16
24	19	20	0.03	0.07	0	32
25	10	20	0.09	0.21	0	32
26	10	17	0.03	0.08	0	32
27	10	21	0.03	0.07	0	32
28	10	22	0.07	0.15	0	32
29	21	22	0.01	0.02	0	32
30	15	23	0.1	0.2	0	16
31	22	24	0.12	0.18	0	16
32	23	24	0.13	0.27	0	16
33	24	25	0.19	0.33	0	16
34	25	26	0.25	0.38	0	16
35	25	27	0.11	0.21	0	16
36	28	27	0	0.4	0	65
37	27	29	0.22	0.42	0	16
38	27	30	0.32	0.6	0	16
39	29	30	0.24	0.45	0	16
40	8	28	0.06	0.2	0.02	32
41	6	28	0.02	0.06	0.01	32

Table A.6 Load data and bus voltage limit data of the 30-bus IEEE test system

Bus No.	Load data		Bus voltage limits	
	P_D (MW)	Q_D (MVAR)	V^{min} (p.u.)	V^{max} (p.u.)
1	0	0	0.95	1.05
2	21.7	12.7	0.95	1.1
3	2.4	1.2	0.95	1.05
4	7.6	1.6	0.95	1.05
5	0	0	0.95	1.05
6	0	0	0.95	1.05
7	22.8	10.9	0.95	1.05
8	30	30	0.95	1.05
9	0	0	0.95	1.05
10	5.8	2	0.95	1.05
11	0	0	0.95	1.05
12	11.2	7.5	0.95	1.05
13	0	0	0.95	1.1
14	6.2	1.6	0.95	1.05
15	8.2	2.5	0.95	1.05
16	3.5	1.8	0.95	1.05
17	9	5.8	0.95	1.05
18	3.2	0.9	0.95	1.05
19	9.5	3.4	0.95	1.05
20	2.2	0.7	0.95	1.05
21	17.5	11.2	0.95	1.05
22	0	0	0.95	1.1
23	3.2	1.6	0.95	1.1
24	8.7	6.7	0.95	1.05
25	0	0	0.95	1.05
26	3.5	2.3	0.95	1.05
27	0	0	0.95	1.1
28	0	0	0.95	1.05
29	2.4	0.9	0.95	1.05
30	10.6	1.9	0.95	1.05

Table A.7 The generator data and cost coefficients of the IEEE 30-bus system

Bus No.	Active power generation		Reactive power generation		Cost coefficient		
	Min (MW)	Max (MW)	Min (MVAR)	Max (MVAR)	*a* ($/hr)	*b* ($/MW/hr)	*c* ($/MW^2/hr)
1	0	80	-20	150	0	2.00	0.02000
2	0	80	-20	60	0	1.75	0.01750
13	0	40	-15	44.7	0	3.00	0.02500
22	0	50	-15	62.5	0	1.00	0.06250
23	0	30	-10	40	0	3.00	0.02500
27	0	55	-15	48.7	0	3.25	0.00834

Table A.8 Generator parameters of the IEEE 30-bus system

	G1	G2	G3	G4	G5	G6
X_d'	0.06	0.30	0.30	0.30	0.30	0.30
H (s)	10	3	13	3	3	3

Table A.9 Shunt data of the 30-bus IEEE test system

Bus no.	B (p.u.)
5	0.19
24	0.04